BAG6 AS A NOVEL HIV-1 HOST FACTOR

A Dissertation
Submitted to
the Temple University Graduate Board

In Partial Fulfillment
of the Requirements for the Degree
DOCTOR OF PHILOSOPHY

---

by
Ivan Tashovski
December 2016

Examining Committee Members:

Dr. Alexander Y. Tsygankov, Ph.D. (Advisory Chair, Department of Microbiology-Immunology)
Dr. Mario P.S Chin, Ph.D. (Department of Microbiology-Immunology)
Dr. Doina Ganea, Ph.D. (Department of Microbiology-Immunology)
Dr. Toby K. Eisenstein, Ph.D. (Department of Microbiology-Immunology)
Dr. Weidong Xiao, Ph.D. (Department of Microbiology-Immunology)
Dr. Sara Ward, Ph.D. (External Member, Department of Pharmacology)

ABSTRACT

The human immunodeficiency virus type-1 (HIV-1) is the major etiological agent of acquired immunodeficiency syndrome (AIDS), the cause of over 30 million deaths worldwide. Highly active antiretroviral therapy (HAART) has demonstrated great efficacy at suppressing viral load and is therefore the standard therapeutic treatment for HIV-1 infection. Noncompliance due to severe HAART-associated side effects significantly undermines therapeutic efficacy. Dronabinol, the synthetic form of the cannabinoid THC found in marijuana, is FDA-approved for countering some of these side effects. Studies have reported that cannabinoids restrict HIV-1 replication, although no mechanism has yet been proposed. Thus the purpose of this study was to characterize the effects of cannabinoids on HIV-1 infection and to determine the molecular basis of cannabinoid-induced viral suppression. By transcriptomic sequencing of T cells treated with cannabinoids, we have found that the expression of BAG6, a protein uncharacterized within the context of HIV-1 infection, was downregulated. To identify the role of this protein during infection, we knocked down BAG6 and were able to recapitulate the protective effects of cannabinoids by observing reduced severity of viral challenge. Moreover, we have also identified BAG6 to be a binding partner of two HIV-1 viral accessory proteins, Vif and Vpr. Importantly, we have discovered that Vpr mediates targeted degradation of BAG6 by leveraging the host proteasome during the early stages of the viral lifecycle, revealing a hitherto unknown function of this poorly-understood viral protein. We thus establish modulation of BAG6 expression as a novel mediator of the effects of cannaninoids on HIV-1 infection.

To my brother Vasil, for his never-ending support and love.

ACKNOWLEDGEMENTS

I would like to express my gratitude to Dr. Mario Chin for accepting me into his laboratory four years ago. His demeanor, knowledge, and humbleness always made for a very encouraging working environment. And even from across the globe, Dr. Chin always made himself available and was always willing to lend his expertise in any way he could. In the laboratory both Natalia Ristic and Janaki Purushe were great conversationalists who were more than eager to lend a helping hand, or say a prayer to the Science Gods on my behalf if need be - at times, very often indeed.

Upon Dr. Chin's departure, the Department was absolutely wonderful in permitting me to resume the project and follow it through completion. My committee members, Dr. Doina Ganea, Dr. Toby Eisenstein, and Dr. Weidong Xiao always showed sincere enthusiasm towards the research progress I was making, very much helping to assuage any of my reservations before every research review, while Dr. Sara Ward was very kind in agreeing to join the committee as an external member. I would like to especially thank Dr. Alex Tsygankov for assuming a supervisory role, being encouraging, and always ready to discuss my thoughts and ideas until they materialized into testable hypotheses. Thank you all for letting me mature as a scientist, and for being members of our great Microbiology and Immunology department.

TABLE OF CONTENTS

Page

LIST OF TABLES

Table Page

LIST OF FIGURES

Figure Page

LIST OF ABBREVIATIONS

AIDS	Acquired Immunodeficiency Syndrome
BAG6	BCL2-associated athanogene 6
CCR5	C-C chemokine receptor type 5
CD4	Cluster of differentiation 4
CDC	Centers for Disease Control and Prevention
CXCR4	CXC-chemokine receptor type 4
DCAF-1	DDB1-CUL4A-associated factor 1
DDB-1	DNA damage-binding protein 1
DMEM	Dulbecco's modified eagle medium
DNA	Deoxyribonucleic Acid
ELISA	Enzyme Linked Immunosorbent Assay
ESCRT	Endosomal sorting complex required for transport
FDA	US Food and Drug Administration
Gag	group specific antigen
GAPDH	Glyceraldehyde 3-phosphate dehydrogenase
GFP	Green fluorescent protein
gp	Glycoprotein
HAART	Highly Active Anti-Retroviral Therapy
HIV	Human Immunodeficiency Virus
LTR	Long terminal repeat
MHC	Major Histocompatibility Complex
Nef	Negative regulatory factor
NFκB	Nuclear factor kappa
NNRTI	Non-nucleoside Reverse Transcriptase Inhibitor

NRTI	Nucleoside Reverse Transcriptase Inhibitor
PCR	Polymerase Chain Reaction
PI	Protease Inhibitor
PIC	Pre-initiation complex
Pol	polymerase
qPCR	quantitative polymerase chain reaction
Rev	Regulator of expression of virion proteins
RIPA	Radioimmuno-precipitation Assay Buffer
RNA	Ribonucleic Acid
RT	Reverse transcriptas
shRNA	small hairpin RNA
siRNA	small interfering RNA
Tat	Trans-activator
TM	trans-membrane
UPS	ubiquitin proteasome system
Vif	Viral infectivity factor
Vpr	Viral protein R
VPRBP	Vpr binding protein
Vpu	Viral protein U

CHAPTER 1

INTRODUCTION

Overview of the HIV-1 Life Cycle

HIV-1 is a member of the genus lentivirus within the *Retroviridae* family. Retroviruses are characterized by their viral RNA genome, which is reverse-transcribed into a double-stranded DNA provirus prior to integration within the host genome, followed by a long incubation period preceding disease onset (Baltimore, 1971). Encapsidated are two copies of the viral genome, roughly 9kb in size and flanked by two long terminal repeat sequences (LTR), which encodes for three polyproteins and several regulatory and accessory proteins (Frankel and Young, 1998). The expression of the three traditional retroviral genes *gag* (name derived from group-antigen), *pol* (polymerase), and *env* (envelope) are all transcribed as large polyproteins prior to subsequent processing and cleavage into functional viral proteins (Wong-Staal, 1991). Gag is initially translated as polyprotein Pr55 and is processed by the viral protease (PR) during viral particle maturation into the matrix (MA), capsid (CA), nucleocapsid (NC), p6 and spacer peptides (SP1, SP2), which together constitute the viral core (Gelderbloom et al., 1993). MA is associated with the inner membrane of the viral particle, while CA forms a shell around the NC in complex with the viral RNA genome. Protease (PR), Reverse Transcriptase (RT) and Integrase (IN) are all derived from the Pol precursor polyprotein. Lastly, the Env polyprotein is cleaved into surface gp120 (SU) and transmembrane gp41 (TM), which together constitute the viral envelope spike, which is critical for initial infection of the host cell (Manel et al., 2010). Viral proteins Tat and Rev function in viral

transcription and viral RNA export, respectively (Wei, 1998; Collins, 1998). The viral accessory proteins such as Vif, Vpr, Vpu and Nef, however, are usually required to overcome cellular restriction factors and are generally considered to be dispensable for HIV-1 replication in cell culture (Rasaiyaah et al., 2013; Yan et al., 2010; Nazli et al., 2013) (Figure A).

The viral life cycle begins with the interaction of the viral gp120 envelope protein and its receptor CD4, expressed on the surface of the target cell (Dalgleish et al., 1984) (Figure B). This binding induces a conformational change within gp120 (Sattentau and Moore, 1991) that exposes additional binding sites and promotes its interaction with one of the two HIV-1 co-receptors, CCR5 or CXCR4. In fact, it is due to the specificity of viral attachment to either CCR5, expressed primarily on macrophages, or CXCR4, expressed primarily on CD4+ T lymphocytes, that a particular HIV-1 strain is either M-tropic or T-tropic (Berger, 1998). This tropism for cells of the immune system ultimately enables HIV-1 to dysregulate immune function, evade immune control and ultimately cause immunodeficiency (Ugolini et al., 1997; Deng et al., 1996; Dragic et al., 1996; Feng et al., 1996). Binding of gp120 to the co-receptor induces further conformational changes that expose a fusion peptide within the transmembrane domain, gp41 (Chan et al., 1997; Gallaher et al., 1987; Veronese et al., 1989). Subsequent exposure of the gp41 fusion peptide enables the lipid membrane surrounding the viral capsid to fuse with the target cell membrane (Melikyan et al., 2000).

Upon membrane fusion, the viral capsid undergoes uncoating, which allows for the release of the viral RNA genome and associated viral proteins into the cytoplasm. Although the exact location and timing of uncoating require further characterization, the

process is likely to be regulated through modulation of capsid stability by both viral and host cellular factors (Aiken, 2006; Arhel, 2010). RT, released into the cytoplasm, then catalyzes the translation of viral RNA into proviral double-stranded DNA, followed by subsequent degradation of the viral RNA template (Charneau et al., 1992; Charneau et al., 1994). Reverse transcription may in fact occur within a semi-intact viral capsid in the cellular cytoplasm to protect the viral genome from recognition by cellular sensors (reviewed in Arhel, 2010). The pre-integration complex (PIC), which is a large nucleoprotein complex composed of both viral and cellular proteins, then forms and serves to facilitate the transport of the viral DNA into the nucleus. This complex utilizes microtubules and actin filaments to reach the nuclear pore complex, which gates the nucleus away from the cytoplasm, prior to nuclear entry (Arhel et al. 2006; Suspene et al., 2006; McDonald et al., 2002). The large size of the PIC necessitates active transport into the nucleus, and it is believed to involve the interplay between the viral MA, Vpr, and IN proteins, all released into the cytoplasm by the uncoating of the capsid, and a number of cellular factors such as nucleoporins and importin (Suzuki and Craigie, 2007). Once in the nucleus, IN cuts the host chromosome DNA and facilitates the insertion of the viral DNA into the host chromosomal DNA (Engelman, 1991). Once integration into the chromosome is complete, the viral DNA is now called a provirus and can serve as the template for new virion synthesis by utilizing the host cell machinery to complete the remaining stages of the viral cycle (Jegede et al., 2008). Alternatively, the provirus may become dormant by establishing latency, by which HIV-1 gained its retroviral classification. Latency is at least in part mediated by histone modifications and other epigenetic factors that restrict transcription (Bushman and Craigie, 1991; Hakre et al.,

2011). In fact, it is a pool of latently-infected cells within an individual, which mediates HIV-1 persistence in spite of HAART administration (Chun et al., 1997; Finzi et al., 1997; Wong et al., 1997).

Following integration, the HIV-1 provirus acts as a template for mRNA synthesis. The cellular RNA polymerase machinery is recruited to the provirus by promoter elements within the LTR to transcribe viral genes into a single mRNA transcript (Ott et al., 2011). The viral mRNA is then alternatively spliced to produce numerous variants, leading to the translation of different viral gene products (Stoltzfus and Madsen, 2006). The regulatory proteins Tat and Rev are among the first to be translated and exported to the cytoplasm. Once Tat accumulates to a sufficient level, viral transcription is actively up-regulated through its interaction with cellular transcription factors (Ott et al., 2011). Rev then mediates the export of unspliced and partially spliced viral RNAs from the nucleus into the cytoplasm to enable translation of other viral proteins and eventual packaging of viral genomic RNA into nascent virions (Pollard and Malim, 1998). In fact, it is the HIV-1 structural proteins Gag, Env, and Pol, that once translated facilitate virion assembly. Gag is specifically targeted to the plasma membrane where it multimerizes to drive membrane curvature formation, therein initiating the process of virion egression out from the cell surface (Ono et al., 2000). This is turn helps facilitate the packaging of the viral RNA within the budding virion (Clever et al., 1995). Cellular ESCRT machinery interacts with Gag p6 at the plasma membrane, enabling budding virions to pinch off and be released from the infected cell (von Schwedler et al., 2003). The Env glycoprotein is synthesized as a precursor, gp160, which is processed into its gp120 and gp41 subunits by host furin protease in the endoplasmic reticulum (Hallenberger et al., 1992). The

processed forms of Env interact to form trimers that are retained within cellular membranes by a transmembrane domain in gp41 (Liu et al., 2008). Incorporation of Env into virions is required for infectivity (Gheysen et al., 1989). Importantly, it is the Env trimers on the surface of infected cells that may interact with CD4 on neighboring cells to initiate recruitment of Gag and assembling virions to intercellular contact sites enriched for Env (Jolly et al., 2004). This mechanism has direct implications for HIV-1 spread.

Two models of HIV-1 cell-to-cell spread have been proposed, with the first model involving free-floating virions that largely by chance attach to and fuse with target cells. The second model on the other hand is thought to be far more efficient as it involves cell-to-cell contact (Sattentau, 2008). Specifically, the contact between an infected cell expressing Env and CD4 expressed by an uninfected cell leads to the formation of a structured called the virological synapse (Jolly et al., 2004). This is turn leads to actin cytoskeletal rearrangement in both cells, resulting in efficient virion assembly within the infected, producer cell and rapid entry of mature virions within the target cell (Del Portillo et al., 2011).

HIV-1 Transmission, Viremia, and Latency

HIV-1 is transmitted predominantly through sexual intercourse by contact of HIV-1-containing bodily fluids with the blood or mucosal tissue of another non-infected individual, as well as from mother to child during childbirth or breastfeeding (Bryson, 1996). Needle sharing between intravenous drug users however also contributes significantly to transmission (Chaisson et al., 1987). One of the first major challenges HIV-1presents is the difficulty involved with initially diagnosing the infection, as many

HIV-positive individuals are unaware of their infection status (Hall et al., 2012). Upon initial infection, many exhibit no significant symptoms, while others may exhibit transient flu-like symptoms such as fever, rash, or swollen lymph nodes, which quickly clear (Hecht et al., 2002). Thus it is easy to confuse the symptoms of HIV-1 infection with other less severe infections, thereby potentially increasing the likelihood of viral spread. During the early phases of acute infection, CD4+ T lymphocytes are rapidly depleted as a result of the quick spreading of the virus throughout the body and subsequent seeding of the thymus, bone marrow, and lymph nodes, with high titers in the bloodstream (Busch and Satten, 1997). Soon thereafter a strong immune response is elicited such that viral loads become substantially decreased, enabling a partial recovery of CD4+ T lymphocyte counts (Moss and Bacchetti, 1989) (Figure C). In fact, in certain HIV-1-infected individuals called long-term nonprogressors, the infection is indefinitely controlled in this manner, nor is treatment required to prevent further disease progression or transmission (Gea-Banacloche et al., 2000). Moreover, other individuals may carry a mutation in the CCR5 co-receptor, known as CCR5-Δ32, that effectively protects target cells from HIV-1 binding and entry (Huang et al., 1996). Most typically however, if left untreated HIV-1 ultimately evades the immune response and causes gradual, but constant depletion of CD4+ T cells with viremia continuing to be detectable in the bloodstream (Trono et al., 2010).

As HIV-1 establishes life-long persistent infection in most infected individuals, it is imperative that the virus is able to evade the immune response for the lifetime of the individual. One defining characteristic of HIV-1 is its extremely high genomic mutagenic rate. This is a consequence of the very error-prone nature of viral RT that facilitates DNA

transcription from viral RNA, leading to the accumulation of genetically diverse quasi-species (Goodenow et al., 1989; Hubner et al., 1992). Although such mutations often reduce the replication capacity of HIV-1, the vast diversity that is generated allows for a subset of HIV-1 clones to persist within the individual in spite of a mounted immune response by remaining CD4+ cells. Thus, this form of immune evasion contributes towards the gradual depletion of immune cells (Smythe, 2012). Even in infected individuals who respond to HAART very well, as defined by suppressed viral loads, the virus can quickly rebound if treatment is interrupted. This is attributable to the establishment of a latent reservoir (Chun et al., 2010), which is a pool of latently-infected cells that are still poorly defined, although resting memory CD4+ T lymphocytes are considered to comprise a substantial portion (Siliciano et al., 2003). In fact, effector memory and central memory cells have been shown to contribute to persistence through their reactivation upon cessation of HAART treatment (Buzon et al., 2014). Additionally, long-lived hematopoietic stem and precursor cells in the bone marrow may also contribute to long-term persistence (McNamara and Collins, 2011). It is also possible that low-level viral replication in cells and/or parts of the body with sub-optimal drug concentrations may contribute to persistence (Zhang et al., 1999). For instance, infected macrophages, in addition to supporting long-term latent infection (Watters et al., 2013), are able to cross the blood-brain barrier and contribute to HIV-1-associated neuropathological afflictions (Burdo et al., 2013). Therefore, many cell types and mechanisms potentially contribute to viral persistence and improved characterization of these pools of cells, as well as the understanding of such mechanisms, will facilitate improved treatment strategies.

Most relevant to the ultimate development of AIDS is the loss of CD4+ T lymphocytes as they are critical mediators of adaptive immunity; depletion of these cells below a functional threshold, defined as less than 200 CD4+ cells per cubic millimeter of blood (CDC, 1993), increases the susceptibility to an array of fatal opportunistic infections caused by microbes that are normally innocuous to individuals with intact immune systems, including commensal strains of bacteria, viruses and fungi. Thus infections such as *M. tuberculosis, C. albicans*, *P. jirovecii*, hepatitis C virus, and cytomegalovirus are a defining hallmark of the AIDS epidemic as it emerged in the 1980s (Chu et al., 2011, Pantaleo and Fauci, 1996). Although CD4+ T lymphocytes, the major target cell of HIV-1, are profoundly depleted by the infection, the virus continues to replicate even when very few T lymphocytes remain; macrophages and other target cell types are believed to contribute significantly to replication during this stage of infection (Orenstein et al., 1997). Despite the advent of antiretroviral drugs that prevent this late stage of HIV-1 disease, this immunodeficiency still affects many people in many parts of the world where treatment remains prohibitively expensive or is outright unavailable.

Antiretroviral Therapy

Rapid characterization of the nature of the virus and its viral life cycle allowed for therapeutic approval of early antiretroviral drugs soon after the virus was first clinically isolated (Fischi et al., 1987). In fact, the first HIV-inhibitor Zidovudine (AZT) saw clinical use in the United States in 1987, only a few years since the original identification of AIDS in the early 1980s (CDC, 1981). Since then more agents within the same class of nucleoside reverse transcriptase inhibitors (NRTIs), as well as a second class of drugs

called the non-nucleoside transcriptase inhibitors (NNRTIs), became available (Mocroft et al., 2003). This led to the development of dual therapy treatment in the early 1990s that unfortunately saw limited success due to rapid rise of drug-resistant strains of HIV-1 (Palella et al., 1998; McNabb et al., 2001). With the approval of protease inhibitors in the mid-1990s however, combination therapy utilizing all three drug types, called Highly Active Anti-Retroviral Therapy (HAART), has proven to be successful in inhibiting the development and reproduction of HIV-1, reducing CD4+ lymphocyte loss, decreasing viral load to undetectable levels, and eliminating wasting-related morbidity (Palella, 1998 et al., Wainberg et al., 1998). In fact HAART has become the standard treatment for HIV-positive patients and has resulted in a tremendous decline in HIV and AIDS-related mortality (Hecht et al., 1998; McNabb et al., 2001). Although this treatment is not curative, continuous, lifelong treatment with antiretroviral therapy has significantly improved life expectancy and turned HIV-1 from a terminal infection into a more chronic disease (Deeks et al. 2013). Despite the success of HAART, the risk of development of drug resistance that may lead to treatment failure is a significant risk of continued HAART administration (Boden et al., 1999). Additionally, incomplete adherence has been found to be a very common cause of virological failure (Paterson, 2000). Drug interactions leading to insufficient plasma and cellular levels of the medication are other causes of viral rebound. Unfortunately, all antiretroviral drugs can cause both short-term and long-term side effects that might lead to the discontinuation of HAART (Hugen, 2002). Chronic use of HAART can lead to significant health problems and complications, such as diabetes, cardiovascular disease, nausea, anorexia, gastrointestinal pain, hepatitis,

and nephritis, all of which compromise adherence likelihood and therefore undermine HAART efficacy (Day, 2003).

Since the introduction of HAART, further progress has been made in terms of development of new classes of drugs, such as entry inhibitors and integrase inhibitors (Hoxia and June, 2012) (Figure D). Their further development may thus contribute towards simpler regiments against multi-drug-resistant viruses (Low-Beer et al., 2000; Paterson, 2000). Nevertheless, strict adherence will remain of the utmost importance for the success of treatment, as the risk of transmission of resistant viruses will always remain a strong public health concern (Bangsberg et al., 2000; Dybul et al., 2001; Sierra-Aragon et al., 2012). Thus the further characterization of the viral lifecycle is paramount for the development of novel drug therapies whose prospects of failure are lower than that of HAART currently.

Host Protein-Viral Protein Interactions

As an obligate intracellular parasite, HIV-1 relies on its capacity to usurp the host cell machinery for successful completion of its life cycle (Sorin and Kalpana, 2006). Thus the virus may manipulate the numerous host cellular factors to facilitate efficient replication (Adamson et al., 2010). Some of these host factors however have evolved as antiretroviral restriction factors against HIV-1, and effectively function as the first line of defense against viral infection (Malim and Emerman, 2008; Malim and Bieniasz 2012). Extrapolated further, investigating the relationship between viral and host proteins may be a highly effective method for identifying novel therapeutic targets. In fact, targeting host protein activity by drug treatment, as opposed to pathogen protein

activity, has been shown to be an effective approach in the fight against infectious disease (Dorr et al., 2005; Kellam, 2006).

Following the discovery of the first restriction factor in the early 2000s (Sheehy, 2002), more than 30 different anti-HIV1 host restriction factors have been characterized thus far (Abdel-Mohsen et al., 2013). Some of the best-studied restriction factors include apolipoprotein B mRNA-editing, enzyme-catalytic, polypeptide-like 3G (APOBEC3G, or A3G) (Sheehy et al., 2002), Tetherin (also known as BST-2) (Neil et al., 2008), Tripartite motif-containing Motif 5 α (TRIM5α) (Stremlau et al., 2004), and Sterile Alpha Motif Histidine-Aspartic (HD) domain-containing protein 1 (SAMHD1) (Hrecka et al., 2011). Although restriction factors target different steps of the viral life cycle, universally they are all germline-encoded, IFN-inducible, and are expressed constitutively at low levels (Malim and Bieniasz, 2012). In spite of their expression however, the virus is able to effectively elude many of these host restriction factors by leveraging the functionality of the host's own methods of protein clearance by means of the viral accessory proteins.

Efficient and tightly-regulated destruction of proteins within the cell is critical for its normal functions and for maintenance of cell viability. The ubiquitin-proteasome system (UPS) is the major pathway by which the cell targets proteins for deliberate degradation. Thus the UPS serves to regulate protein expression and function through the conjugation of a highly structurally related class of ubiquitin-like proteins (Ravid and Hochstrasser, 2008). Ubiquitination is a post-translational protein modification that regulates protein degradation and trafficking, and thus may affect cellular protein dynamics (Ravid and Hochstrasser, 2008). The process involves ubiquitin, a highly conserved 76 amino acid protein (Ozkaynak et al., 1984), and its covalent conjugation to

other proteins via an E1 activating enzyme, an E2 conjugating enzyme, and an E3 ubiquitin ligase. Briefly, cellular E3 ubiquitin ligases facilitate the transfer of ubiquitin from E2 ubiquitin-conjugating enzymes to lysine, serine, or threonine residues on specific target proteins. E3 ligases are often comprised of multiprotein complexes that include a scaffold, an adaptor, and a target protein substrate (Ciechanover et al., 1982; Pickart and Vella, 1988; Haas and Bright, 1988; Pickart and Rose, 1985; Hershko et al., 1991; King et al., 1996). Importantly, in the context of HIV-1, the viral accessory proteins Vif, Vpr, and Vpu can all function as substrate adaptors that simultaneously bind with ubiquitin adaptors and cellular target proteins, inducing their ubiquitination and subsequent proteasomal degradation. Thus by being able to antagonize host restriction factors through the recruitment of targeted degradation machinery, the viral accessory proteins facilitate the successful completion of the viral lifecycle (Gramberg et al., 2009; Harris et al., 2012) (Figure E).

Viral and Host Factors That Utilize the Proteasome

The viral accessory protein Vif is a 24kDa protein that counteracts the antiviral activities of A3G (Sheehy et al., 2002, Malim, 2009). In the absence of Vif, A3G from virus-producing cells is packaged into budding HIV-1 virions and carries out its function in the subsequent round of infection. During the process of virally-mediated reverse transcription, A3G, released into the cytoplasm along with the RT complex, specifically targets minus-strand DNA and deaminates cytidine to uracil. Next, during plus-strand DNA synthesis, adenine is incorporated as the complementary base to uracil, resulting in guanine to adenine (G-to-A) hypermutation in viral plus-strand (Mangeat et al., 2003;

Malim, 2009). As a consequence, the proviral DNA would then encode for viral proteins with premature stop codons or mutated proteins that lose all functionality, effectively resulting in incomplete and nonviable virion formation (Yu et al., 2004). In order to promote the degradation of A3G, Vif recruits an E3 ubiquitin ligase complex, comprising of the Cullin5 (Cul5), Rbx2, as well as Elongins B (EloB) and C (EloC) proteins (Yu et al., 2003). Vif then binds to A3G and drives its ubiquitin-dependent degradation. Importantly, two motifs within Vif have been identified which are important facilitators of the Vif:A3G interplay: the $Y^{40}RHHY^{44}$ motif is essential for A3G binding (Russell et al., 2007), while the conserved motif $Y^{69}XXL^{72}$ has been reported to mediate A3G interaction (Pery et al., 2009). Vif is therefore capable of rescuing HIV-1 from A3G-mediated antiviral restriction, which otherwise would be catastrophic to the virus (Compton et al., 2012).

The viral accessory protein Vpr is a 14kDa pleiotropic lentiviral accessory protein that is conserved among all primate lentiviruses (Planelles et al., 1996; Stivahtis et al., 1997). In fact, Vpr mutations have been associated with long-term nonprogressors (Lum et al., 2003). Vpr was first studied within the cell division context. Specifically, the presence of Vpr caused dividing cells to stall in the G2/M phase of the cell cycle (He et al., 1995; Re et al., 1995). Vpr arrests cell division in both HIV-1 infected cell lines and primary T lymphocytes (Jowett et al., 1995). An early and preliminary model of Vpr function was that Vpr may enhance HIV-1 replication in T cells by arresting cell division in the stage at which HIV-1 replication is most efficient (Goh et al., 1998). Vpr however is not required for HIV-1 replication in these cells (Balliet et al., 1994; Planelles et al., 1995; Rogel et al., 1995). Moreover, cell cycle arrest was shown to require a cellular

factor called Vpr binding protein (VprBP), later named DCAF1 [damaged DNA binding protein 1-cullin 4-associated factor 1 (DCAF1)] (Hrecka et al., 2007; Le Rouzic et al., 2007; Wen et al., 2007). DCAF1 is a substrate adaptor of a cellular ubiquitin ligase complex Rbx1/Cullin4A E3. Thus, Vpr causes the polyubiquitination and proteasomal degradation of its binding partners. Recently, the degradation of the endonuclease complex component MUS81 has been shown to be required for Vpr mediated cell cycle arrest *in vitro* (Laguette et al., 2014). Other host proteins targeted by Vpr include the uracil glycosidases UNG2 and SMUG1 (Schrofelbauer et al., 2005), and the small RNA processing enzyme Dicer (Klockow et al., 2013), although the exact purpose of their targeting by Vpr remains unclear. Interestingly, the VprQ65R mutation has been shown to be deficient for DCAF1 binding (Le-Rouzic, 2008), effectively decoupling Vpr from the proteasomal machinery. Additionally, Vpr is packaged within virions via interaction with Gag p6, suggesting that Vpr acts early in the HIV-1 replication cycle (Paxton et al., 1993). Fittingly, Vpr was found to associate with the PIC and localizes to the nucleus (Heinzinger et al., 1994; Yao et al., 1995). This activity of Vpr remains poorly understood, however, as further studies demonstrated that nuclear import in non-dividing macrophages occurs efficiently even in the absence of Vpr, and that this function overlaps with the functions of IN and MA in promoting nuclear entry of the virus (Haffar et al., 2000).

Notably, Viral Protein X (Vpx), which is not encoded by HIV-1, but by HIV-2 and some viruses of the simian immunodeficiency virus (SIV) family, also interacts with DCAF1 to promote the degradation of a cellular nucleotide triphosphate phosphohydrolase [SAM domain and HD domain-containing protein 1 (SAMHD1)]

(Laguette et al., 2011). In the absence of Vpx, SAMHD1 inhibits reverse transcription by depleting the intracellular pool of dNTPs (Lahouassa et al., 2012).

Lastly, the Viral Protein U (Vpu) promotes viral release by counteracting the antiviral activities of the interferon-induced restriction factor bone marrow stromal antigen 2 (BST-2, or tetherin) (Neil et al., 2008; Van Damme et al., 2008). Vpu also down modulates the HIV-1 receptor CD4 (Harris et al., 2012). In the absence of Vpu, CD4 and BST-2 inhibit the release of infectious viral particles. CD4 binds virions through interactions with Env glycoproteins, and BST-2 tethers virions to the cellular membrane, preventing their release. Vpu therefore functions as an adaptor that promotes the interaction between BST-2 and the ubiquitin ligase substrate adaptor [beta transducing repeat-containing protein (β-TrCP), thereby inducing targeted proteasomal degradation (Harris et al., 2012; Margottin et al., 1998).

Bcl-2-associated athanogene 6 (BAT3, or BAG6), which became the focus of this study, is a universally expressed multi-domain cellular protein of 1132 residues. It was originally identified as a novel gene product encoded within the class III region of the human major histocompatibility complex (Banerji et al., 1990). Although BAG6 contains a nuclear localization sequence, it is in fact masked by a co-factor, which is why BAG6 primarily localizes within the cytoplasm. Moreover, BAG6 is also associated with the intracellular membrane system of the endoplasmic reticulum (ER), consistent with its involvement in ERAD (Wang, 2011). ERAD, or ER-associated protein degradation, is a process by which newly synthesized proteins, which fail to be targeted to the lumen of the ER for further modification or are unable to assume their native conformation, are processed for clearance (Smith et al., 2011) In fact, it is through the N-terminus, which

contains a ubiqutin-like domain, that BAG6 was revealed to associate with ubiquitin-mediated degradation of numerous defective substrates (Minami et al., 2010), while also being involved in the quality control of mislocalized or misfolded proteins (Hessa et al., 2011; Rodrigo-Brenni et al., 2014). It is theorized that these functions are linked to the "holdase" activity of BAG6 whereby certain aggregation-prone proteins may safely be transported between the nucleus and the cytoplasm to the appropriate cellular subcompartments for further processing (Reviewed by Lee and Ye, 2013). The C-terminus of BAG6 on the other hand contains a BAG domain, which is commonly found in a family of proteins that interact with the HSP70 chaperone family (Doong, 2002). Interestingly, HSP70 expression was found to be transiently increased upon HIV-1 infection (Wainberg et al. 1997), while its incorporation within the mature virion is presumed to contribute to structure maintenance (Ott , 2008).

Cannabinoids and HIV-1

Although several new classes of drugs have been developed and approved by the Federal and Drug Administration in recent years (Sierra-Aragon, 2012), currently one of the major limitations of all antiretroviral therapies is the need for strict compliance with regimens. Failure to do so is correlated with clinical and virologic failure (Paterson, 2000). The major cause of imperfect compliance among North American and European HIV+ patients is attributable to the wide range of side effects caused by most drug regimens, all of which compromise adherence likelihood and therefore undermine HAART efficacy (Day, 2003).

For treatment of HAART-associated anorexia, in 1992 the FDA approved dronabinol (Marinol), the synthetic form of the major psychoactive cannabinoid in marijuana, Δ^9-tetrahydrocannabinnol (THC) (Gorter, 1992). Dronabinol is prescribed to HIV+ patients for appetite stimulation and relief from nausea, diarrhea, and clinical depression, symptoms frequently reported for delayed or missed doses of HAART (Catz, 2002; Day, 2003, Abrams, 2007). In addition to THC, many more cannabinoid compounds exist. Marijuana itself contains over 60 cannabinoids (Elsohly, 2002). Cannabinoids can be broadly categorized into three different groups: (1) endogenous cannabinoids produced within the body such as anadamide or 2-arachidonoyl glycerol; (2) plant-derived phytocannabinoids such as THC and cannabidiol; and (3) synthetic cannabinoids such as WIN55,212-2 and CP55,940 (Elsohly, 2002). Two canonical cannabinoid receptors (CB) have been identified thus far: CB1 is expressed predominantly in the CNS (Westlake, 1994, Glass 1997); while CB2 is expressed primarily in immune cells and tissues (Galiegue, 1995). Both receptors belong to the seven-transmembrane, G protein-coupled receptor (GPCR) superfamily (Howlett, 1988). Depending on the specificities they exhibit for CB1 or CB2, in addition to their molecular properties, cannabinoids may initiate or abate downstream signaling cascades. Furthermore, so-called pancannabinoids exhibit high specificity for both receptors (Howlett, 2002).

Upon cannabinoid ligation to either the CB1 or CB2 receptor, the G_α subunit of the receptor-associated G protein leads to inhibition of adenylate cyclase activity, thereby preventing the accumulation of intracellular cAMP. This in turn prevents protein kinase A-mediated phosphorylation of AP-1, NF-κB and other transcription factors that

modulate expression of immune response genes (Kaminski, 1998; Klein, 2000, 2004). Furthermore, the $G_{\beta\gamma}$ subunit of the receptor-associated G protein regulates the p38 MAPK, p42/p44 MAPK, and JNK signaling pathways that lead to phosphorylation of cytoplasmic and nuclear proteins. These in turn modulate gene expression associated with synaptic plasticity, cell survival, and differentiation (Howlett, 2002; Demuth, 2006).

The effects of THC on HIV-positive patients are controversial, as conflicting results have been published as to the effects of cannabinoids on immunity. Numerous *in vitro* studies have reported that THC suppresses immune function. Cell proliferation, antibody production, NK cell activity, and cytokine production by macrophages were all found to be adversely affected by THC (reviewed in Klein, 2003; Cabral and Griffin-Thomas, 2009). Recent clinical studies however have reported that neither marijuana nor dronabinol have significant effects on viral load, percentages of circulating CD4+ or CD8+ T lymphocytes, NK cell number and function, PBMC proliferation status, or metabolism of antiretroviral drugs (Bredt, 2002; Adams, 2003). Additionally, an *in vivo* study using rhesus macaques challenged by simian immunodeficiency virus (SIV) reported that chronic THC administration was associated with decreased early morbidity, decreased viral load, and mass retention (Molina, 2010; Lecapitaine, 2011), all correlating with higher survival rates. The findings of these studies suggest that cannabinoids may mediate suppression of HIV-1 infection by an unknown mechanism.

The synthetic pancannabinoid WIN55,212-2 was initially shown to inhibit HIV-1 infection in human microglial cells and CD4+ lymphocytes in a concentration- and time-dependent manner (Peterson, 2004; Rock, 2007). Furthermore, the pancannabinoid CP55,940 and the CB2 agonist JWH-015 were also found to suppress viral expression

(Rock, 2007). Interestingly, the study reported that two CB1-selective antagonists, SR141716A and AM-251, also exerted inhibitory effects on HIV-1 infection. Thus both CB1 and CB2-mediated signaling cascades may play a role in viral inhibition. Moreover, in human microglial cells, WIN55,212-2 was found to downregulate expression of CCR5, the co-receptor utilized by HIV-1, suggesting a mechanism by which HIV-1 infection was attenuated by cannabinoid treatment (Rock, 2007).

Further studies have demonstrated that cannabinoids 'cross-talk' with the two HIV-1 co-receptors, CCR5 and CXCR4, which like the cannabinoid receptors also belong to the GPCR superfamily (Charo and Ransohoff, 2006). Administration of synthetic cannabinoids or THC *in vitro* inhibited the chemotaxis of several cell types biologically mediated by the natural ligands of CCR5 and CXCR4, CCL5 and CXCL12, respectively (Ghosh, 2006; Raborn, 2008). Yet another recent study reported that CB2 agonists decreased CXCR4-mediated p42/p44 MAPK phosphorylation (Constantino, 2012). This resulted in decreased F-actin levels and altered cytoskeletal architecture of resting CD4+ T lymphocytes, leading to significant modulation of HIV-1 infection.

Scope of Study

The conclusions of these studies therefore suggest that cannabinoids have a suppressive effect on HIV-1 infection. However, the mechanisms of cannabinoid effects on HIV-1 are not well defined. Moreover, the relationship between host cell pathways affected by cannabinoids and host cell pathways that interact with HIV-1 proteins is unclear. After all, viruses are obligate parasites that must hijack the cellular machinery to complete their life cycle. Increasing our knowledge of host factors that may be essential

or may modulate steps in the viral life cycle could therefore lead to a better understanding of the host-pathogen relationship and of prospective therapeutic targets (Goff, 2007). We thus hypothesized that signaling cascades downstream of activated cannabinoid receptors serve to reduce the severity of HIV-1 infection, and that by recapitulating the phenotypic effects of cannabinoids we could mimic their effect on the virus.

To assess this hypothesis, we studied the transcriptomic effects of cannabinoids as they pertain to HIV-1 replication. Importantly, the last couple of years have seen the advent of multiple genome-wide screens to identify candidate factors that may either impair or facilitate viral functions. With rising computational power and the development of next-generation sequencing technology, global siRNA-based approaches have greatly helped to facilitate host genome-wide investigations into HIV-1-dependency factors (Brass et al. 2008, König et al. 2008; Zhou et al. 2008). In fact, certain groups, such as R. Konig et al., have used additional criteria to validate their findings. Specifically, they had cross-referenced different databases, such as a yeast two-hybrid human protein-protein interaction database, to increase the stringency of the analysis of their prospective hits. Moreover, Zhou et al., on the other hand, applied criteria for druggable targets (Hopkins and Groom, 2002), narrowing their number of prospective candidates from 311 hits to 56 (Zhou et al. 2008). Importantly, the overlap between the two genome-scale siRNA screens (Brass, et al. vs. Zhou, et al.) for HIV-1 cofactors is greater than the amount of overlap that would be expected by chance (Zhou et al. 2008, Bushman, 2009), lending further validity to the paradigm of utilizing global studies for further characterization of HIV-1. In fact, this is an attractive direction for drug development, since antiviral medicines targeting host factors required for HIV-1 infection or replication may provide a

higher barrier to the development of resistance (Flexner et al., 2007). Importantly to our study, the NIH curates a database for a considerable number host factors within the NIH NIAID HIV-1 Human Protein Interaction Database (available for access at http://www.ncbi.nlm.nih.gov/RefSeq/HIVInteractions/). We thus sought to capitalize on recent technological breakthroughs, such as the implementation of next-generation transcriptome sequencing by means of RNA-Seq (Wang, 2009), to understand the effects of cannabinoids on HIV-1 replication and to characterize novel host cell factors, modulated by cannabinoids, which affect HIV-1 infection.

Figure 1. The structure of HIV-1. Above) Schematic of HIV-1 showing the envelope glycoproteins, as well as the structural and enzymatic proteins found within the virion (Adapted from Robinson, 2002). Below) Overview of the organization of the HIV-1 genome (adapted from Janeway's Immunobiology, 2008)

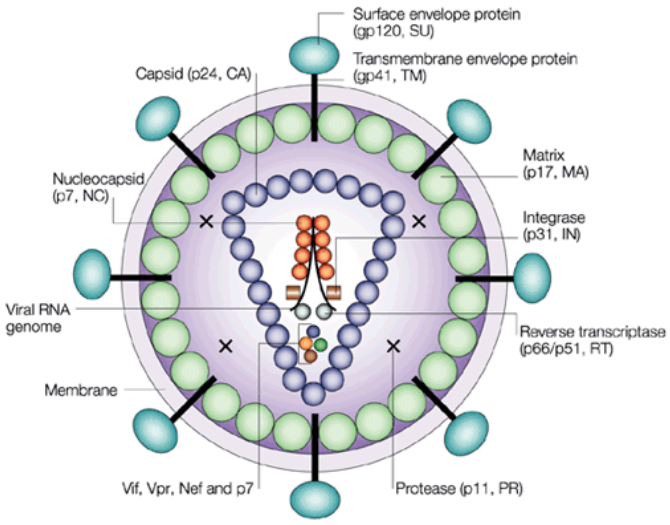

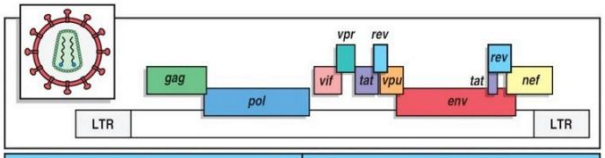

Gene		Gene product/function
gag	Group-specific antigen	Core proteins and matrix proteins
pol	Polymerase	Reverse transcriptase, protease, and integrase enzymes
env	Envelope	Transmembrane glycoproteins. gp120 binds CD4 and CCR5; gp41 is required for virus fusion and internalization
tat	Transactivator	Positive regulator of transcription
rev	Regulator of viral expression	Allows export of unspliced and partly spliced transcripts from nucleus
vif	Viral infectivity	Affects particle infectivity
vpr	Viral protein R	Transport of DNA to nucleus. Augments virion production. Cell cycle arrest
vpu	Viral protein U	Promotes intracellular degradation of CD4 and enhances release of virus from cell membrane
nef	Negative-regulation factor	Augments viral replication *in vivo* and *in vitro*. Decreases CD4, MHC class I and II expression

Figure 11-24 Immunobiology, 6/e. (© Garland Science 2005)

Figure 2. Replication cycle of HIV-1. Schematic overview of the different stages of the HIV-1 replication cycle. The HIV-1 virion, by means of gp120 and gp41, attaches to the cellular CD4+ receptor and the CCR5 or CXCR4 co-receptor. The virion fuses with the host cell and releases its contents into the cell. The viral particles are uncoated, the RNA genome is reverse transcribed and localized to the nucleus. In the nucleus the viral DNA will be integrated into the host genome. Upon activation the viral DNA will be expressed and translated to produce new viral particles, which will bud from the host cell and infect new cells (Pasternak et. al, 2013).

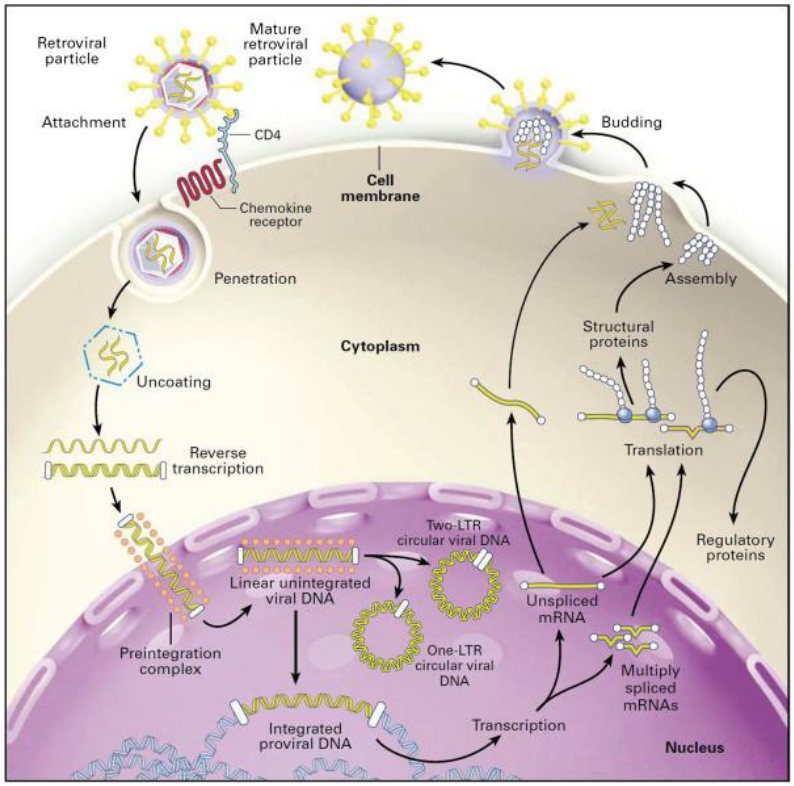

Figure 3. Progression of a typical HIV infection. After the initial acute phase characterized by a strong immune response and rapid virus replication comes the chronic phase when the virus can remain undetected for many years. AIDS is characterized by a high immune activation, low number of CD4+ T cells and high virus replication (Forsman and Weiss, 2008).

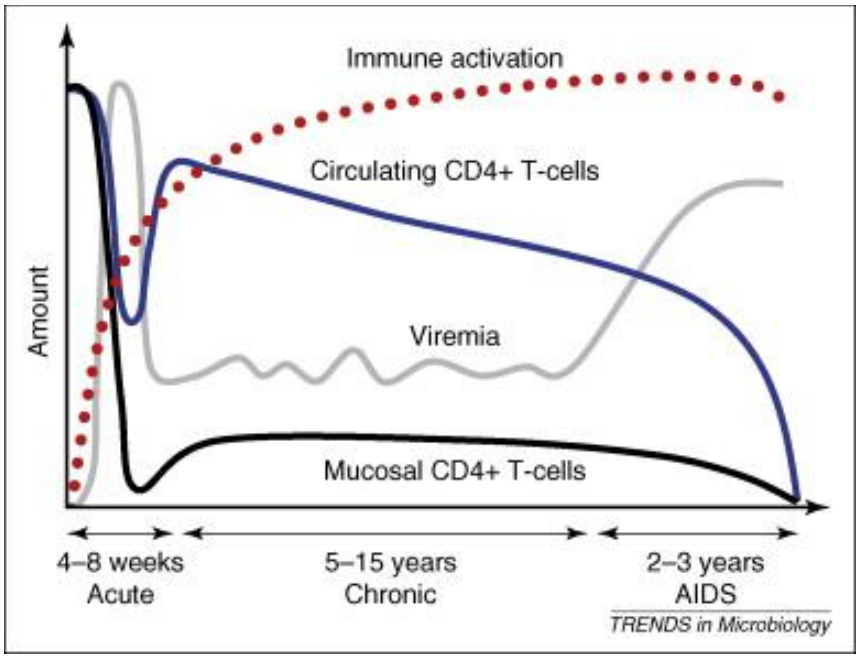

Figure 4. The HIV-1 life cycle and the antiretroviral drug class intervention points. Entry inhibitors interfere with viral entry into the host cell and are comprised of a complex group of drugs with multiple mechanisms of action. By inhibiting the processes of virion attachment, co-receptor binding and fusion, reverse transcription, proviral integration, or viral protease activity, virus spreading can be abrogated. (Adapted from Smith et al., 2012)

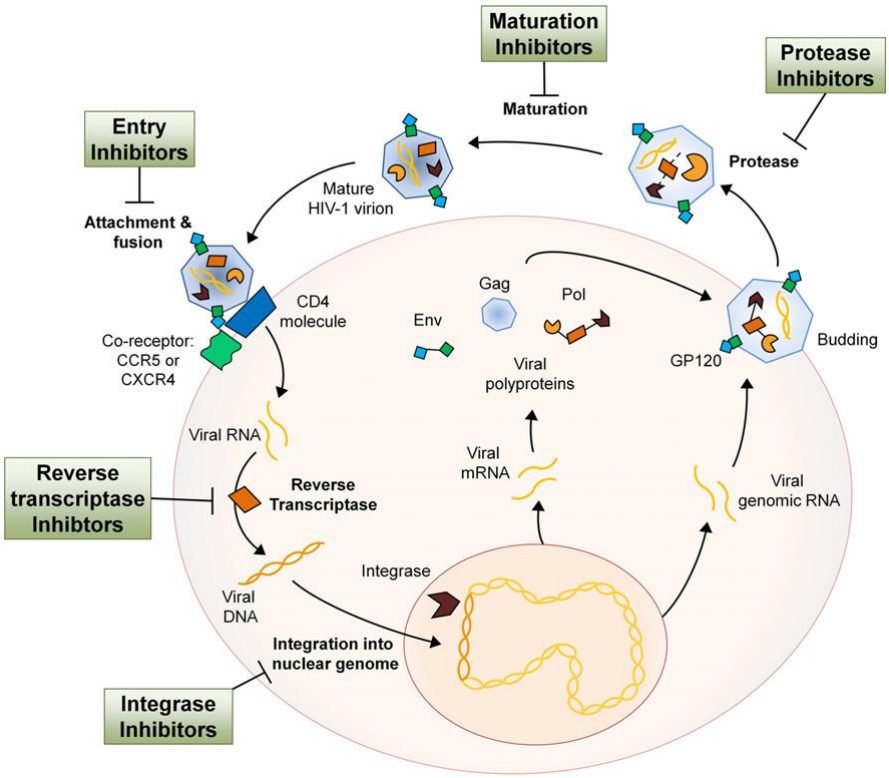

Figure 5. The HIV-1 accessory proteins usurp cellular ubiquitin ligase adapters. Graphical depiction of complexes formed between Vif, Vpu or Vpr and cellular proteins for targeted proteasomal degradation. (A) Vif, in complex with and stabilized by cellular CBF-β, binds to the EloBC/Rbx2/Cullin5 E3 ubiquitin ligase complex to target APOBEC3G (B) Vpu interacts with the Skp1/Cullin/F-Box (SCF) ubiquitin ligase complex via β-TrCP to target BST-2 or CD4 (C) Vpr interacts with the DCAF1/DDB1/Rbx1/Cullin4A E3 ubiquitin ligase complex to target UNG2.Collins, D.R. (2015). Vpr mediates immune evasion and HIV-1 spread (Doctoral dissertation). Retrived from https://deepblue.lib.umich.edu/bitstream/handle/2027.42/113293/davrcol_1.pdf?sequence=1&isAllowed=y

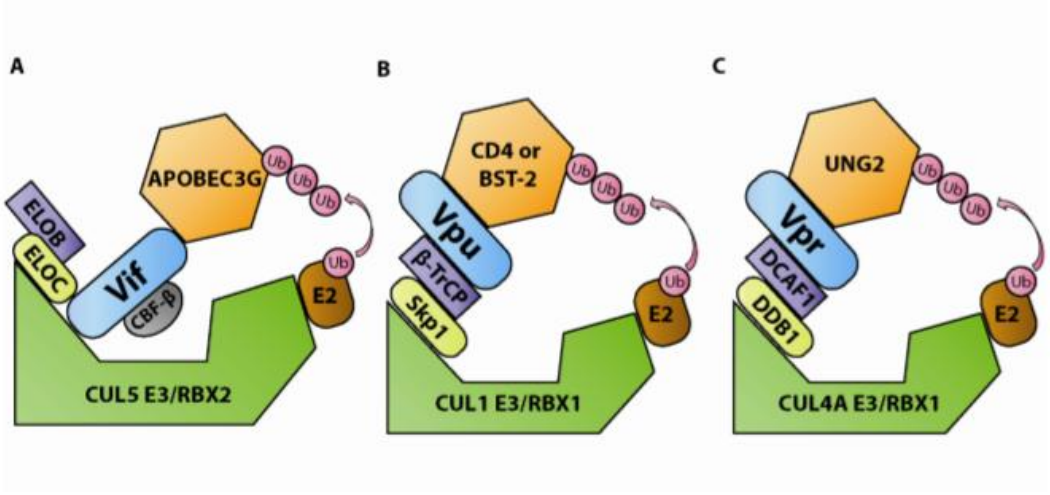

CHAPTER 2

MATERIALS AND METHODS

Cells

The following T-cell lines were obtained through the NIH AIDS Reagent Program, Division of AIDS, NIAID, NIH: Jurkat (E6-1) (Cat# 177, originally from Dr. Arthur Weiss), CEM-SS (Cat# 776, Dr. Peter L. Nara), PM-1 cells (Cat# 3038, Dr. Marvin Reitz), CEM (Cat# 117, Dr. J.P. Jacobs), and JLTRG reporter cells (Cat# 11587, Dr. Olaf Kutsch). Cells were all maintained in Roswell Park Memorial Institute (RPMI)-1640 medium supplemented with 10% fetal bovine serum (FBS) and at 37°C in a humidified 5% CO_2 incubator. All five T-cell lines express both the CD4 and CXCR4 receptors, necessary for successful infection by T-cell tropic virus, and so were utilized for all subsequent HIV-1 infection-based experiments and amplifications. TZM-bl cells were also obtained through the NIH AIDS Reagent Program (courtesy of Dr. John C. Kappes, Dr. Xiaoyun Wu and Tranzyme Inc) This is a modified HeLa reporter cell line that constitutively express the aforementioned HIV-1 co-receptors in addition to having integrated copies of the luciferase and ß-galactosidase genes under control of the HIV-1 promoter. These cells may therefore be used to determine viral infectivity (explained later below). Both TZM-bl and human embryonic kidney 293T/17 [HEK 293T/17] cells, which were obtained from ATCC (Cat# CRL-11268), were maintained in Dulbecco's Modified Eagle's Medium (DMEM) supplemented with 10% FBS and at 37°C in a humidified 5% CO_2 incubator. Due to high transfectability, 293T cells were utilized for

all transfection-based overexpression experiments, as well as for the generation of recombinant lentiviral particles.

Cannabinoids

The cannabinoids WIN55212-2 (Cat# 1038), CP 55,940 (Cat# 0949), L-759,656 (Cat# 2434), AM 251 (Cat# 1117), JWH 133 (Cat# 1343), and CB 65 (Cat# 2663) were obtained from Tocris Bioscience (Bristol, United Kingdom). SR 144528 (Cat# 9000491), SR 141716 (Cat# 9000484), JWH 015 (Cat# 10009018), AM 630 (Cat# 10006974), ACPA (Cat# 91053), and CB 13 (Cat# 10010398) were purchased from Cayman Chemical (Ann Arbor, MI). JWH-210 (CAS 824959-81-1), JWH-213 (CAS 824959-83-3), and Palmidrol (CAS 544-31-0) were obtained from the National Institute on Drug Abuse Drug Supply Program, Division of Neuroscience and Behavioral Research (Bethesda, MD). All cannabinoids were resuspended in DMSO to a 10^{-3}M concentration and aliquots were stored at -20°C.

Antibodies

The following antibodies were purchased: mouse anti-BAG6 (D-1) (Santa Cruz, sc-365928), mouse anti-GFP (B-2) (Santa Cruz, sc-9996), rabbit anti-GFP (FL) (Santa Cruz, sc-8334), mouse anti-β-actin (Sigma-Aldrich, Cat# A5316), rabbit anti-V5 (G-14-R) (Santa Cruz, sc-83849), mouse anti-V5 (Invitrogen, R960-25), mouse anti-FLAG (Sigma-Aldrich, F1804-200UG). HIV-1 Vif Monoclonal Antibody (#319) obtained through the NIH AIDS Reagent Program, Division of AIDS, NIAID, NIH: HIV-1 Vif Monoclonal Antibody (#319) from Dr. Michael H. Malim (Cat# 6459).

Plasmids

Plasmids were obtained from the Addgene plasmid repository: HSP70-GFP (from Lois Greene, plasmid# 15215), and psPAX2 (Didier Trono, plasmid# 12260), and pLKO.1 - TRC cloning vector (from David Roote, plasmid# 10878). pLX304-BAG6 was obtained from the DNASU Plasmid Repository (Drs. David E. Hill, David E. Root, Cat# HsCD00442162). Lastly, following plasmids were all obtained through the NIH AIDS Reagent Program, Division of AIDS, NIAID, NIH: pHEF-VSVG (Dr. Lung-Ji Chang, Cat# 4693), pNL4-3 (Dr. Malcolm Martin, Cat# 114), Apobec3G-V5 (Drs. B. Matija Peterlin and Yong-Hui Zheng, Cat# 10102), DCAF1-FLAG (Dr. Vicente Planelles, Cat# 11690), Vpr-GFP (Dr. Warner C. Greene, Cat# 11386), pcDNA-HVif (Dr. Stephan Bour and Dr. Klaus Strebel, Cat# 10077) , pNLdE-GFP (Drs. Haili Zhang, Yan Zhou, and Robert Siliciano, Cat# 11100), HIV-1 NL4-3 5´ Clone (p83-2) (Dr. Ronald Desrosiers, Cat# 2479), HIV-1 NL4-3 3´ Clone (p83-10) (Dr. Ronald Desrosiers, Cat# 2480), HIV-1 NL4-3 5´ Clone (p83-2) (Dr. Ronald Desrosiers, Cat# 2479), p197-1 (ΔVif) (Dr Ronald Desrosiers, Cat# 2481), and p210-19 (ΔVpr) (Dr Ronald Desrosiers, Cat# 2482).

Transfections

293T cells were seeded either at 4 x 10^5 cells/well in 6-well plates or at 2x10^6 cells in 10cm plates the day prior to transfection, which were performed utilizing 1mg/mL polyethylenimine (PEI) (cat# 23966, Polysciences, Inc., Warrington, PA). 500mg of PEI were first stirred into 450mL of water and concentrated 12M HCl was added drop-wise until the solution reached pH<2.0. Once the PEI was fully dissolved, 10M NaOH was then gradually added to restore the pH to 7.0, with the final volume of

the solution adjusted to 500mL. The PEI solution was then filter-sterilized through a 0.22um filter and aliquots were stored at -80°C. For 6-well plate based transfections, 0.4mL serum-free DMEM medium was added to 20uL of 1mg/mL PEI and mixed well. Plasmid DNA was then supplemented and the solution mixed again. After a 15 minute incubation at room temperature, additional 1.6mL DMEM was pipetted and the 2mL transfection mix was transferred to 293T cells aspirated of old media. After a further 6h incubation, transfection media was replaced by fresh DMEM and cells were collected 48h later. For 10cm plate based transfections, 2.4mL serum-free DMEM and 180uL of 1mg/mL PEI were used instead to account for increased cell number and plasmid DNA amount, with 9.6mL of DMEM added prior to pipetting the transfection mix onto the cells.

For proteasomal inhibition experiments, transfected cells were treated with 20uM of the proteasomal inhibitor MG-132 (Sigma Aldrich, Cat# M7499-1ML) at 32 hours post-transfection, with cells collected 16 hours post treatment.

Generating Knockdown Cells

RNA interference was utilized to generate stable BAG6 knockdown cell lines. MISSION® TRC-Hs 1.5 (Human) bacterial glycerol stocks containing a set of individual shRNA species targeting BAG6 (Cat# SHCLNG-NM_004639) were purchased from Sigma-Aldrich (St. Louis, MO), while a scrambled shRNA plasmid to serve as a non-knockdown control (pLKO) was originally from David Roote (Addgene plasmid# 10878) Each BAG6 shRNA glycerol stock was inoculated into LB medium cultures containing 100ug/mL ampicillin and incubated with shaking at 37°C overnight. Plasmid DNA

containing the individual shRNA sequences was extracted the next morning from bacterial cultures using the PureYield Plasmid Miniprep System by Promega (Madison, WI, Cat# A1223), and DNA concentration was measured by spectrophotometry utilizing the NanoDrop 1000 system (Thermo Scientific). To generate lentiviral stocks with which to transduce target T-cells, producer 293T cells maintained in 10cm plates were transfected with 10ug psPAX2, 7ug pVSVG, and 14ug BAG6 shRNA or pLKO plasmid DNA. Supernatants containing lentiviral particles were collected 48h later and spun down at 800g to remove cellular debris. Next, to generate stable BAG6 knockdown cell lines, Jurkat cells were transduced with the collected supernatants. Jurkat cells ($1x10^6$) were resuspended in 500uL RPMI-1640 medium and incubated with 250uL infectious supernatant for 24 hours, after which they were fed with 2mL of RPMI medium. Two days later, cells were washed and resuspended in RPMI medium containing 2.0ug/mL puromycin that served as a selection agent for successful transductants. Forty eight hours later, $1x10^6$ cells were collected and their BAG6 expression was assessed by immunoblotting with anti-BAG6 antibody and compared to the expression of BAG6 in pLKO controls, in which it remains at endogenous levels.

Puromycin Response

Puromycin was purchased from Sigma-Aldrich (cat# P8833). The powdered form was resuspended in water to a 50mg/mL concentration and stored at -20°C. Jurkat cells ($2x10^5$) were seeded in 24-well plates in 700uL RPMI and treated with increasing amounts of puromycin (0 - 4.0ug/mL). 72 hours post treatment, cells were collected and

flow cytometry was performed to assess cell viability on forward- and side-scatter gated live populations.

Immunoblotting and immunoprecipitation

Cells were washed with cold PBS, spun down, and homogenized for 5 minutes on ice in 100uL of lysis buffer consisting of 78.6uL RIPA Lysis and Extraction Buffer (Cat # 8900, Thermo Scientific) and 21.4uL of cOmplete Mini Protease Inhibitor Cocktail (Cat # 4693124001, Roche) wherein per manufacturer's instructions a single tablet was dissolved in 1.5mL of water. Lysates were then spun for 10 minutes at 14,000g and 4°C. 11.2uL of lysate was added to 0.8uL β-mercaptoethanol and 4.0uL 4x NuPAGE LDS Sample Buffer (Cat # NP0008, Thermo Scientific) and heated for 10 minutes at 70°C. Samples were briefly cooled on ice, spun down, and 14ul were loaded onto NuPAGE Novex 4-12% Bis-Tris Protein Gels (Cat # NP0323BOX, Thermo Scientific). Gel electrophoresis was performed with NuPAGE MOPS SDS Running Buffer (Cat # NP0001, Thermo Scientific) for 45 minutes at constant 200V. The gel containing separated proteins was first washed in water for 5 minutes and placed in Western Blot Transfer Buffer (Cat # 35045, Thermo Scientific) for 10 minutes. Filter papers were equilibrated in transfer buffer for 10 minutes as well. PVDF membranes (Novex) were washed in methanol for 20 seconds, rinsed with water, and placed in transfer buffer for 10 minute. Transfer was performed using the Fast Semi-Dry Blotter system (Cat # 88217, Thermo Scientific). Specifically, the gel was placed on top of the PVDF membrane flanked on top and bottom sides by dual layers of filter paper and the transfer was ran for 9 minutes at 25V. The PVDF membrane containing transferred proteins was then rinsed in water and blocked with 5% BSA in 1x TBS with 1% Tween-20 (TBS-T) for one hour

prior to immunoblotting with the appropriate antibodies, which themselves were suspended in TBS-T with 5% BSA.

To study protein-protein interactions, transfected 293T cells in 10cm plates were washed twice with cold PBS, spun down, and homogenized for 5 minutes on ice with 786uL of Co-IP lysis buffer (50mM Tris-HCl pH 7.4, 150mM NaCl, 1mM EDTA, 1% Triton X-100) supplemented with 214uL protease inhibitor cocktails, prepared as above. Lysates were then spun down at 4°C for 10 minutes at 10,000g. Magnetic beads (Dynabeads Protein G Immunoprecipitation Kit, Life Technologies) were pre-incubated with either 2.5ug rabbit anti-V5 or 4.0ug mouse anti-GFP antibodies for 15 minutes at room temperature under rotating conditions. Beads were washed once and added to 500uL of cell lysates and allowed to incubate at 4°C for 2 hours under rotating conditions. Beads were washed once and proteins were eluted with a mix of 21uL water, 7.5uL 4x NuPAGE LDS Sample Buffer, and 1.5uL β-mercaptoethanol at 70°C for 10 minutes. Samples (14uL) were loaded onto Novex gels and all western blotting steps were performed as above.

For protein detection, IRDye 800CW goat anti-mouse IgG (Li-COR, Cat# 926-32210) and IRDye 800CW goat anti-rabbit IgG (Li-COR, Cat# 926-32211) secondary antibodies were utilized when scanning membranes with the Li-Cor Odyssey 9120 system, per manufacturer's instructions.

Virus Generation

Wildtype NL4-3 HIV-1 used in the cannabinoid and knockdown experiments was generated by PEI transfection of a 6-well plate seeded with 293T cells with 1.2ug pNL4-

3 plasmid DNA per well. Forty eight hours post transfection, infectious supernatants were spun down for 5 minutes at 800g to remove cellular debris, and NL4-3 was quantified by p24 ELISA (Cat # 5421, ABL Inc., Rockville, MD). HIV-GFP was generated by transfecting 1.2ug pNL4-3-ΔEnv-eGFP and 0.2ug pHEF-VSVG DNA per well. HIV-GFP is a pseudotyped replication-deficient variant of NL4-3 that expresses the GFP marker. This variant is also deficient for the *env* gene and so does not express the viral envelope protein, which is why the VSVG envelope is provided *in trans*. More importantly, HIV-GFP virus cannot successfully complete the latter stages of the viral life cycle, as no progeny virions are able to be produced, making it useful for single cycle replication experiments. All viral aliquots were stored at -80°C and allowed to thaw on ice prior to use.

Viruses utilized in BAG6 knockdown infection experiments were generated as follows: 3ug each of the plasmids p83-2 (5' portion of NL4-3), p83-10 (3' portion of NL4-3), p197-1 (5' portion of NL4-3 containing the ΔVif mutation) and p210-19 (5' portion of NL4-3 containing the ΔVpr mutation) were first individually digested with 5 units of the restriction enzyme EcoRI overnight to generate linearized plasmids. The next day, the respective linearized 5' and 3' fragments were ligated together using the DNA Ligation Kit, Ver. 2.1, (Cat # 6022, Takara, Mountain View, CA) to reconstitute full-length NL4-3, NLΔVif, or NLΔVpr proviruses. 5ug of these proviruses were then used to transfect $2x10^6$ 293T cells in 10cm plates. Seventy-two hours later, supernatants were collected and used to infect $1x10^6$ JLTRG reporter cells seeded in a single well of a 6-well plate to amplify viral output. As these are modified Jurkat cell lines stably expressing HIV-LTR, which will therefore fluoresce upon infection, convenient

visualization of infection progression was possible. Using light microscopy, cells were monitored daily for viral cytopathicity, while fluorescent microscopy was used to observe the extent of viral replication. Four days later cells were transferred to T25 flasks to avoid overcrowding. Twelve days post infection, at both the peak of cytopathicity and fluorescence, supernatants were collected and viral production was quantified by p24 ELISA. Viral aliquots were stored at -80°C and allowed to thaw on ice prior to use.

Infectionss

Prior to investigating the effects of cannabinoids on HIV-1 challenge in detail, infection protocols yielding detectable levels of virus first needed to be established. Jurkat, CEM-SS, and PM-1 cells were seeded at a density of 2 x 10^5 cells/well in 24-well plates in 700uL RPMI and pretreated with DMSO vehicle or 10^{-6}M of the cannabinoids WIN55212, CP55940, SR141716, or SR144528 for 3 hours. Cells were then challenged with 2.0ng NL4-3, as quantified by p24 ELISA. Twenty four hours later cells were washed with PBS and resuspended in fresh RPMI media infused with cannabinoids or DMSO. Supernatants (300uL) were then collected every 2 days post infection, up to 12 days. Cells were replenished by the addition of 300uL fresh RPMI containing cannabinoids. Furthermore, cells were passaged in a 1:3 dilution on a per need basis to prevent overcrowding. Supernatants were stored at -80°C prior to viral quantification by TZM-bl assay, as described below. Infection of CEM cells was performed similarly as above. Cells were not however treated with cannabinoids prior to viral challenge.

Once the time of detectable viral production was determined, Jurkat, CEM-SS, and PM-1 cells were seeded at a density of 2 x 10^5 cells/well in 24-well plates, pretreated

with cannabinoids or DMSO vehicle for 3h at 10^{-6}M and subsequently challenged with 2.0ng of p24-quantified NL4-3. Cells were then washed 24 hours later and incubated for 6 days in the case of Jurkat and CEM-SS, and 4 days in the case of PM-1 cells. Cells were washed, pelleted, and processed for genomic DNA extraction and determination of infection by real-time qPCR. (below).

Similarly, for infections utilizing viruses generated by ligating 5' and 3' portions (NL, NLΔVif, NLΔVpr), Jurkat control and BAG6-knockdown cells were incubated with 2.0ng of each virus for 6 days prior to genomic DNA extraction.

As the infectivity of each batch of HIV-GFP is determined in large extent by the overall efficacy of the transfection by which the virus was generated, the volume to be used was previously determined by infecting $1x10^6$ Jurkat-pLKO cells with increasing amounts of HIV-GFP for 24 hours and measuring fluorescence as a proxy for viral potency. Too much volume added to cells may be deleterious to the overall cell health, possibly due to the carryover of the cytotoxic pVSVG plasmid or other cell debris released by virion egression of 293T cells, and so the overall effect of HIV-GFP on the number of still-viable cells was monitored as well. Thus the optimal amount of virus used resulted in the highest number of GFP+ cells with the least amount of cytotoxicity, as measured by gating for the live cell population via forward- and side-scatters.

Determining Peak Viral Production by TZM-bl Assay

TZM-bl cells were seeded in 96-well plates at 4000 cells/well in a total 100uL volume of DMEM. The next day, media was aspirated and cells were first given 100uL of 10ug/mL polybrene diluted in DMEM. 100uL of infectious supernatants were added to

cells. Cells were incubated for 48 hours, rinsed with PBS, and processed per the Galacto-Star System protocol (Applied Biosystems, Bedford, MA): cells were incubated for 12 minutes at RT with 50uL of Lysis Solution. 10uL of lysated extract was then transferred to white polystyrene flat bottom 96-well plates (Cat # 3922, Costar, Corning Inc., Corning, NY). 100uL of reaction buffer containing 2% Galacton-Star substrate in reaction buffer diluent was then added to each well. 20 minutes later, luminescence was measured using a FLUOstar Omega Microplate Reader (BMG Labtech, Ortenberg, Germany) and results analyzed to determine optimal infection termination endpoints.

Genomic DNA Extraction and qPCR

To accurately quantify the extent of infection, pelleted cells were washed and resuspended in 200uL PBS. Genomic DNA was then extracted via the QIAamp DNA Blood Mini Kit (Qiagen). Per the manufacturer's suggestion for increased final DNA concentration, a five minute incubation with 50uL of elution buffer was performed as the last step of the extraction procedure. Real-time quantitative PCR (qPCR) reactions were then performed utilizing 10uL of Fast SYBR Green Master Mix (Cat # 4385616, Applied Biosystems), 5.76uL water, 4uL sample, and 0.12uL each of forward and reverse primers, which had been resuspended in water to a stock 100uM concentration. Specifically, *gag*-specific primers were used to evaluate cannabinoid-induced changes in viral replication (forward: 5'- CTAGAACGATTCGCAGTTAATCCT; reverse: 5'- CTATCCTTTGATGCACACAATAGAG). Target gene amplification was normalized to the amplification of the reference housekeeping gene GapDH (forward: 5'- GGAAGGTGAAGGTCGGAGTC; reverse: 5'- GCTCAGTGTAGCCCAGGATG). The

reactions, done in duplicates, were performed per the manufacturer's suggested program using an Applied Biosystems StepOne Plus system. Results were quantified via the ΔΔCt method as compared to DMSO controls, which were set to 0% inhibition, to determine the effects of cannabinoid treatment on viral replication.

As the pLKO.1-puro vector backbone that contains the BAG6 shRNA species is lentiviral based and contains modest homology to the aforementioned HIV-1 *gag* sequences used as primer pairs, qPCR reactions using genomic DNA derived from shRNA-transduced cells could not be performed under identical conditions. New *gag* primers, which did not share homology between HIV-1 and the pLKO.1-puro vector were instead designed and utilized to measure BAG6-knockdown-induced changes in viral replication: forward: 5'-GTACATCAGGCCATATCACCTA; reverse: 5'-GCTTCCTCATTGATGGTCTCTT. For quantification using the ΔΔCt method, BAG6 knockdown-induced changes in infection were represented as a percent of infected pLKO control cells, which were set to 100%.

Flow Cytometry

Five hundred thousand 293T-pLKO or 293T-BAG6 knockdown cells per well were seeded in 24-well plates and challenged with varying amounts of HIV-GFP. Infected cells were washed 72 hours later in PBS twice and resuspended in 200uL fresh 1% paraformaldehyde. Using a BD FacsCANTO II cytometer, live cell populations were enumerated by means of gating via forward- and side-scatters at 5V and 450V, respectively. GFP+ cells, as a function of viral infection, were then detected by the FITC

channel and measured within the live gate, and results were analyzed using FlowJo software (TreeStar).

RNA-Seq Data Analysis

Next-generation RNA sequencing (RNA-Seq) was utilized to evaluate cannabinoid-induced transcriptomic changes in two T cell lines. $1x10^6$ Jurkat cells were treated with 10^{-6}M of the cannabinoids WIN55212, CP55940, JWH-210, or DMSO vehicle for 27 hours, while $1x10^6$ CEM-SS cells were treated with 10^{-6}M AM630, JWH-210, or DMSO vehicle for 27 hours. Cells were then pelleted at 800g for 5 minutes and total RNA was isolated via the RNeasy Mini Kit (Cat # 74104, Qiagen) per the manufacturer's instructions, with optional DNase treatment performed to ensure maximum purity. RNA quality control was then assessed using the Agilent 2100 Bioanalyzer system (Agilent Technologies, Santa Clara, CA) to ensure sample quality was compatible with next-generation sequencing platforms, as per submission guidelines. RNA was then stored at -80°C prior to being shipped out for RNA-Seq utilizing the Illumina HiSeq2500 platform. Services were provided by GeneWiz, Inc. (South Plainfield, NJ). Four weeks later RNASeq results were then returned to us on an external storage device and accessed using Lasergene Genomics Suite software (DNASTAR, Madison, WI). Over 22,000 transcripts were revealed to be modulated by each cannabinoid treatment, compared to DMSO treatment controls, for both Jurkat and CEM-SS cells. To negotiate these large data sets, lists of genes that are significantly upregulated or downregulated by each cannabinoid treatment were manually compiled and sorted. Next, to focus the investigation on those transcripts that are salient to HIV-1

infection, we capitalized on the knowledgebase of HIV-1-associated host genes that had been previously curated within the NIAID HIV-1-Human Protein Interaction Database (HHPID), as well as those genes identified in several genome-wide screenings for HIV-1 host cell factors (Ptak, 2009; Brass, 2008; Konig, 2008; Zhou, 2008, Fellay, 2007, Bushman, 2009). The HHPID is an annotated database which at the time of analysis contained ~1400 distinct HIV-1 viral protein - human protein interactions, while an additional ~ 900 genes had been identified among the multiple global studies. In total, over 2300 gene products via which cannabinoids may mediate the moderating effects on HIV-1 infection we observed were identified.

The transcriptomic data was then overlayed and cross-examined with the ~2300 virally-associated genes to specifically enrich for host factors that are functionally important within the HIV-1 infection context, which drastically reduced the total number of genes that needed further characterization. These genes were then processed using Qiagen's Ingenuity Pathway Analysis software (IPA, QIAGEN Redwood City, www.qiagen.com/ ingenuity) to generate highly scored, robust network maps. Finally, these networks were then subjected to further literature review to select for potential mediators of cannabinoid-induced HIV-1 suppression to be experimentally investigated in further detail.

Cycloheximide Assay

To assess the effects of viral challenge on endogenous BAG6 expression during the early phase of infection, cycloheximide, a *de novo* protein synthesis inhibitor, was utilized to counter rapid BAG6 protein turnover. Jurkat-pLKO cells ($1x10^6$), as they retain endogenous BAG6 protein, were seeded in 24-well plates in 1mL RPMI media and

pretreated with 75ug/mL cycloheximide or DMSO vehicle for 30 minutes prior to mock infection or challenge with an optimal amount of HIV-GFP. Cells were then collected at 0h, 2h, and 4h post-infection, pelleted at 800g for 5 minutes and stored at -80°C to ensure all samples are processed simultaneously. Longer incubations with cycloheximide were highly cytotoxic and were therefore not considered. The next day, cell lysates were generated and western blotting with anti-BAG6 antibody was performed.

CHAPTER 3

RESULTS

Determining the Effects of Cannabinoids on Viral Infection Among T Cells

To begin our study on the effects of cannabinoids on HIV-1 infection, we first needed to assess the viral infection kinetics among multiple T-cell lines. This would in turn allow us to determine both the sufficient amount of virus to be utilized and the optimal duration of all subsequent infection experiments involving cannabinoid compounds (Table 1). All viruses used in this study were derived from NL4-3, a very standard T-cell-tropic HIV-1 variant used in many laboratories. Briefly, NL4-3 virus was generated by transfecting 293T cells with the pNL4-3 provirus, and 48 hours later supernatants were collected and viral production was quantified by p24 ELISA, a standard method of measuring physical titer. Importantly. we determined by qPCR that the commonly available T-cell lines Jurkat, CEM-SS, and PM-1 all expressed CB2 more abundantly than CB1, as expected. Cells were then pretreated with the cannabinoids WIN55212, CP55940, SR141716, SR144528, or DMSO vehicle at a final concentration of 10^{-6}M for three hours prior to challenge with the amount of NL4-3 corresponding to 2.0ng of p24. Cells washed 24 hours later, and clarified supernatants were collected every 48 hours over a span of 12 days. The CEM cell line however was only pretreated with DMSO prior to infection. Since we expected the infection to progress very poorly in CEM cells due to the expression of the host restriction factor A3G (Sheehy et al., 2002), this cell line served as a negative control for the TZM-bl assay, which we utilized to assess the collected supernatants for infectivity (Figure 6). Specifically, the assay relies

on a modified HeLa cell line that not only expresses the HIV-1 co-receptors, but also contains integrated reporter genes for firefly luciferase and E. coli β-galactosidase under control of an HIV-1 LTR promoter. By measuring β-gal activity of these cells as a function of the amount of virus contained in collected supernatants from challenged T cells, we were able to accurately measure infection progression. It was determined that in Jurkat and CEM-SS cells, 6-day incubations with NL4-3 virus yielded detectable amounts of virus, while a 4-day incubation in PM-1 cells was sufficient. In the case of the CEM cell line however infection was very low even at 12 days post infection, confirming that the TZM-bl assay was functioning as expected. We therefore determined that the Jurkat, CEM-SS, and PM-1 cell lines are all capable of harboring robust infection at time points practically convenient for all future experiments, as these time points would not require cell passage to prevent extensive overcrowding, reducing the risk of viral removal. Notably, the TZM-bl assay was not sufficiently sensitive in resolving any changes in viral infection caused by cannabinoid treatment. In fact, several publications reported a roughly 50% reduction in infection (Peterson, 2004; Rock, 2007, Costantino, 2012), a difference which may certainly be below the ability of this assay to resolve. Having determined that the TZM-bl assay was inadequate for our attempts at characterizing potentially moderate effects of cannabinoids on HIV-1 infection, we proceeded to ascertain the effects of cannabinoids on the viral infection in T-cells through the application of a more sensitive assay.

As HIV-1 relies on integration into the host chromosome for successful completion of its viral life cycle, HIV-1 sequences unique to the viral genome can be leveraged by quantitative real-time PCR (qPCR) using targeted primers to accurately

determine the number of integrated viral copies among a virally-challenged cell population. Here, we generated primers specific to the HIV-1 *gag* sequence, encoding for the large Gag polyprotein. Although the HIV-1 sequence in general has a very high mutational rate, *gag* itself is relatively stable and amplifies readily without necessitating any special considerations. Analogously, total cell amount was normalized via the housekeeping gene *GapDH*. We then pretreated Jurkat, CEM-SS, and PM-1 cells with a panel cannabinoids or DMSO vehicle for 3 hours prior to challenge with the amount of NL4-3 corresponding to 2.0ng of p24.The panel largely consists of pancannabinoids that express affinities towards both CB1 and CB2 receptors, and of CB2 agonists, although CB2 antagonists as well as CB1-specific members were represented as well. At six, six, and four days post infection, respectively for Jurkat, CEM-SS, and PM-1 cells, genomic DNA was extracted and qPCR using SYBR Green dye was performed (Figure 7). In Jurkat cells, the cannabinoids WIN552122, CP55940, SR141716, JWH-210, AM251, and CB13 all significantly reduced viral replication by 2-fold. In CEM-SS cells, the cannabinoids JWH210, ACPA, AM251, JWH133, and AM630 all significantly reduced viral replication by 2-fold as well. In PM-1 cells however, cannabinoid treatment exerted no significant effects on viral challenge. Overall, treatment was therefore sufficient in decreasing HIV-1 infection in multiple T-cell lines, although these suppressive effects were found to be both cell-type and cannabinoid-specific, consistent with prior findings of the inhibitory properties of cannabinoids on viral challenge (Peterson, 2004; Rock, 2007, Costantino, 2012).

Cannabinoids and Cell Health

To verify that cannabinoids are not adversely affecting cells independently of infection, cell viability was next assessed. The effect of cannabinoid treatment on cell viability in the absence of viral challenge was determined using flow cytometry in two ways: by forward- and side-scatter gating for the live population, and by gating for 7-AAD dye exclusion. Briefly, 7-AAD, normally excluded by viable cells, is an intercalating DNA dye that permeates the nuclear membranes of nonviable cells, permitting the gating of live cells (Figure 8a). From these results, cannabinoids at a concentration of $1x10^{-6}$ M, which was utilized for all infection experiments, did not affect cell viability compared to DMSO alone. For verification of our results, a ten-fold increase in cannabinoid concentration however was found to be cytotoxic, corroborating previous reports that increased concentrations are lethal to cells (Peterson, 2004; Rock, 2007, Costantino, 2012). The observed changes in HIV-1 infection in Jurkat cells are therefore not a consequence of compromised cell health, but may in fact be attributed to some specific effects of cannabinoids that confer anti-viral properties.

Identifying Cannabinoid-Induced Gene Modulation

As it has been shown that cannabinoid treatment has pleiotropic effects on cell expression profiles (Kaminski, 1998), alterations in gene expression may explain our observed modulation in pretreated cells challenged with HIV-1. In other words, the consequence of cannabinoid treatment is that large numbers of genes are both up- and down-regulated, with the net effect being that the normal progression of the viral lifecycle is adversely affected. Thus to characterize the broad effects of cannabinoids on

viral infection, we next utilized a targeted transcriptomic analysis approach to identify molecular regulatory mechanisms through which suppressive effects on HIV-1 infection may be occurring. Thus total RNA from uninfected Jurkat and SEM-SS cells, treated with cannabinoids for 27 hours, was extracted and utilized as the input for RNA-Seq. We chose a 27-hour incubation because that was the amount of time cells were incubated with treatment prior to washing: a 3-hour pretreatment followed by a 24-hour challenge with the virus. RNA-Seq was specifically employed for transcriptome analysis because, unlike hybridization-based expression microarrays, this approach utilizes next-generation sequencing technology that can detect the expression of a much greater range of transcripts without *a priori* knowledge of the existing genomic sequence (Wang, 2009). Importantly, as RNA-Seq characterizes the global transcriptome (Wang, 2009), many of the genes we identified possessed minimal or uncertain relevancy to the HIV-1 context. Thus to specifically focus our investigation on the genes salient to HIV-1 infection, we capitalized on several knowledge bases: that of known HIV-1-associated genes published in a curated database that is publically available, as well as those of genes identified in several genome-wide screenings (Ptak, 2009; Brass, 2008; Konig, 2008; Zhou, 2008, Fellay, 2007, Bushman, 2009). Particularly, we utilized the NIAID HIV-1-Human Protein Interaction Database (HHPID), an annotated database containing roughly 1400 genes that have been shown to be important during HIV-1 infection (Ptak, 2009). An additional ~900 genes identified in several genome-wide screenings for HIV-1 host cell factors (Brass, 2008; Konig, 2008; Zhou, 2008, Fellay, 2007, Bushman, 2009) were included in our analysis as well. Among the 22,000 genes RNA-Seq results generated, we were able to specifically enrich for host factors that are functionally important within the

HIV-1 context.by generating highly scored, robust network maps using Ingenuity Pathway Analysis software based on gene ontology (Figure 9). By subjecting these networks members to further literature review, we were able to select for potential mediators of cannabinoid-induced HIV-1 suppression that would then be experimentally investigated in further detail (Table 2). Thus our transcriptomic workflow revealed 11 host factors, expressed in Jurkat and CEM-SS cells, that are not only modulated by cannabinoids, but implicated in HIV-1 infection.

Identifying BAG6 as a potential mediator of cannabinoid effects on HIV-1 infection

Among the factors identified by RNA-Seq, HLA-B associated transcript 3 (BAG6, also known as BAT3) emerged as our top candidate. BAG6 is a protein with diverse chaperoning functions, which is universally expressed in mammalian tissues (reviewed in Kawahara, 2012; Lee & Ye, 2013). Within the context of HIV-1 infection, the role of BAG6 was previously recognized by a global siRNA study. A HeLa-derived reporter cell line was silenced for BAG6 expression and then challenged with HIV-1, resulting in a 2-fold reduction in viral replication (Zhou, 2009). Notably, our sequencing data revealed that the pancannabinoids WIN55212, CP55940, and JWH210 reduced BAG6 RNA expression in Jurkat cells by at least 6-fold. Similarly, there was a 9-fold decrease in BAG6 expression in CEM-SS cells treated with AM630 (Figure 10), suggesting that the downregulation of BAG6 expression by cannabinoids may be responsible for the observed reduction in viral replication. As our targeted transcriptomic workflow was successful in identifying well-scored targets among host factors that are

both modulated by cannabinoids and critical for HIV-1 replication, we proceeded to characterize the role of BAG6 during HIV-1 infection, as no prior characterization of this was previously available.

Generating BAG6 Knockdown Cell Lines

To confirm if reduction in BAG6 expression, as shown by RNA-Seq, correlates with decreased infection due to cannabinoid treatment, we first needed to recapitulate the low-expressing BAG6 phenotype by ablating BAG6 protein expression. As T-cells are difficult to transfect with siRNA (Zhao, 2005), we alternatively utilized an shRNA approach by a lentiviral transduction system to generate stable Jurkat BAG6 knockdown cells. As multiple BAG6 shRNA species were available to us, with each one targeting a unique portion of the *BAG6* sequence (Table 3), we needed to assess each species for their capacity to abolish BAG6 expression. To accomplish this, we needed to generate lentiviral particles for each individual BAG6 shRNA species, in addition to a non-encoding sequence (pLKO) to control for non-specific and off-target effects. Particles were generated by transfecting 293T cells with three plasmids, and 48 hours post transfection supernatants containing particles were clarified and stored at -80°C. The plasmids utilized to this end were: pVSVG which provides a pleiotropic envelope; the psPAX2 packaging vector that provides structural proteins needed for assembly; and transfer plasmids containing either the individual BAG6 shRNA species or pLKO control. Importantly, each transfer plasmid contains a puromycin resistance gene to facilitate the selection of successful transductants (Figure 11). And so prior to the utilization of these generated lentiviral particles to generate BAG6 knockdown cell lines,

we first needed to assess the puromycin-dose dependency in Jurkat cells to determine the optimal antibiotic concentration to be used for cell selection (Figure 12). We determined that 2.0ug/mL of puromycin was sufficient in eliminating the vast majority of the cell population. While a very minute antibiotic-resistant population could be observed, our experimentally-determined concentration was in fact also recommended by the shRNA manufacturer for use in these cell lines, corroborating our supposition prior to proceeding towards transduction.

Cells were then transduced with 250uL, 1mL, or 2mL of lentiviral supernatant and three days-post transduction washed and incubated with fresh media containing 2.0ug/mL puromycin. Three days later a portion of cells was collected and cell viability assessed by flow cytometry to determine which volume of particles yielded highest transduction (Figure 13). In our case, 250uL generally resulted in the highest survival. Higher cyotoxicity at 1mL or 2mL volumes may be attributed to excessive plasmid carryover from transfections of 293T cells, or possibly due to an overwhelming number of particles adversely affecting the total cell population. In any case, 250uL-transduced cells were transferred to T25 flasks for expansion. Four days later transduced cells were then assessed for BAG6 protein expression by western blot. shRNA "species A" reduced BAG6 protein expression by 30-fold, normalized to β-actin expression, as compared to untranduced cells, which were set to 100% of BAG6 expression (Figure 14). pLKO control cells expressed BAG6 levels very similarly to untransduced cells, while the other shRNA species B, C, D, E, F, and G exhibited varying efficiency in ablating protein expression. Transduced cells appeared to resemble the parental cell line in terms of growth and expansion by visual inspection with light microscopy. Indeed, flow cytometry

revealed that BAG6 knockdown did not affect the proliferative capacity of these cells (Figure 15). We were therefore able to recapitulate a single, particular effect of cannabinoid treatment by successfully knocking down BAG6 in Jurkat and cells via shRNA, permitting the further characterization of the role of this protein during HIV-1 challenge.

Role of BAG6 During HIV-1 Challenge

To determine if targeted knockdown of BAG6 expression in Jurkat cells mimics the suppressive effects of cannabinoids, BAG6 knockdown and pLKO–control cells were challenged with 2.0ng of p24-quantified NL4-3 virus as before. Cells were washed 24 hours later and qPCR was performed on extracted gDNA at 6 days post infection. Compared to control cells, HIV-1 challenge of BAG6 knockdown cells resulted in a 2-fold decrease in infection (Figure 16), similarly to the effect of cannabinoid treatment on HIV-1 infection in the parental Jurkat cell line (see Figure 7). It should be noted that these infection experiments occur during a relatively long six-day incubation with the virus. In tandem with rapid viral replication turnover, there is sufficient time for multiple generations of progeny virus to form. In other words, virions from, at least, secondary or tertiary infection events may in fact be found within the supernatant. These emergent infection events may therefore constitute a larger contribution towards the overall infection state of the cell population beyond the parental virus introduced at day zero of the experiment. Thus the observed decrease in infection due to BAG6 knockdown may be explained in two ways: either there is an accrued effect of modestly decreased infectivity per viral generation; or alternatively the consequences of BAG6 knockdown may

manifest at a particular stage of the viral lifecycle, effectively bottlenecking each progeny generation at the same step within the replication cycle.

To further our understanding of BAG6, we generated HIV-GFP, a GFP-expressing pseudotyped replication-deficient variant of NL4-3, by transfecting 293T cells with the pNLΔEnv-GFP and pVSVG plasmids. HIV-GFP is deficient for the *env* gene and so does not express the viral envelope protein, which is why the VSVG envelope is provided *in trans*. More importantly, HIV-GFP virus cannot successfully complete the latter stages of the viral life cycle due to the absence of viral Env protein, as no progeny virions are able to be produced. By utilizing HIV-GFP, we effectively remove the contribution of newly-generated virus as a function of long incubation times and are able to better isolate those stages of the viral lifecycle preceding involvement of progeny virions. We thus challenged knockdown and control cells with varying volumes of HIV-GFP, and at 48 hours post-infection detected GFP intensity within the gated live cell population by flow cytometry (Figure 16). Again, we observed a ~2-fold reduction in infection, suggesting that BAG6 deficiency is indeed a rate-limiting event that equally affects both replication-competent and -deficient virus. Thus the knockdown of BAG6 in cells challenged with NL4-3 or HIV-GFP was sufficient in recapitulating the protective effects of cannabinoid treatment on HIV-1 infection. We were thus successful in characterizing BAG6 as a host factor, modulated by cannabinoids, that serves an important role during viral challenge. Notably, by observing a similar rate of decrease in infection when using either replication-competent or -deficient virus, we also conclude that the knockdown of BAG6 has an effect on the early stages of the viral cycle.

The Interplay between BAG6 and the Viral Accessory Protein Vif

The completion of the HIV-1 lifecycle is intimately coupled to the host cell machinery (Lever et al., 2011). Accessory viral proteins, oftentimes found within incoming virions, are key facilitators of the usurpation of host factors to the benefit of the virus, especially during the early stages of infection prior to integration and subsequent translation of viral proteins (Malim et al., 2008). We were thus interested in the interplay between viral accessory proteins and BAG6 as they pertained to BAG6-knockdown-mediated suppression of infection, for we suspected BAG6 plays an important role during the early phases of the viral cycle. A recent finding utilizing a purification mass-spectrometry approach (Jäger et al., 2011) revealed BAG6 to be a binding partner to the viral accessory protein Vif. This 24-kDa protein has been well characterized within the context of its role in degrading the host restriction factor APOBEC3-G (A3G) (reviewed in Feng et al., 2014). Beyond this global study, the relationship between Vif and BAG6 remains uncharacterized. To first validate this putative interaction, we performed co-immunoprecipitation experiments by overexpressing FLAG-tagged Vif and V5-tagged BAG6 proteins in 293T cells. We did not investigate endogenous BAG6 because we were unable to validate any of the α-BAG6 antibodies in our possession for the purpose of co-immunoprecipitation. 293T cells were transfected with 6ug pLX304-BAG6 and with 6ug Vif-FLAG. As confirmation that our co-immunoprecipitation experiments are functional, we also transfected 6ug A3G-V5 with 6ug Vif-FLAG, with the expectation that these two proteins bind, as is known from the literature. Forty-eight hours later cells were lysed in a low-stringent Triton X-100 buffer supplemented with protease inhibitors. Lysates were allowed to incubate with beads conjugated to 2.5ug rabbit α-V5 antibody for 1 hour at

4°C. Antigen-antibody-bead complexes were washed and eluted in LDS gel loading buffer, fractionated by SDS-PAGE, transferred to a PVDF membrane, and probed with mouse α-V5 and mouse α-FLAG antibodies (Figure 17). Comparing lane 6 to lane 4, there is an increase in Vif expression in the presence of A3G as compared to Vif alone, verifying that our experiment is working properly, with Vif demonstrating its ability to degrade A3G efficiently (lanes 6 vs. 3). Importantly, Vif also shows a 2-fold increase in the presence of BAG6 when compared to Vif alone (lane 5 vs. 4), confirming the finding that BAG6 is a novel binding partner to Vif.

We were next interested in discovering the amino acid sequences responsible for this interaction between BAG6 and Vif. Previously, two sequences within Vif, namely $Y^{40}HRRY^{44}$ and $Y^{68}XXL^{72}$, were identified as A3G binding regions (Russel et al., 2007; Pery et al., 2009). By targeted alanine-mutagenesis of these regions, it was determined that Vif-mediated A3G interaction was abrogated. To determine if these two Vif sequences are also responsible for BAG6 binding, by utilizing the same alanine mutagenesis approach, we also reconstituted these two individual mutations: $^{69}YXXL^{72}$>4A and $^{40}YRRHY^{44}$>5A, whereby residues were mutated into four and five alanines, respectively. Furthermore, we also referred to a partial Vif 3D model based on X-ray crystallography (Guo et al., 2014), whereby we could visualize the YXXL and YHRRY sequences. As both appeared proximal to one another (Figure 18a) within a single groove, we generated additional mutant proteins by alanine-scanning mutagenesis to determine if any alterations to the structure of this groove would affect BAG6 binding: $K^{22}RLVK^{26}$>5A, $V^{10}WQVD^{14}$>5A, and $I^{57}PLGD^{61}$>5A, referred to as Mutant 1, Mut. 2, and Mut. 3, respectively. (Figure 18b).

By co-immunoprecipitation of overexpressed BAG6 and mutated Vif proteins, we discovered that Mut. 2, Mut.3, and $Y^{69}XXL^{72}$>4A led to a 3-fold decrease in binding of BAG6 compared to wild-type. Mut. 1 led to a 3-fold increase, while the $Y^{40}RRHY^{44}$>5A mutant was similar to wild-type Vif (Figure 19). Throughout these experiments however, we could not detect any changes in BAG6 expression in the presence of Vif, and so we then slightly shifted our focus to the role of A3G. Although Jurkat cells do not express A3G (Figure 20) and are thus commonly referred to as "permissive cells" to contrast them with those that do express A3G, such as CEM cells, we were compelled to examine whether or not BAG6 interacts with A3G. Overexpression with 6ug pLX304-BAG6 and 6ug A3G-HA revealed an unexpected 3-fold increase in A3G expression in the presence of BAG6 as compared to A3G alone (Figure 21, lane 3 vs 2). As Vif was first characterized in the context of its targeted degradation of A3G, we investigated if BAG6 could protect A3G from Vif-mediated proteolysis. From our results however, BAG6 overexpression was not able to rescue A3G from wildtype or mutant Vif-mediated degradation (Figure 22). Taken together it is conceivable that the Vif:BAG6 complex has a function during HIV-1 infection that we simply cannot appreciate via the experiments we had conducted.

These findings were corroborated by challenge of BAG6-knockdown and control cells with 2.0ng NL5097m, an NL4-3 derived virus with a point mutation at the 5097 nucleotide residue that terminates Vif translation (previously generated in the lab by N. Ristic). Cells were washed 24 hours later, and by qPCR on extracted gDNA 6-days post infection a 2-fold decrease was revealed, which was similar to that previously seen with wild-type virus (Figure 23), thereby downplaying the importance of Vif for the infection

of HIV-1 in these cells. These results however do not exclude the possibility that the importance of the BAG6:Vif interaction becomes apparent during challenge of cells that do express A3G, as both Vif and BAG6 act as binding partners to A3G. With Jurkat cells not expressing A3G, they may not represent the optimal model for the further investigation of Vif within the context of BAG6.

Infection of BAG6 Knockdown Cells with Vpr-deficient Virus

In recent years, several findings have investigated the interplay between Vif and Vpr, another small (14-kDa) viral accessory protein (Wang, et al., 2008; Wang et al., 2011; Zhou et al., 2015). As certain overlap in their functionalities, including the capacity to degrade A3G, had been reported, we examined the effect of Vpr on the infective capacity of the virus in BAG6 knockdown cells.

Unlike the case with the NL5097m virus that is deficient in Vif expression, we did not have in our possession virus that is lacking in Vpr. Instead we used a complementary dual proviral approach to generate NLΔVpr. In parallel, we generated both wildtype NL and NLΔVif viruses using this same approach to serve as controls to corroborate our previous infection results with NL4-3 and NL5097m, respectively. The following plasmids were first obtained from the NIH AIDS Reagent Program: p83-2 (5’ portion of NL4-3), p83-10 (3’ portion of NL4-3), p197-1 (5’ portion of NL4-3 containing the ΔVif mutation) and p210-19 (5’ portion of NL4-3 containing the ΔVpr mutation). Importantly, each of these plasmids includes a single EcoRI sequence, which is critical because it allows for an EcoRI-digested 5' portion to be ligated with an EcoRI-digested 3' portion to reconstitute a full-length provirus. Thus 3ug of each of the appropriate 5’ and

3’ plasmids were digested with EcoRI and ligated to generate NL, NLΔVif, and NLΔVpr proviruses (Figure 24). These were then used to transfect 293T cells. Due to the relatively large size of these plasmids, in addition to potentially poor ligation, we anticipated transfection efficiency to be low. For that reason, seventy-two hours later supernatants were collected and used to infect $1x10^6$ JLTRG reporter cells for the purpose of amplifying the viruses. As these are modified Jurkat cell lines stably expressing HIV-LTR and therefore fluoresce upon infection ((Ochsenbauer-Jambor et al., 2006)), convenient visualization of infection progression was possible. By light microscopy, cells were monitored daily for viral cytopathicity, while fluorescent microscopy was used to observe the extent of viral replication as a function of GFP expression. Four days later cells were transferred to T25 flasks to avoid overcrowding. Twelve days post infection, at the peak of both cytopathicity and fluorescence, supernatants were collected and viral production was quantified by p24 ELISA.

We then challenged BAG6 knockdown and control cells with 2.0ng of p24-quantified NL, NLdVif, and NLdVpr. As expected, we again observed a 2-fold decrease in infection upon NL or NLΔVif challenge in BAG6 knockdown cells (Figure 25), as seen before in experiments utilizing NL4-3 and NL5097m (see Figure 23). Very surprisingly however, NLΔVpr showed a 4-fold decrease in infection as compared to infected control cells. These results thus indicate that Vpr, and not Vif, is likely to be the viral accessory protein that assumes a physiological role during the infection of BAG6-deficient Jurkat cells. Therefore, we next assessed the interplay between these two proteins.

The Protein:Protein Interplay between BAG6 and Vpr

Analogously to Vif, Vpr too mediates the proteasomal degradation of A3G, along with other host proteins, such as UNG2 and SMUG1, through the recruitment of a cellular E3 ubiquitin ligase complex (Zhou et al., 2015, Schrofelbauer et al., 2005; Wen et al., 2012) and through the subsequent use of the host cell's ubiquitin machinery. Moreover, prior findings have shown that BAG6 possesses chaperoning functions by acting upstream of numerous ubiquitin ligases (reviewed in Kawahara et al., 2012; Lee & Ye, 2013) and is often required for substrate ubiquitination. Taken together with our data that BAG6 forms a complex with A3G (Figure 21), we asked if BAG6 assumes a role in the Vpr-mediated degradation of A3G. With overexpression of Vpr-GFP, A3G-V5, and pLX304-BAG6, we confirmed that Vpr is sufficient in degrading A3G efficiently (Figure 26, compare lanes 5 vs. 3). Moreover, Vpr-mediated A3G degradation was not modified in the presence of BAG6 (lanes 6 vs 4). More importantly however, BAG6 expression was significantly reduced in the presence of Vpr (lane 6 vs. 3 and 4), which represents a hitherto novel, never previously reported function of this viral accessory protein.

To confirm if Vpr and BAG6 form a complex, which may be essential for this degradation, we overexpressed 6ug Vpr-GFP and 4ug BAG6-V5 and performed co-immunoprecipitation with 2.5ug rabbit α-V5 as described earlier. Immunoblotting was performed with mouse α-V5 and mouse α-GFP antibodies (Figure 27). Although the expression of BAG6 was lower in cells expressing BAG6+Vpr (lane 3) compared to those expressing BAG6 alone (lane 2) due to Vpr-mediated degradation, importantly our results showed that Vpr expression is increased ~6-fold in the presence of BAG6 (compare lanes 1 and 3). Vpr was thus revealed to be a novel binding partner of BAG6.

BAG6 Degradation via Vpr-mediated Protealysis

We next investigated if Vpr leverages the proteasome for targeted BAG6 degradation. The targeted proteasomal degradation of A3G by Vpr was previously identified (Zhou et al., 2015) through overexpression experiments utilizing the VprQ65R mutant, a Vpr variant that is unable to bind to the host adapter protein DCAF1 (Le Rouzic et al., 2007), previously known in the literature as Vpr-Binding Protein (VprBP) (Zhao et al., 1994; Zhang et al., 2001). DCAF1 is the substrate-binding subunit of the CRL4 ubiquitin ligase complex and functions through diverse mechanisms that include ubiquitination and phosphorylation (Guo et al., 2015). The proposed model for Vpr-mediated degradation consists of Vpr binding to the CRL4-DCAF1 complex through DCAF1 for the purpose of recruiting a target to the E3 ligase. This target is then subsequently ubiquitinated and degraded (Le Rouzic et al., 2007). Thus Vpr effectively ferries a target protein towards DCAF1 for proteolysis. However, by disrupting the interaction between Vpr and DCAF1, such as through the utilization of the DCAF-1-binding-deficient variant Vpr65R, there is effectively an uncoupling of Vpr from the cullin 4 E3 ubiquitin ligase complex, thereby reversing targeted Vpr-mediated proteolysis (Zhao et al., 2011, Romani & Cohen, 2012; Zhou et al., 2015). And so to assess if Vpr utilizes the proteasome for BAG6 degradation, we performed overexpression experiments utilizing 1.5ug pLX304-BAG6 (all lanes), 0.1ug DCAF1-FLAG (lane 2, 5, 6), 1.0ug Vpr-GFP (lanes 3 and 5), and 6ug VprQ65R-GFP (lanes 4 and 6). We determined that in contrast to the low BAG6 expression observed in the presence of wild-type Vpr, BAG6 expression in the presence of VprQ65R did not significantly differ from BAG6 alone (Figure 28a). Additionally, we found that the extent of Vpr-induced degradation of BAG6

was enhanced in the presence of DCAF1 (Figure 28b). The fact that expression of DCAF1 alone was sufficient in degrading BAG6 corroborates the proposed model that DCAF1 acts as an upstream adapter, linked to the proteasome, which Vpr utilizes for specific degradation of its targets. Conversely, we examined the role of the proteasome during BAG6 degradation more directly by utilizing the protease inhibitor MG-132 (Figure 29). Here, we wanted determine if MG-132 treatment, effectively halting the proteasomal pathway, could reverse the degradation of BAG6 in the presence of Vpr. We overexpressed 293T cells with 1.5ug pLX304-BAG6 (lanes 1-4), 1.0ug Vpr-GFP (lane 2 and lane 4, which was treated with 25μM MG-132 16h prior to harvesting), and 6ug VprQ65R-GFP (lane 3). Here again, BAG6 expression was diminished in the presence of Vpr, but not VprQ65R. Looking at lane 4 however, which was treated with MG-132, BAG6 was rescued from Vpr-mediated degradation to a level similar to that seen with the VprQ65R mutant (lane 3). Thus if Vpr cannot leverage the proteasome, and if BAG6 cannot be marked for subsequent degradation, our results then indicate that Vpr engages the host ubiquitin machinery to promote degradation of BAG6.

As we had observed that DCAF1 expression alone was able to induce BAG6 degradation, we were then prompted to investigate if the two proteins acted as binding partners. We thus overexpressed pLX304-BAG6 (4ug in lanes 1 and 3) and DCAF1-FLAG (6ug in lanes 2 and 3) and performed co-immunoprecipitation as before (Figure 30). In spite of extensive degradation of BAG6 in the presence of DCAF1 (compare lanes 1 and 2), there was a noticeable increase in DCAF1 binding in the presence of BAG6 (lanes 1 vs. 3). Thus we were able to confirm that BAG6 co-precipitates with DCAF1. Taken together, our data suggest that DCAF1 may normally be a putative regulator of

BAG6 expression, as DCAF1 alone is sufficient inducing BAG6 degradation. Thus upon infection, Vpr usurps DCAF1 for the targeted degradation of BAG6, a paradigm that has been shown to be the case for Vpr-mediated degradation of UNG2 and ZIP (Wen et al., 2012; Maudet et al., 2013).

Characterizing the Regions of BAG6 Important for its Degradation

We next sought to characterize the regions within BAG6 essential for interaction with either Vpr or DCAF1. To that end we systematically generated multiple truncated BAG6 proteins by subcloning the *BAG6* sequence, utilizing mutagenic primers, to first roughly map areas of BAG6 that may be critical for binding. We were thus able to generate the ΔN, ΔC, ΔUBL and ΔBAG mutants. Notably, the last two mutant constructs are missing the UBL or BAG regions, which are the two known domains located on either the N- or C-terminus, respectively (Figure 31a). Presence of the UBL domain within BAG6 implies a role in protein turnover by the ubiquitin–proteasome system (Binici and Koch, 2014). The BAG region however has been studied largely within the context of HSP70 binding of other members of the BAG-family of proteins (Reviewed by Kawahara, 2012) When assessing the expression of the ΔN, ΔC, ΔUBL and ΔBAG mutants, we could not detect ΔN (Figure 31b). This could be due to extensive alterations in protein folding leading to instability and rapid clearance of the misfolded protein. ΔC and ΔUBL were expressed similarly to wildtype BAG6, while ΔBAG had decreased expression, again possibly due to the adverse effect of this deletion on protein stability. We then overexpressed normalized amounts of wildtype BAG6, ΔUBL, ΔBAG, and ΔC in tandem with Vpr-GFP to determine if the introduced truncations affected BAG6

degradation. Results revealed that although ΔBAG was degraded similarly to wild-type BAG6, the ΔUBL mutant was resistant to Vpr-mediated degradation (Figure 31c). Next, to determine if the missing UBL domain is a potential binding site for BAG6 with Vpr, we performed co-immunoprecipitation to verify if the ΔUBL mutant retains the ability to bind to Vpr (Figure 32a). Our results indicate that the ΔUBL mutant, much like wildtype BAG6, is still able to complex with Vpr. In other words, the protective consequences of the ΔUBL mutation are independent of Vpr binding to BAG6, and may in fact result from decreased binding capacity to DCAF1. We then overexpressed ΔUBL and DCAF1 to determine if the upstream proteasomal member is hindered in its ability to bind to BAG6 that is deficient in the UBL domain. Our results show that the binding of ΔUBL to DCAF1 is indeed reduced compared to wild-type BAG6 (Figure 32b). Taken together, these results indicate that the region where BAG6 binds to Vpr may reside outside of the UBL domain, which explains our observations that Vpr is still able to bind to ΔUBL. Importantly, the ΔUBL mutant however has a diminished DCAF1 binding capacity, which is consistent with our VprQ65R data, suggesting that BAG6 is protected from proteasomal degradation.

Viral Vpr and Endogenous BAG6 during Early Infection

Lastly, with the knowledge that Vpr binds to and degrades BAG6, as well as previous findings that Vpr is packaged into the virion and released into the cytoplasm (Gallay et al., 1995), we wanted to confirm the importance of BAG6 during the early stages of viral infection. At any point in time during challenge of BAG6-expressing pLKO control cells with HIV-GFP, including very soon post infection, we could not detect any changes in

BAG6 protein expression by western blot. Presumably, high BAG6 turnover effectively conceals any loss of BAG6 as a direct consequence of Vpr-mediated degradation. Thus to better study the immediate impact of virion-associated Vpr on endogenous BAG6 expression, we required an approach that would effectively prevent synthesis of new BAG6 protein and allow us to compare the rates of BAG6 degradation both with and without viral presence to verify if HIV-1 is able to enhance BAG6 clearance. For this reason, we performed a cycloheximide chase assay. Cycloheximide is a *de novo* protein synthesis inhibitor that is very toxic to cells. As we were interested in very early time points following HIV-1 infection, this did not concern us very much as it would not interfere with what we were attempting to assess. We thus challenged pLKO control cells with HIV-GFP or empty DMEM, as that was the medium in which the virus was originally generated by transfection of 293T cells, and treated these cells with cycloheximide for up to 4 hours. From Figure 33, natural degradation of BAG6 can be observed in the absence of virus at 2 hours post-treatment, indicating that BAG6 has a short-half life. The results at this time point revealed that the presence of HIV-1 virus accelerated the degradation of BAG6 by roughly 2-fold. This finding thus suggests the existence of a physiological link between early events of the viral life cycle and the targeted degradation of BAG6 by virion-associated Vpr. Although the precise biological role of Vpr-mediated proteasomal degradation of BAG6 remains to be further characterized, taken together our data reveal BAG6 to be a novel host factor that is critical for optimal HIV-1 infection.

Table 1. Panel of cannabinoids under current investigation. Cannabinoids exhibiting varying affinities for either cannabinoid receptor (CB1 or CB2) which were utilized in this study to assess their effects on HIV-1 replication *in vitro*. List of cannabinoids with receptor affinities is shown in the table (Tocris Bioscience; Cayman Chemical). All compounds were reconstituted to 10^{-3}M in DMSO, aliquoted, and stored at -20°C.

Drug	Property	CB1 Ki	CB2 Ki	Amount	Solvent (C_F = 1mM)
ACPA	CB1 Agonist	2.2 nM	700 nM	5 mg	14.6 mL DMSO
AM251	CB1 Antagonist	7.5 nM	22292 nM	5 µmol	5 mL DMSO
SR141716	CB1 Antagonist	1.8 nM	negligible	9.65 mg	20.81 mL DMSO
CB65	CB2 Agonist	>1000 nM	3.3nM	10 mg	23.9 mL DMSO
JWH-133	CB2 Agonist	677 nM	3.4 nM	10 mg	32.0 mL DMSO
L-759,646	CB2 Agonist	4888 nM	11.8 nM	10 mg	25.0 mL DMSO
JWH-213	CB2 Agonist	1.5nM	0.42nM	10 mg	26.07 mL DMSO
Palmidrol	CB2 Agonist	negligible	10 µM	10 mg	33.39 mL DMSO
JWH 015	CB2 Agonist	383 nM	13.8 nM	5 mg	15.3 mL DMSO
SR144528	CB2 Antagonist	400 nM	0.6 nM	11.51 mg	24.2 mL DMSO
AM630	CB2 Antagonist	5.2 µM	31.2 nM	5 mg	9.9 mL DMSO
WIN55,212	CB1/CB2 Agonist	62.3 nM	3.3 nM	10 mg	19.3 mL DMSO
CP55,940	CB1/CB2 Agonist	0.6-5.0 nM	0.7-2.6 nM	10 mg	26.5 mL DMSO
JWH-210	CB1/CB2 Agonist	0.46nM	0.69nM	10 mg	27.06 mL DMSO
CB13	CB1/CB2 Agonist	15 nM	98 nM	10 mg	27.13 mL DMSO

Table 2. Target genes modulated by cannabinoids and involved in HIV-1 infection. RNA-Seq data was overlayed with ~2300 virally-associated genes found among multiple global studies and within the NIAID HIV-1-Human Protein Interaction Database (HHPID) to generate enriched gene lists. Using Ingenuity Pathway Analysys software (IPA, Ingenuity Systems), highly scored, robust network maps were established. Upon extensive literature review, 11 unique host factors in either Jurkat or CEM-SS cells were revealed by our transcriptomic workflow that are both recruited during HIV-1 infection and affected by cannabinoids. Positive values correspond to fold-change increase over DMSO-treated controls, while negative values correspond to fold-change decrease. (ND: not detected)

	JURKAT			CEM-SS	
Transcript	WIN55212	CP55940	JWH-210	AM-630	JWH-210
NF2	-7.1	-6.9	-8.0	1.9	-7.5
BAG6, isoform b	-8.0	-6.4	-6.2	-8.7	-1.0
CAPN3	-3.1	-3.7	-6.0	4.8	4.8
PRDM10, isoform 3	1.5	-10.9	-1.3	3.9	5.1
PRDM10, isoform 4	-8.7	9.6	-1.3	3.2	-1.7
CRYAB	-1.7	-12.2	-8.2	1.8	-1.3
KCNIP3	-1.4	-7.2	-1.6	-1.6	-2.9
NOL3	-1.8	-6.7	-1.2	-2.1	-1.2
PTPN6	-2.5	ND	-1.2	-2.8	-4.4
RHOB	1.6	ND	ND	2.1	2.8
CAPN9	2.0	2.1	2.9	4.5	1.9

Table 3. BAG6 shRNA sequences.

Individual BAG6 shRNA clones were provided as frozen bacterial glycerol stocks (*E. coli*). Following amplification of bacterial cultures from glycerol stocks in LB broth supplemented with 100ug/mL ampicilin, shRNA plasmid DNA was then purified and utilized for the generation of recombinant lentiviral particles (LVPs).

Table of shRNA Sequences Targeting BAG6

Designation	TRC Number	BAG6 shRNA Sequence	Clone ID
shRNA A	TRCN0000279975	CCGGGCTGTTATCAATGGCCGAATTCTCGAGAATTCGGCCATTGATAACAGCTTTTTG	NM_004639.3-2991s21c1
shRNA B	TRCN0000279905	CCGGCCTTGGACTCTCAAACTCGTACTCGAGTACGAGTTTGAGAGTCCAAGGTTTTTG	NM_004639.3-382s21c1
shRNA C	TRCN0000279904	CCGGCCTATTATCCAGCAGGACATTCTCGAGAATGTCCTGCTGGATAATAGGTTTTTG	NM_004639.3-3372s21c1
shRNA D	TRCN0000279903	CCGGGCCATTCCCATACAGATCAATCTCGAGATTGATCTGTATGGGAATGGCTTTTTG	NM_004639.3-1434s21c1
shRNA E	TRCN0000007353	CCGGGCTGTTATCAATGGCCGAATTCTCGAGAATTCGGCCATTGATAACAGCTTTTT	NM_004639.2-2961s1c1
shRNA F	TRCN0000007354	CCGGGCCATTCCCATACAGATCAATCTCGAGATTGATCTGTATGGGAATGGCTTTTT	NM_004639.2-1404s1c1
shRNA G	TRCN0000007356	CCGGCAGTGAAAGTATTGCTGCCTTCTCGAGAAGGCAGCAATACTTTCACTGTTTTT	NM_004639.2-2450s1c1

Figure 6. Assessing the effects of cannabinoids on NL4-3 challenge of Jurkat, CEM-SS, PM-1, and CEM cells. $2x10^5$ **(a)** Jurkat, **(b)** CEM-SS, and **(c)** PM-1 cells were seeded in 24-well plates and maintained in 700uL RPMI media throughout the experiment. Cells were pretreated with 10^{-6}M WIN55212, CP55940, SR141716, SR144528, or DMSO vehicle for 3 hours prior to mock challenge or infection with 2.0ng of NL4-3, as quantified by p24 ELISA. Cells were washed 24 hours later and clarified supernatants were collected every 2 days post infection. Removed volume replenished with fresh drug-infused media. CEM cells **(d)** were seeded as above and challenged with mock or 2.0ng NL4-3 without any pretreatment. Infectivity of supernatants was then determined by TZM-bl assay; β-galactosidase activity, as a function of viral infectivity, was plotted as the log of relative units of luminescence.

Figure 6, continued.

a)

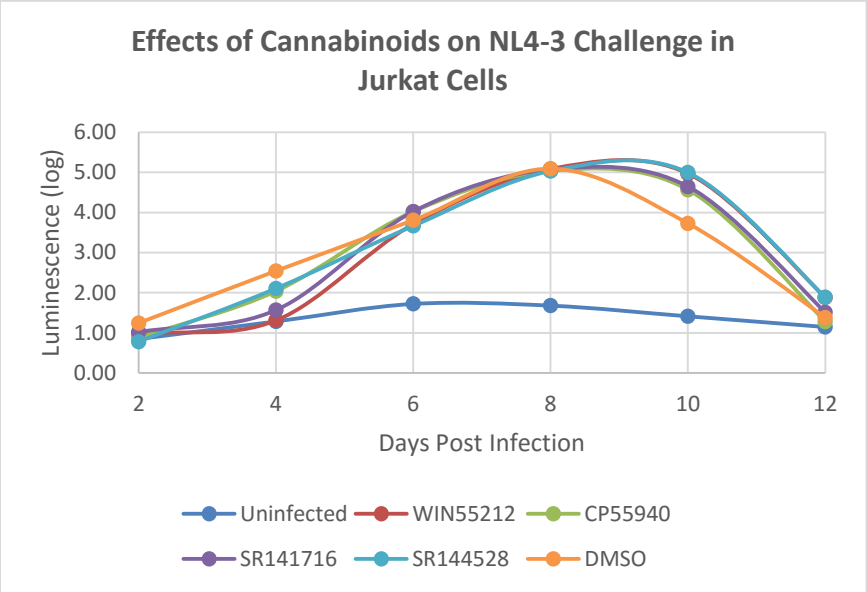

b)

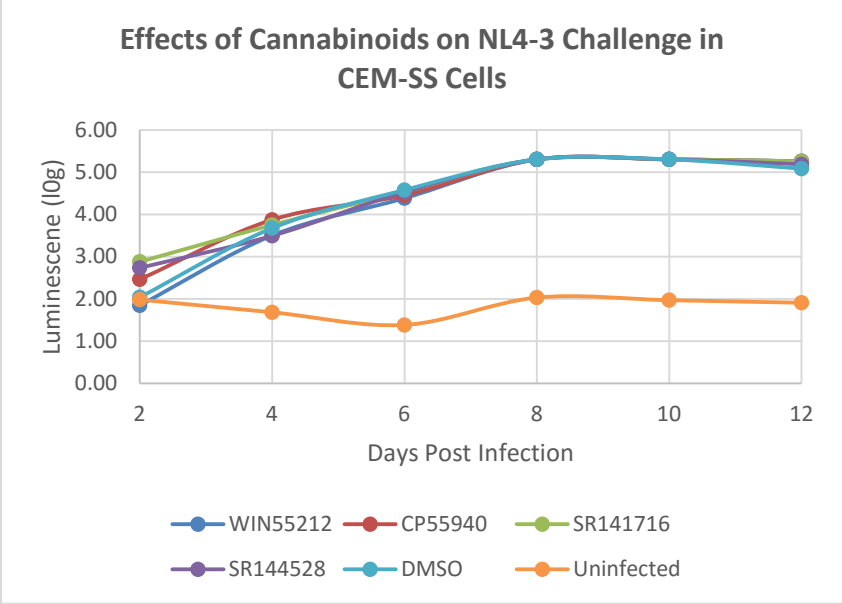

Figure 6, continued.

c)

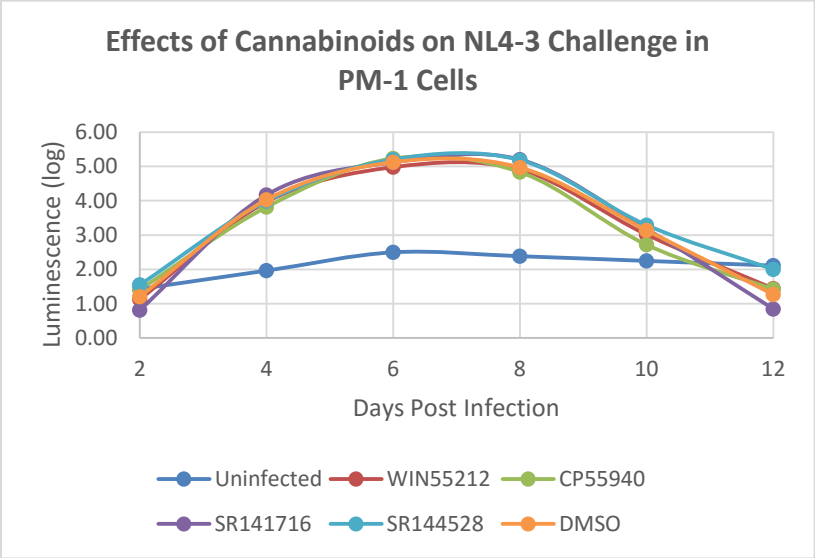

d)

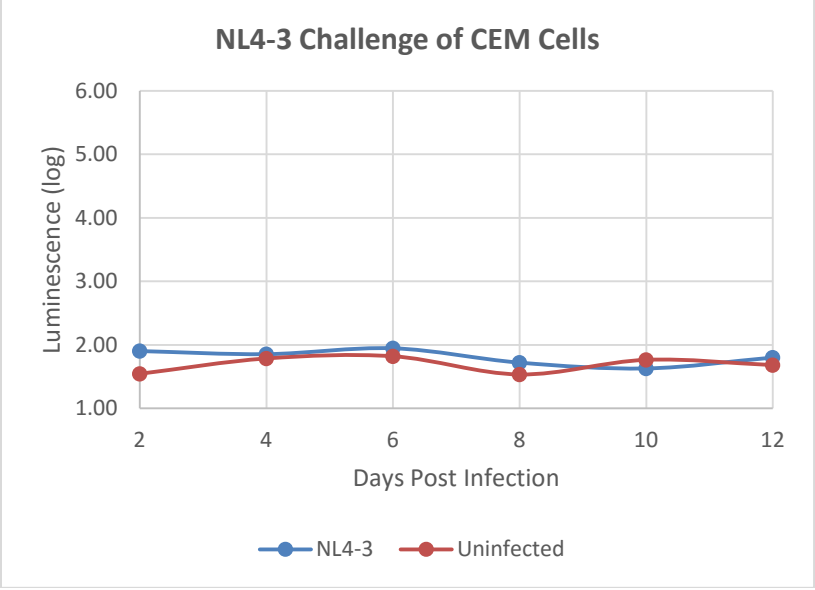

Figure 7. The effects of cannabinoids on HIV-1 infection in multiple T cell lines. $2x10^5$ Jurkat (a), CEM-SS (b), or PM-1 (c) cells were seeded in 24-well plates in 700uL RPMI and pretreated with cannabinoids or DMSO vehicle at a final concentration of $1x10^{-6}$M for 3 hours prior to challenge with 2.0 ng of p24 ELISA-quantified NL4-3. Cells were then incubated with the virus for 24 hours, washed, and maintained in cannabinoid-infused media. 6 days post-infection, genomic DNA from infected cells was extracted and qPCR utilizing primers specific to the *gag* and *GapDH* sequences was performed. Results are presented as percent inhibition relative to DMSO-treated control cells, which were set to 100%. (*P<0.05, Student's t-test).

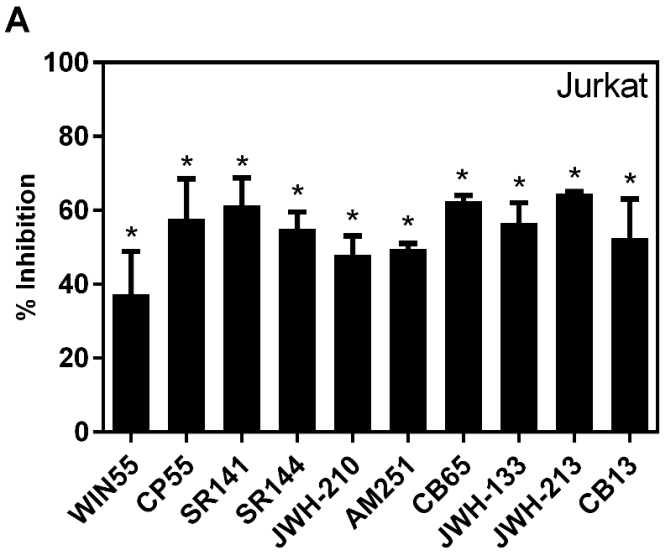

Figure 7, continued.

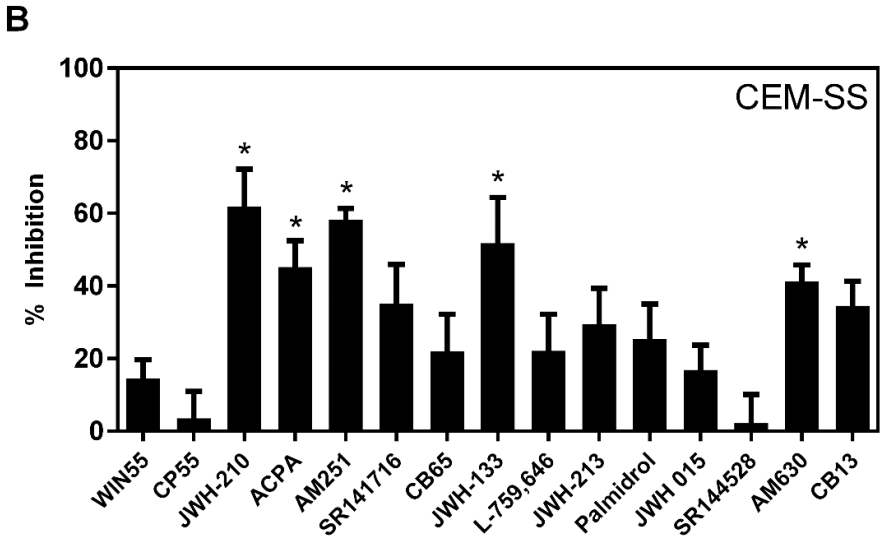

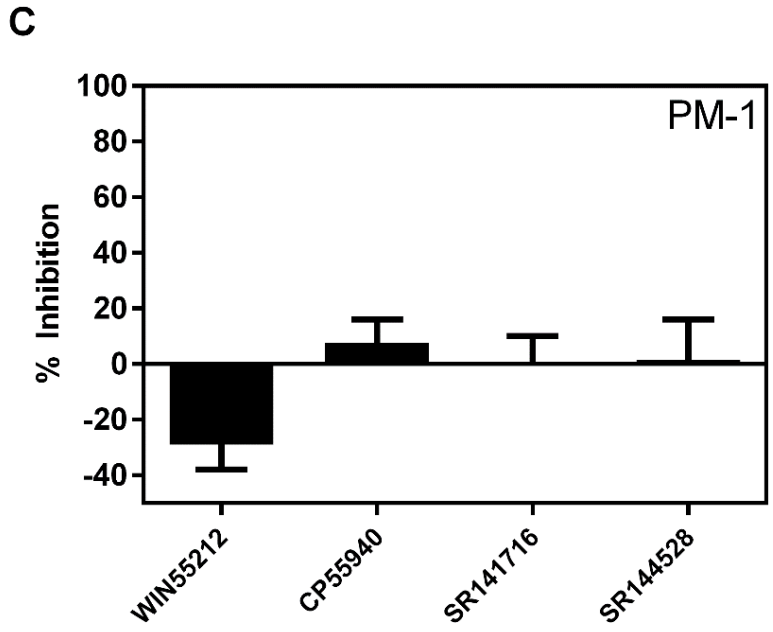

Figure 8. Effects of Cannabinoids on Cell Viability. Cells were treated with 10-5M or 10-6M cannabinoids or DMSO vehicle. 6 days later, flow cytometry was performed to assess cell viability. a) Shown below is a representative example of forward- and side-scatter gating of the live cell population, followed by plotting of live cells as a percent of all cells within the live gate, as a function of cannabinoid treatment. b) Cells were stained with 7-AAD dye and gated by forward-scatter and PerCP-Cy5-5A (7-AAD channel). The percent of 7-AAD-positive as a function of cannabinoid treatment are plotted as well.

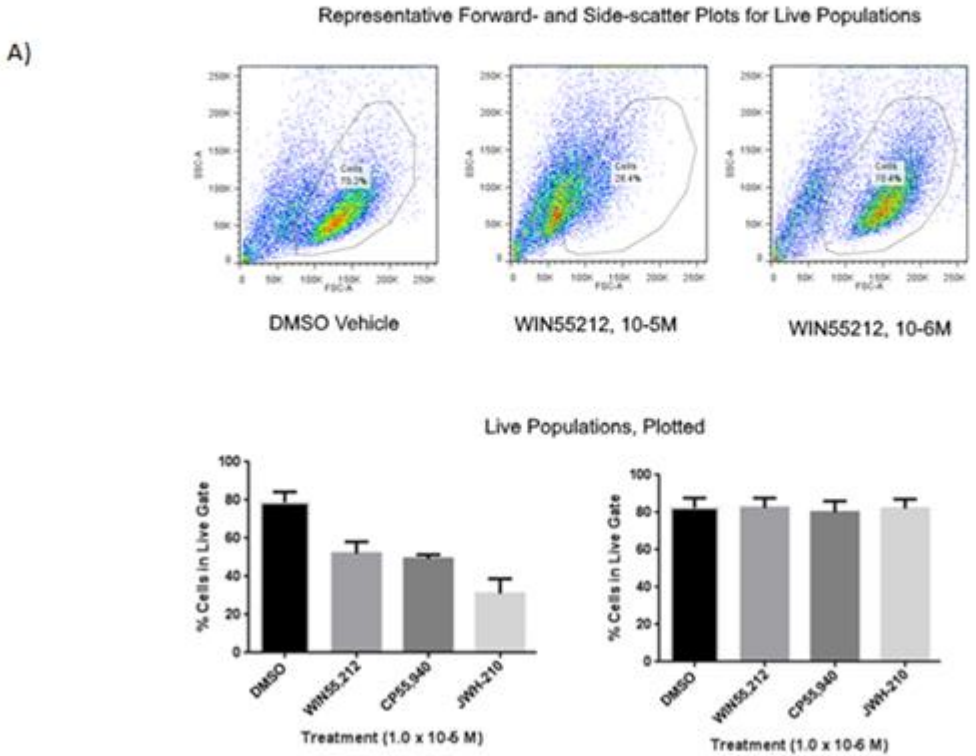

Figure 8, continued.

B) Representative 7-AAD Staining, Live/Dead Gating

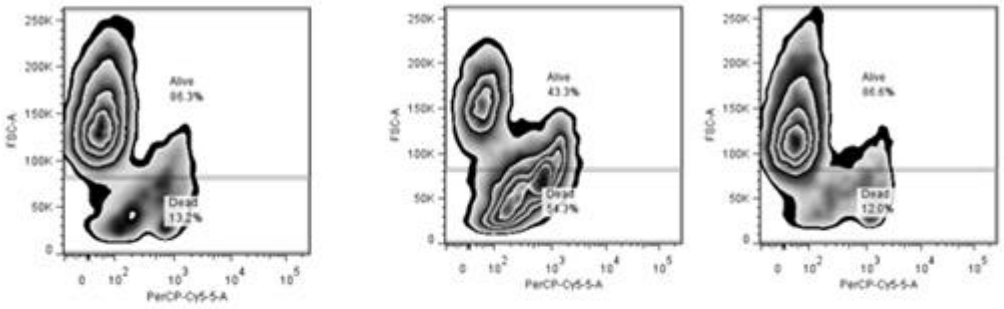

DMSO, 1.0 x 10-5 M

WIN55,212-2, 1.0 x 10^{-5} M

WIN55,212-2, 1.0 x 10^{-6} M

Live/Dead Cells, Plotted

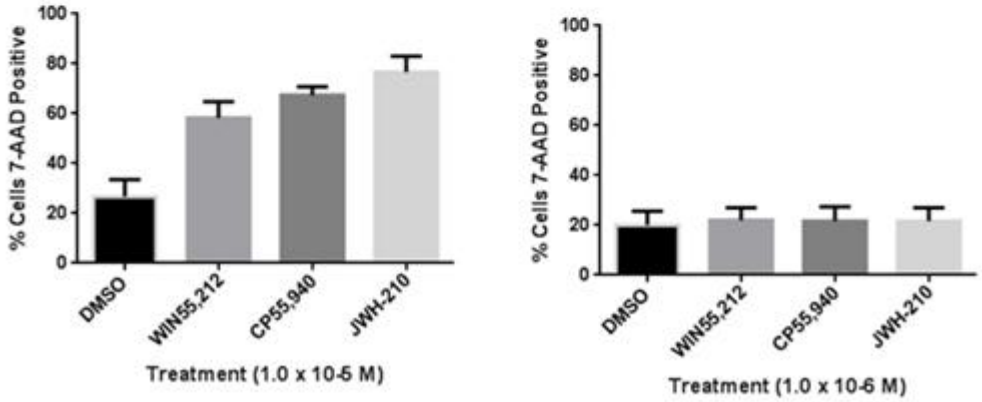

Figure 9. Schematic overview of utilizing RNA-Seq for the identification of novel factors, modulated by cannabinoids, that are important during HIV-1 infection. (a) Cannabinoids are known to exert pleiotropic effects on cell expression, particularly modulating numerous signaling pathways. Analogously (b), HIV-1 viral proteins (red) are known to interact (yellow) with hundreds of host proteins (blue), while many other more interactions remain to be identified. (c) Thus to reveal those host factors that are both modulated by cannabinoids and involved during HIV-1 infection, we employed RNA-Seq to assess global transcriptomic changes in Jurkat and CEM-SS cells treated with WIN55212, CP55940, and JWH210, compared to DMSO vehicle control. RNA-Seq was performed on extracted total RNA from $2x10^5$ Jurkat and CEM-SS cells treated with the aforementioned cannabinoids for 27 hours, resulting in the modulation of over 22,000 genes per treatment. Focusing on those genes modulated 2-fold, 4-fold, or even 6-fold still resulted in large, numbers of non-enriched genes that would need further investigation. Thus to focus our investigation on those genes involved in HIV-1 replication, we capitalized on the knowledge bases provided by several genome-wide screenings that had identified ~900 novel host factors, (Ptak, 2009; Brass, 2008; Konig, 2008; Zhou, 2008, Fellay, 2007, Bushman, 2009), as well as the NIAID HIV-1-Human Protein Interaction Database (HHPID), which is an annotated database containing roughly 1400 genes experimentally determined to interact with HIV-1. By overlaying these gene sets with our transcriptomic data and applying fold-change filters, we were able to enrich for prospective HIV-1-salient factors while drastically reducing the total number of genes that needed to be further characterized (shown in red and green). (d) Using the 3-fold filter as a starting point, we then manually removed histones and other non-specific proteins before generating preliminary molecular interaction networks by Ingenuity Pathway Analysis software (IPA). These predicted interactomic networks were then subjected to further literature review prior to experimental validation (see Table 2).

Figure 9, continued.

a.

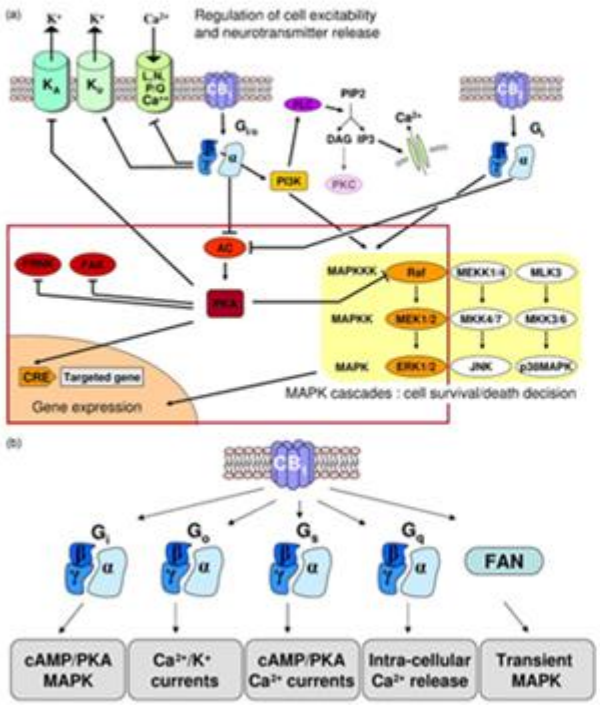

b.

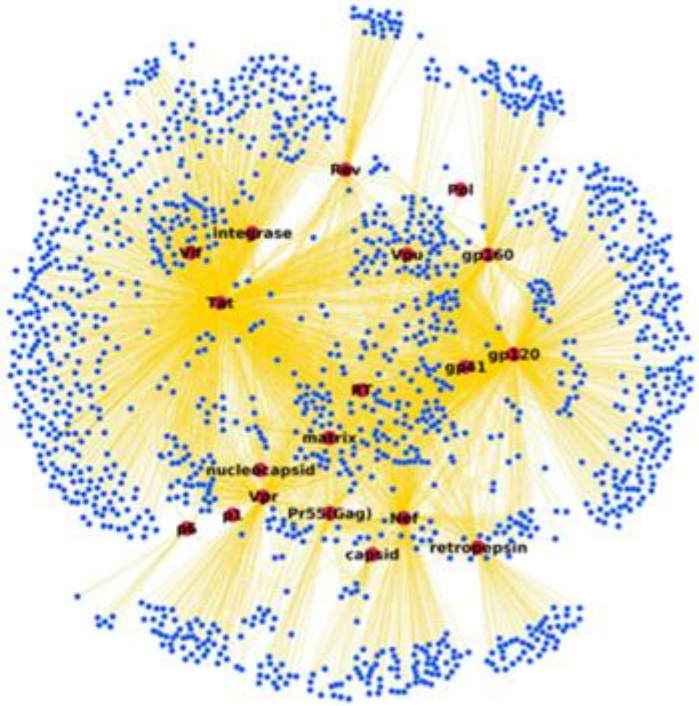

Figure 9, continued.

c.

List	Name	Number of Genes	Description
1	siRNA HIV König	293	siRNA screen for host factors promoting HIV replication
2	siRNA HIV Brass	283	siRNA screen for host factors promoting HIV replication
3	siRNA HIV Zhou	303	siRNA screen for host factors promoting HIV replication
4	SNP HIV Fellay	63	GWA study of HIV set point in infected individuals
5	Particle Associated HIV	248	Proteins in HIV particles identified by mass spec
6	HARC Nef	6	Cellular proteins that interact with HIV Nef protein (mass spec)
7	HARC Tat	69	Cellular proteins that interact with HIV Tat protein (mass spec)
8	HARC Rev	56	Cellular proteins that interact with HIV Rev protein (mass spec)
9	BIND INT HIV	23	Cellular proteins that interact with HIV IN protein (yeast two hybrid)
10	NCBI Interactions	1434	Published interactions between an HIV protein and a cellular protien

Genomic/Interactomic Studies

~900 genes

	RNA-Seq	2x Fold	3x Fold	4x Fold	6x Fold
WIN55,212-2	23,888	1863 ↓ 126	630 ↓ 38	294 ↓ 20	122 ↓ 11
CP55,940	23,494	3311 ↓ 228	1178 ↓ 76	598 ↓ 58	252 ↓ 34
JWH-210	23,729	1708 ↓ 128	559 ↓ 43	268 ↓ 21	131 ↓ 11

~ 1400 genes

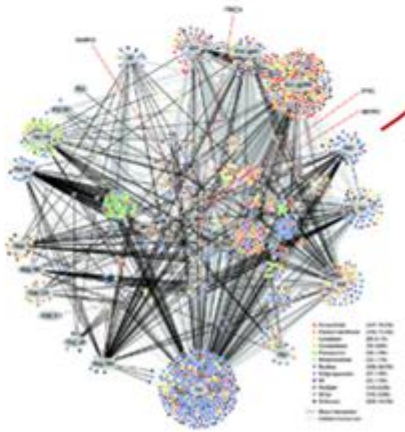

HIV-1, Host Protein Interaction Database (NCBI)

Figure 9, continued.

d.

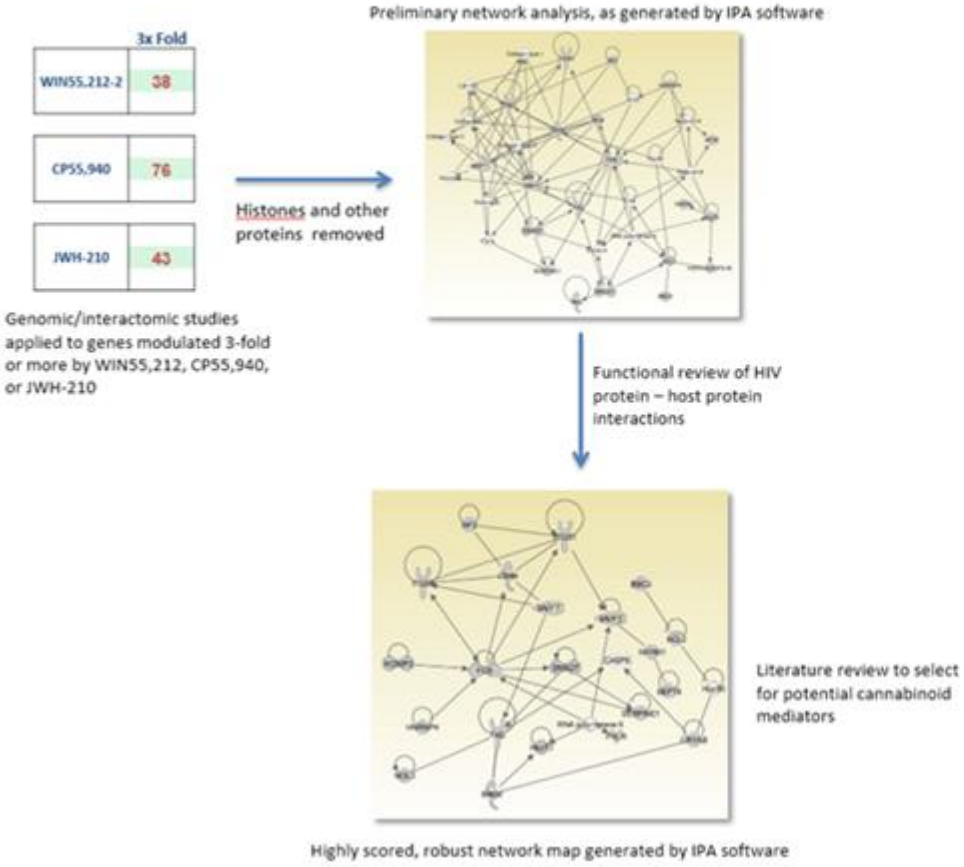

Figure 10. Cannabinoids reduce BAG6 RNA expression in Jurkat and CEM-SS cells. $2x10^5$ Jurkat cells were seeded in 24-well plates in 700uL RPMI were pretreated with the pancannabinoids WIN55212, CP55940, JWH210 or DMSO vehicle, while $2x10^5$ CEM-SS cells were pretreated with AM630, JWH210, or DMSO vehicle for 27 hours. Total RNA was then extracted, assessed for quality by use of the Agilent Bioanalyser 2100 system, and processed for transcriptomic sequencing by RNA-Seq. Analysis of BAG6 gene expression modulation by cannabinoids, as compared to DMSO-treated cells, was quantified by DNASTAR QSeq software.

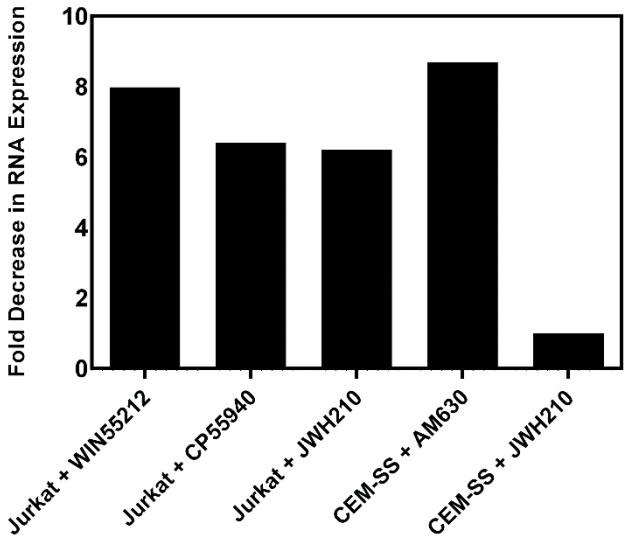

Figure 11. Schematic overview of LVP generation (adapted from Sigma Aldrich). 293T cells were transfected with the following plasmids: 14ug shRNA or non non-coding pLKO control plasmid DNA; 7ug pVSVG, which provides a pleiotropic envelope facilitating efficient transduction; and 10ug pSPAX2, which provides the Gag, Pol, Rev, and Tat genes, which are essential for transcription and packaging of the shRNA sequences into recombinant pseudoviral particles. 48 hours post-transfection, clarified supernatants were aliquoted and stored at -80°C.

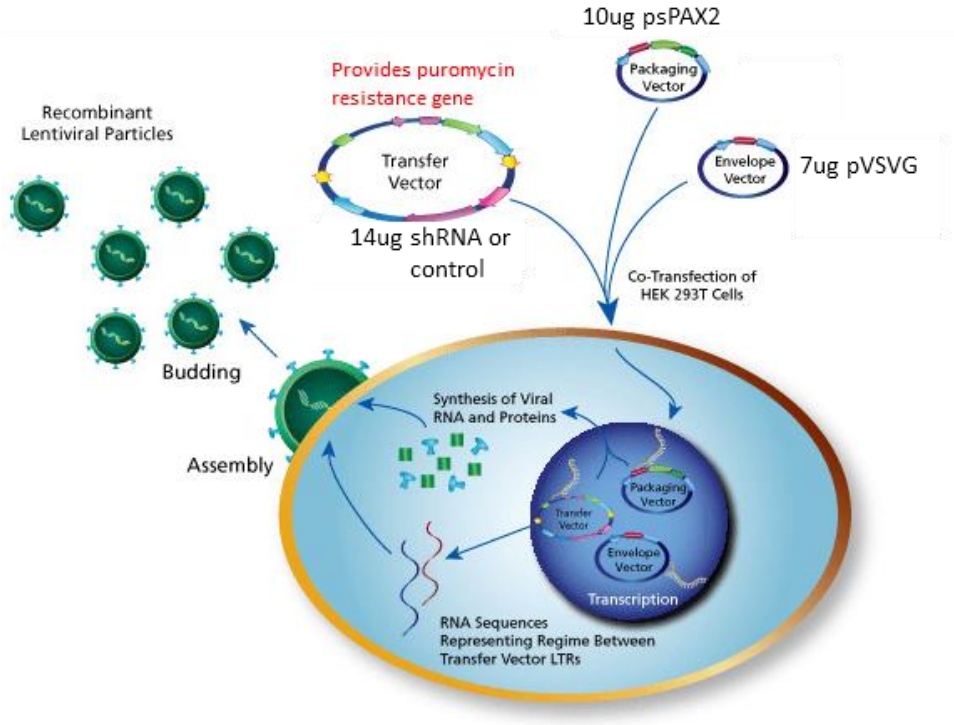

Figure 12. Puromycin Response Curve in Jurkat Cells. $2x10^5$ Jurkat cells were seeded in 24-well plates and treated with increasing amounts of puromycin. 72 hours post treatment, cells were collected and flow cytometry was performed to assess cell viability on forward- and side-scatter gated live populations. Shown below are representative examples of (left) untreated cells and (right) cells treated with 2ug/mL puromycin. The total percent of live cells as a function of increasing concentration of puromycin at 72 hours is plotted below.

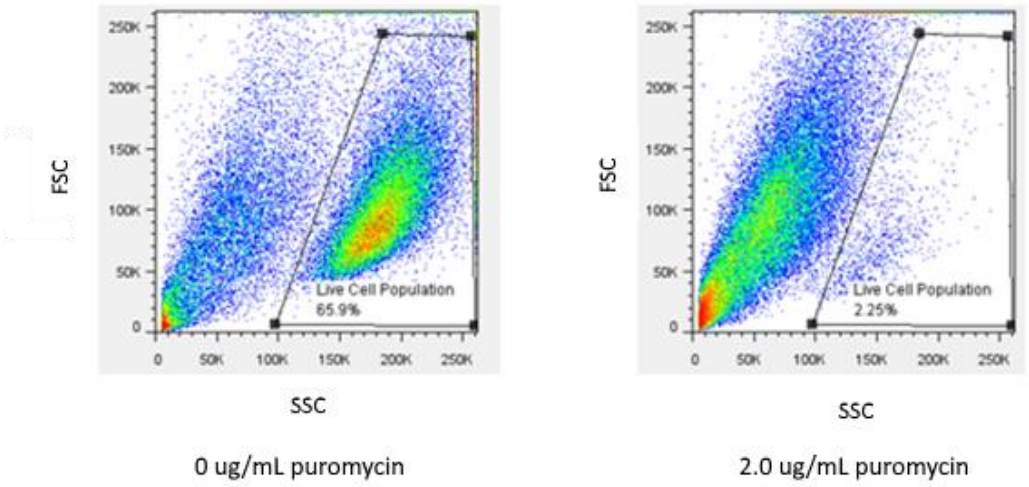

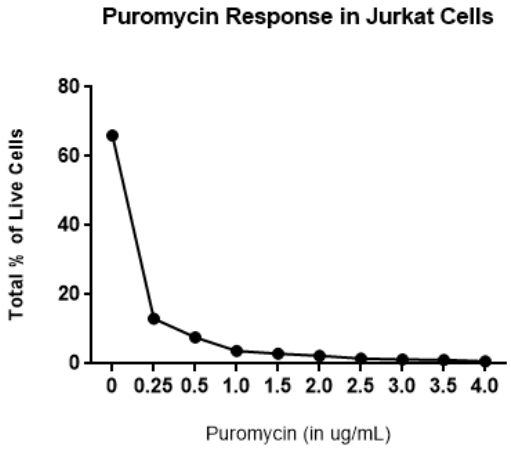

Figure 13. BAG6 knockdown does not have deleterious effects on cell health. Upon transduction with LVPs containing individual BAG6 shRNA species or control, cells were treated with 2.0ug/mL purmomycin (a). 3 days later, flow cytometry was performed to assess for cell viability. Shown below is a representative example of forward- and side-scatter gating of the live cell population. Upper left: untransduced Jurkat cells, no puromycin addition. Upper right: untransduced Jurkat cells with puromycin treatment. Lower left: Jurkat cells transduced with 250uL of BAG6 shRNA "A" LVPs. Lower right: Jurkat cells transduced with 2mL BAG6 shRNA "A" LVPs. (b) 10 days post-puromycin selection, cells were stained with 7-AAD and cell viability was assessed by flow cytometry. Forward-and and side-scatter gating was first employed prior to subsequent gating by 7-AAD dye uptake ("Dead") or exclusion ("Live"). Shown is a representative example of 10-day puromycin treated transduced cells (b), as well as the plotted results of the percent of "Live" cells among all cells (c).

a.

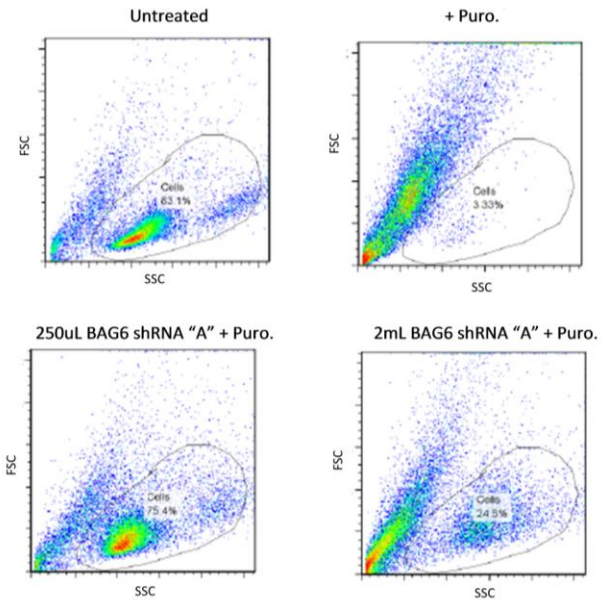

Figure 13, continued.

b.

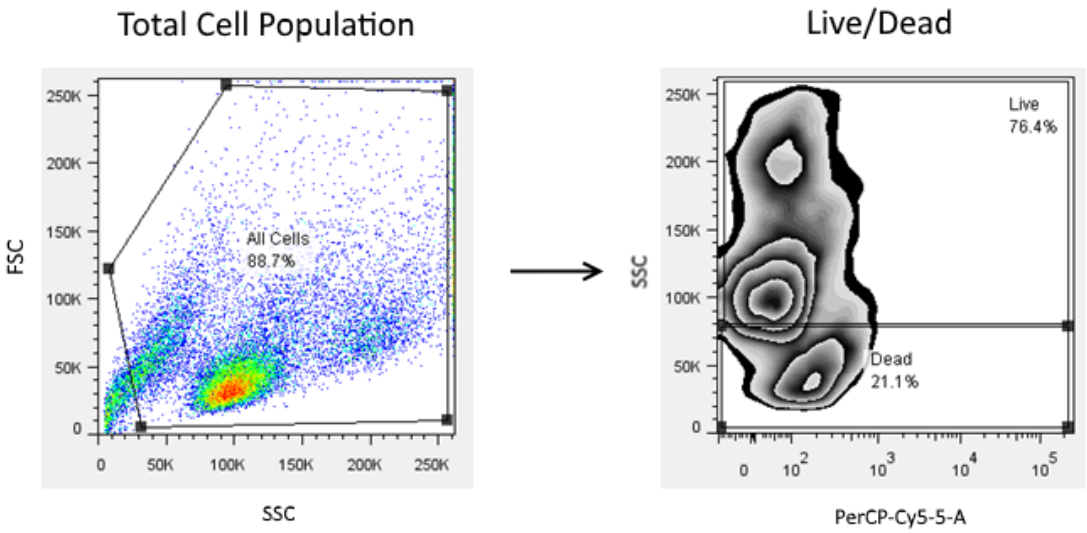

c.

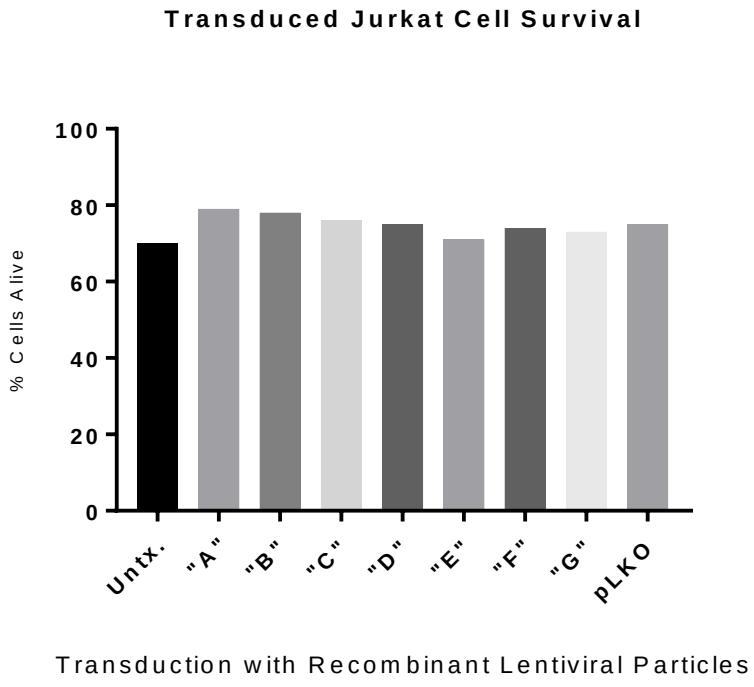

Figure 14. Knockdown of BAG6 expression in Jurkat and 293T cells by RNA interference. Cells were transduced with recombinant lentiviral particles expressing control shRNA (pLKO) or shRNA species specifically targeting BAG6. Seven different BAG6-targeting shRNA species, labeled "A" through "G," were tested. Cells were assessed for protein ablation by immunoblotting 4 days after transduction using mouse α-BAG6 antibody. Mouse antibody specific for β-actin was used as the loading control. Shown is a representative western blot for the BAG6 shRNA species "A" and "B," for which BAG6 knockdown was the most potent, as compared to expression in untransduced Jurkat or in pLKO-transduced control cells. A summary of all BAG6 shRNA species efficacies is shown as well.

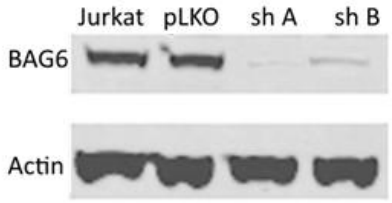

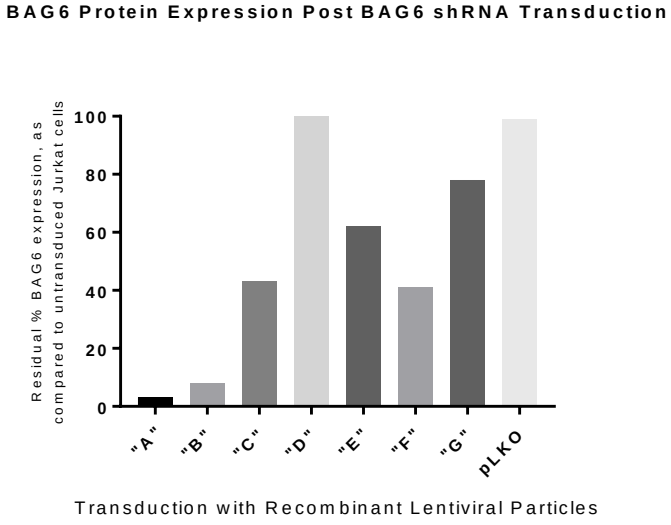

Figure 15. Viability of BAG6 shRNA-transduced Jurkat cells. Cells were initially transduced with 0, 250uL, or 2mL lentiviral particles. a) Upon a 3 day selection for successful transductants with puromycin, the live population was visualized by forward- and side-scatter plotting by means of flow cytometry. b) 10 days post selection, the percent of cells found within the live gate, as a function of the various lentiviral particles utilized, was plotted.

a)

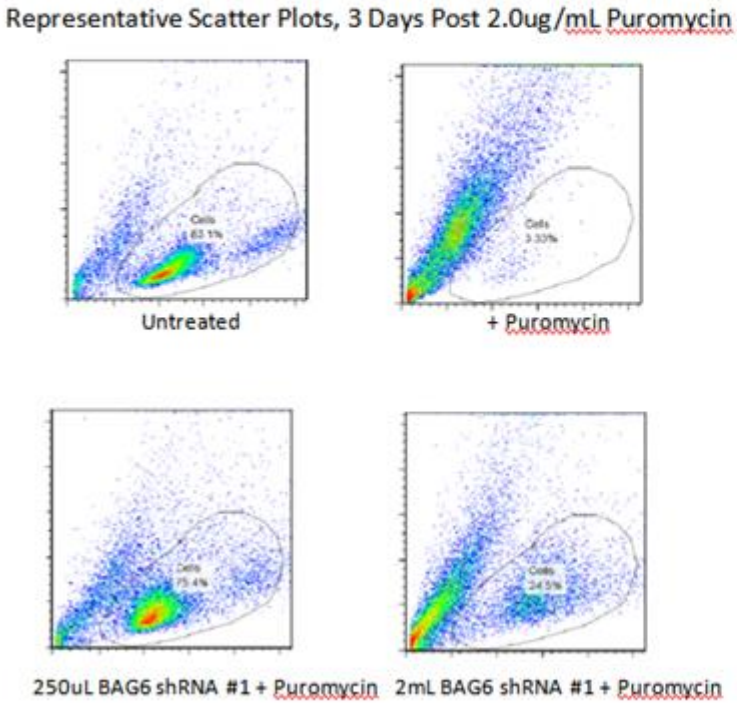

b)

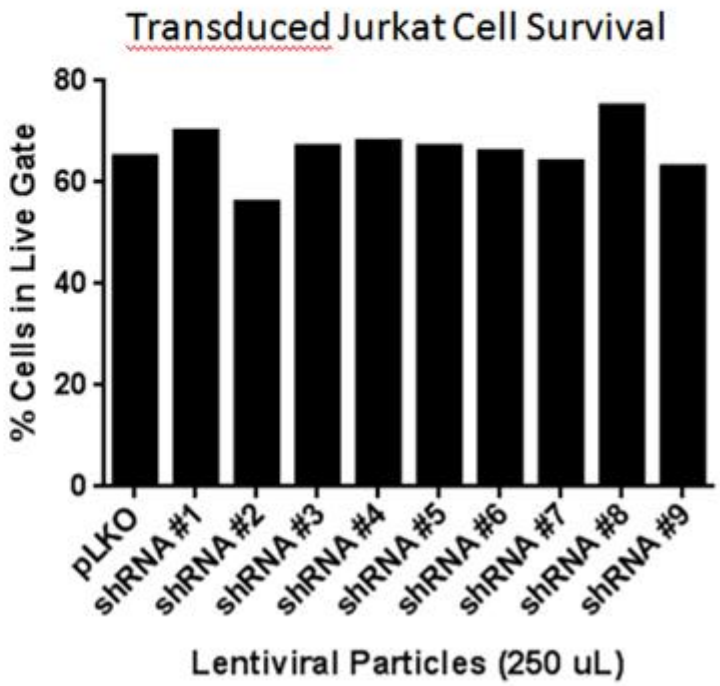

Figure 16. Infection by NL4-3 or HIV-GFP is Reduced in BAG6 knockdown cells. $2x10^5$ Jurkat-BAG6 knockdown and Jurkat-pLKO cells were seeded in 24-well plates in 700uL RPMI media prior to challenge with 2.0ng NL4-3 or different amounts of HIV-GFP. 6 days post-infection with NL4-3, cells were harvested and genomic DNA from infected cells was extracted. qPCR utilizing primers specific to the gag and GapDH sequences was performed to determine the effects of BAG6 knockdown during viral challenge. For HIV-GFP challenge, cells were fixed in 1% paraformaldehyde prior to flow cytometry. The live cell population was gated by forward- and side-scatter plotting and fluorescence as a function of viral infection was acquired. pLKO control cells were set as 100% for both viruses.

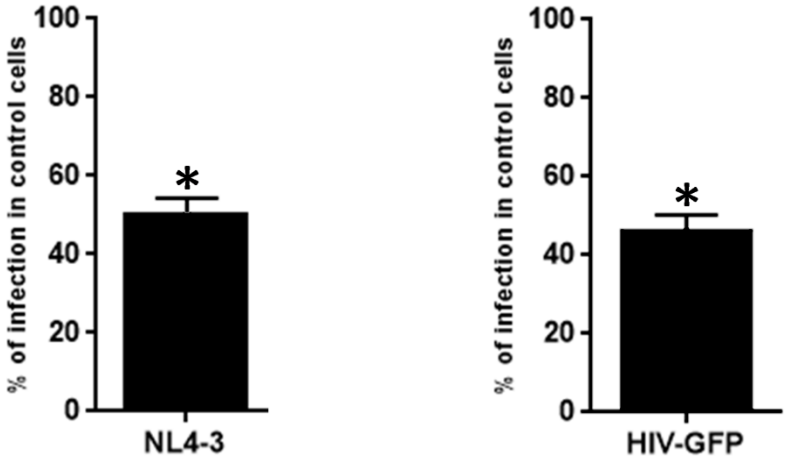

Figure 17. BAG6 co-immunoprecipitates with Vif. $2x10^6$ 293T cells were plated in 10cm plates the day before transfection with 6ug BAG6-V5 (lane 1), 6ug pcDNA-Vif (lane 2), or 6ug each of BAG6-V5 and Vif-FLAG (lane 3). Forty-eight hours later, cell lysates were generated and used for Co-IP with rabbit anti-V5 antibody. IP samples were detected by immunoblotting with mouse anti-V5 or mouse anti-FLAG antibodies to detect BAG6 or Vif expression, respectively.

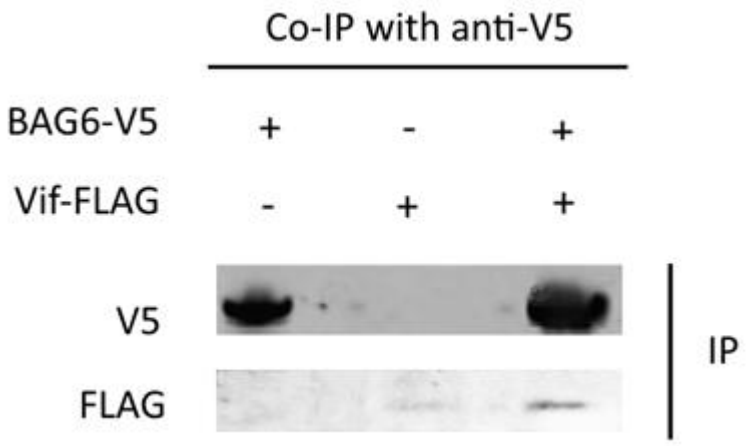

Figure 18. Schematic overview of generated Vif mutants. (a) Wildtype Vif is schematically depicted, with the two well known mutations involved in A3G binding, Y40RHHY44 and Y69XXL72, shown as well. (b) Furthermore, a partial 3D model of Vif based on X-ray crystallography is available as well, with the A3G-binding pocket circled in red (Guo et al., 2014). Based on this, by targeted alanine mutagenesis along the Vif sequence (c), we generated the Vif mutant proteins 22KRLVK26>5A ("Mutant 1"), 10VWQVD14>5A ("Mutant 2"), and 57IPLGD61>5A ("Mutant 3").

a.

b.

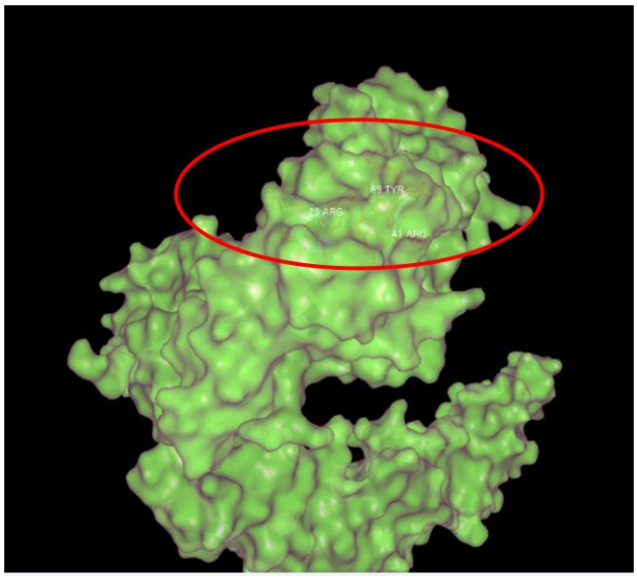

Figure 18, continued.

C.

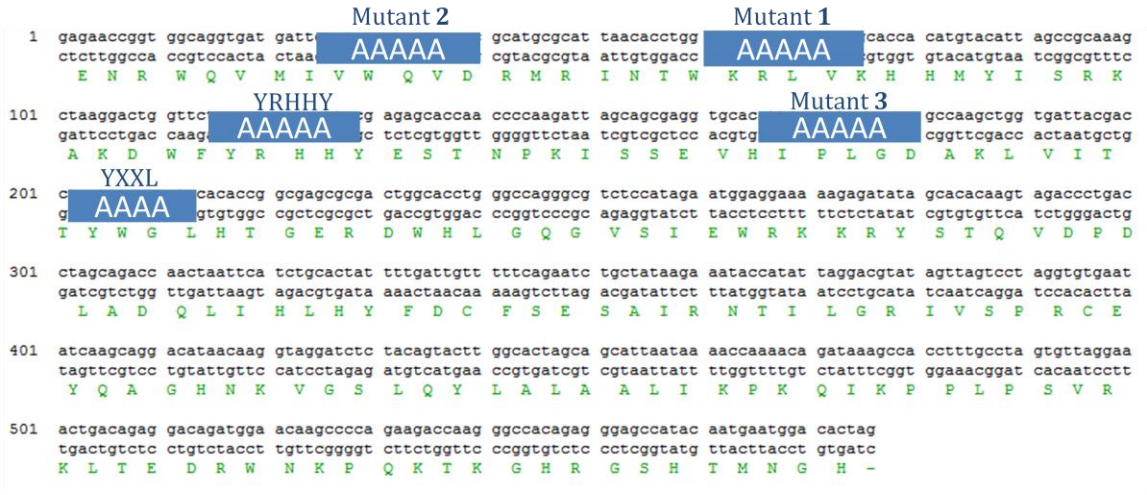

Figure 19. Binding affinities of Vif mutant proteins to BAG6. 2x106 293T cells were plated in 10cm plates the day before transfection with 6ug BAG6-V5 together with 6ug of each of the following Vif-FLAG-based constructs: WT Vif, Mutant 1, Mutant 2, Mutant 3, YHRRY, and YXXL. Forty-eight hours later, cell lysates were generated and used for Co-IP with rabbit anti-V5 antibody. Protein expression was detected by immunoblotting with mouse anti-V5 or mouse anti-FLAG antibodies to detect BAG6 or Vif expression, respectively. A representative western blot of the differences between wildtype Vif and Mutant 2 in the ability to bind to BAG6 is shown in (a). Semi-quantification of mutant Vif:BAG6 interactions, compared to the binding ability of wildtype Vif, which was set to 100%, is depicted in (b). Semi-quantification was performed by measuring band intensities of western blot membranes using Image Studio Lite Software (Li-Cor) and using the following forumula: ratio of lysate Vif to lysate BAG6 multiplied by the ratio of co-ip Vif to co-ip BAG6.

a.

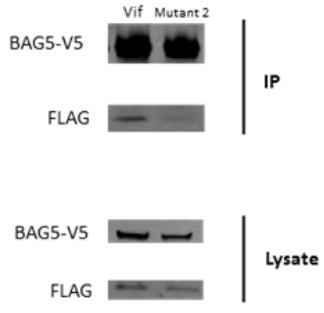

b.

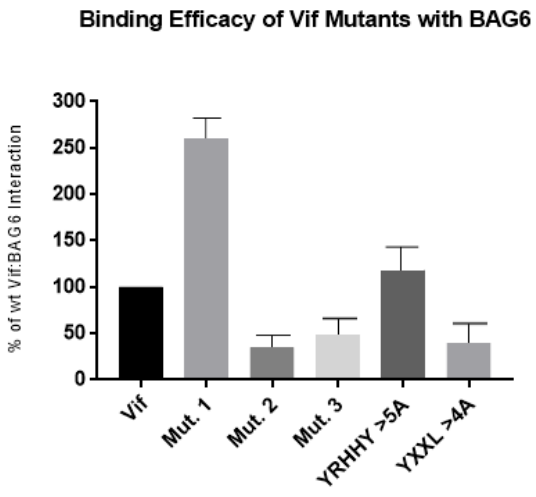

Figure 20. Jurkat cells do not express A3G. Cell lysates were generated from 1x106 million Jurkat or CEM cells, which serve as the A3G-expressing positive control. Protein expression was determined by immunoblotting with anti-A3G and anti-β-actin antibodies, which served as the loading control.

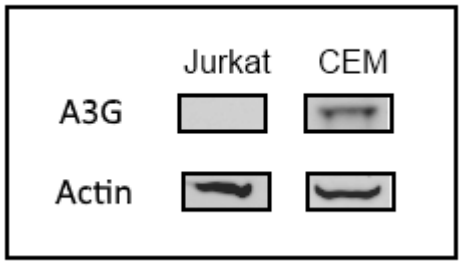

Figure 21. BAG6 co-immunoprecipitates with A3G. 2x10^6 293T cells were plated in 10cm plates the day before transfection with 6ug BAG6-FLAG (lane 1), 6ug A3G-V5 (lane 2), or 6ug each of BAG6-FLAG and A3G-V5 (lane 3). Forty-eight hours later, cell lysates were generated and used for Co-IP with rabbit anti-V5 antibody. IP and raw lysate samples were detected by immunoblotting with mouse anti-V5 or mouse anti-FLAG antibodies to detect A3G or BAG6 expression, respectively.

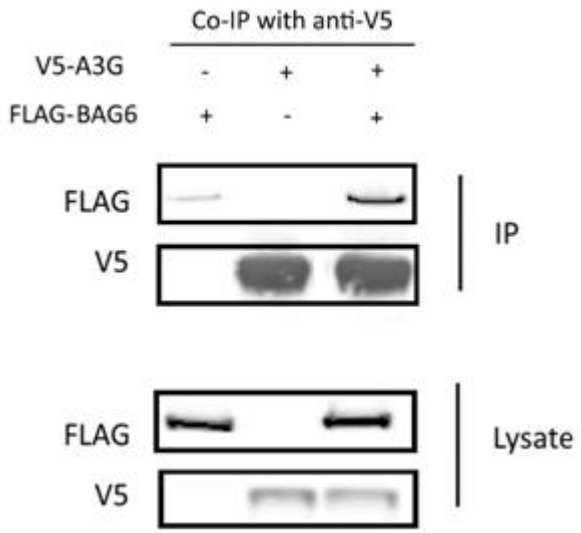

Figure 22. BAG6 does not protect A3G from Vif-mediated degradation. $4x10^5$ 293T cells were plated in 6-well plates the day before transfection with 1) 0.50ug A3G-V5, 2) 1.0ug pLX304-BAG6, 3) 0.25ug Vif-VLAG, 4) A3G+BAG6, 5) A3G+Vif, 6) BAG6+Vif, and 7) A3G+BAG6+Vif, as depicted below. 48 hours later, cell lysates were generated and protein expression was detected by immunoblotting with anti-B-Actin, anti-V5, and anti-FLAG antibodies.

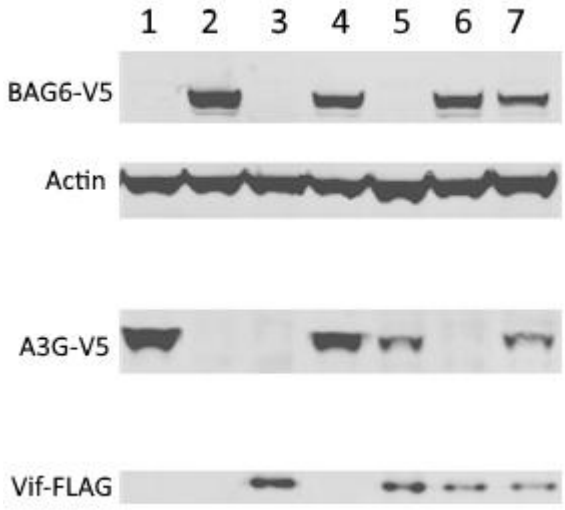

Figure 23. Challenge of BAG6-KD Cells with NL4-3 or with NL5097m. 2x10^5 Jurkat-BAG6 knockdown and Jurkat-pLKO cells were seeded in 24-well plates in 700uL RPMI media prior to challenge with 2.0ng NL4-3 or NL5097m. 6 days post-infection, cells were harvested and genomic DNA from infected cells was extracted. qPCR utilizing primers specific to the *gag* and *GapDH* sequences was performed to determine the effects of BAG6 knockdown during viral challenge. pLKO control cells infected with the respective viruses were set as 100%.

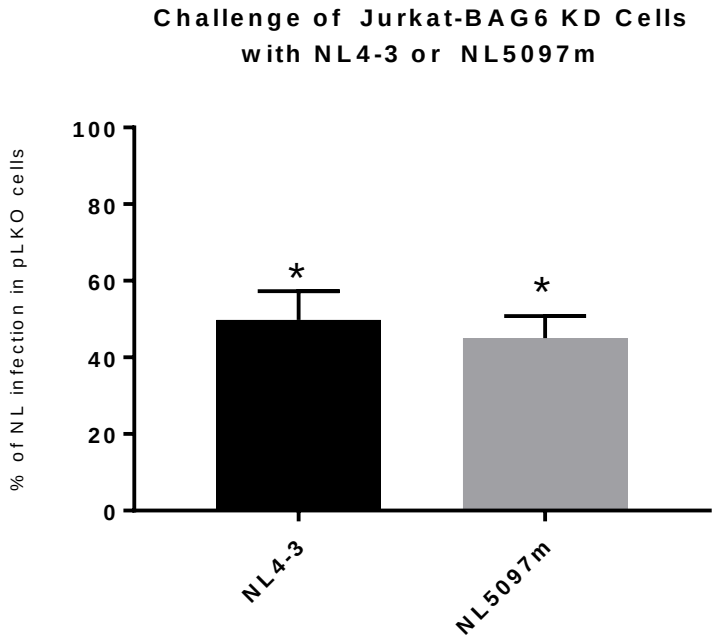

Figure 24. Schematic overview of mutant viral generation. Multiple plasmids were obtained from the NIH AIDS Reagent Program, each one containing a fragment of the wildtype NL4-3 provirus: p83-2 (5’ portion), p83-10 (3’ portion), p197-1 (5’ portion containing the ΔVif mutation) and p210-19 (5’ portion containing the ΔVpr mutation). Critically, each plasmid contains a single EcoRI sequence, allowing for its linearization. Once linearized, 5' fragments may then be ligated with 3' fragments to reconstitute full-length proviruses. Thus by digesting with EcoRI and ligating 3ug of the 5' fragments containing the appropriate mutations with 3ug of the 3' end, we were able to generate the NL, NLΔVif, and NLΔVpr proviruses.

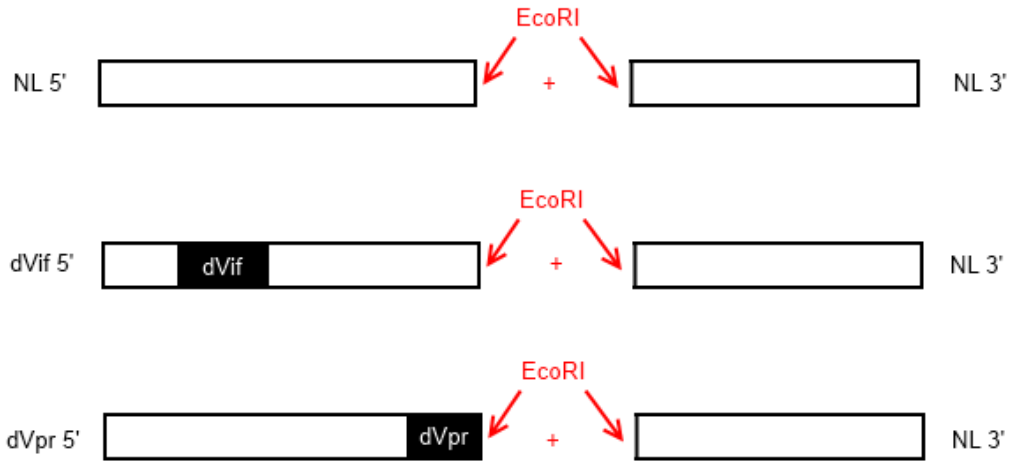

Figure 25. Infection of BAG6-KD Cells with HIV-1 Mutants. 2x105 Jurkat-BAG6 knockdown and Jurkat-pLKO cells were seeded in 24-well plates in 700uL RPMI media prior to challenge with 2.0ng NL4-3, NLΔVif, or NLΔVpr. 6 days post-infection, cells were harvested and genomic DNA from infected cells was extracted. qPCR utilizing primers specific to the gag and GapDH sequences was performed to determine the effects of BAG6 knockdown during viral challenge. pLKO control cells infected with NL were set to 100%, and all other infections are presented as a percentage of that.

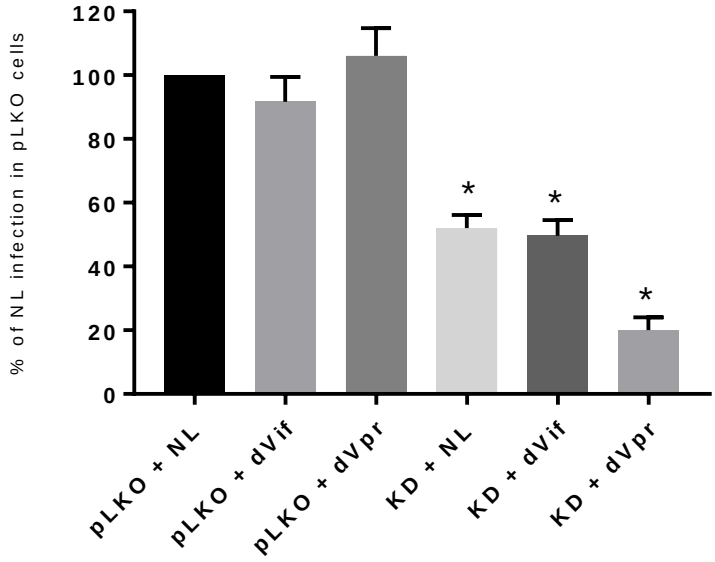

Figure 26. BAG6 is degraded by the HIV-1 accessory protein Vpr. 4x105 293T cells were plated in 6-well plates the day before transfection with 2.0ug of: A3G-V5 (lane 1), 0.5ug Vpr-GFP (lane 2), 1.0ug BAG6-V5 (lane 3), A3G-V5 + BAG6-V5 (lane 4), A3G-V5 + Vpr-GFP (lane 5), and A3G-V5 + BAG6-V5 + Vpr-GFP (lane 6). 48h later, immunoblotting with anti-GFP and anti-V5 antibodies was performed on the cell lysates.

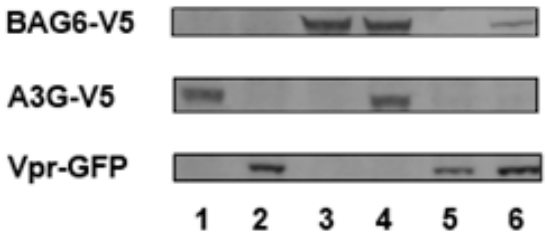

Figure 27. BAG6 is a binding partner to the HIV-1 accessory protein Vpr. 293T 2x106 293T cells were plated in 10cm plates the day before transfection with Vpr-GFP (6ug in lanes 1 and 3) and BAG6-V5 (4ug in lanes 2 and 3), as depicted. 48 hours later, cell lysates were generated and used for Co-IP with rabbit anti-V5 antibody. IP and raw lysate samples were detected by immunoblotting with anti-V5 or anti-GFP antibodies to detect BAG6 and Vpr, expression, respectively.

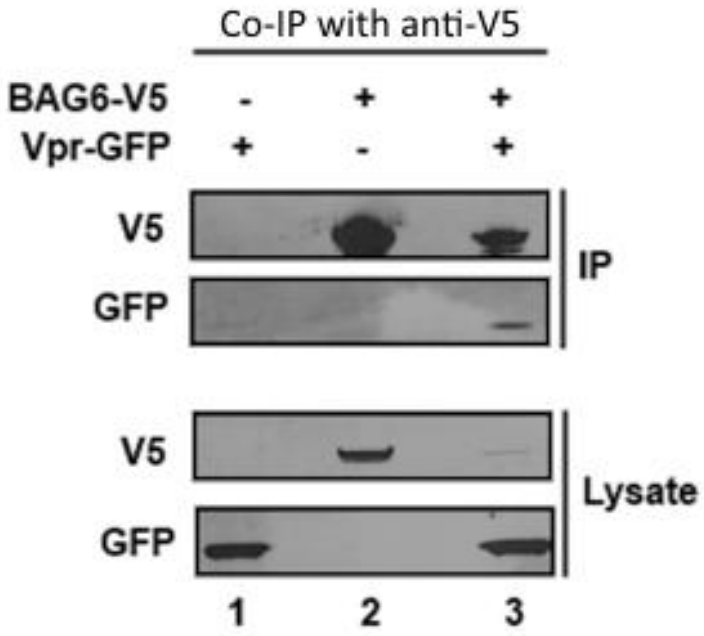

Figure 28. In the presence of Vpr, the ability of DCAF1 to degrade BAG6 is enhanced. 4x10^5 293T cells were plated in 6-well plates the day before transfection with 1.5ug BAG6-V5 (all lanes), 0.1ug DCAF1-FLAG (lane 2, 5, 6), 1.0ug Vpr-GFP (lanes 3 and 5), and 6ug VprQ65R-GFP (lanes 4and 6). Forty-eight hours later, immunoblotting with mouse anti-V5, anti-GFP, and anti-actin antibodies was performed.

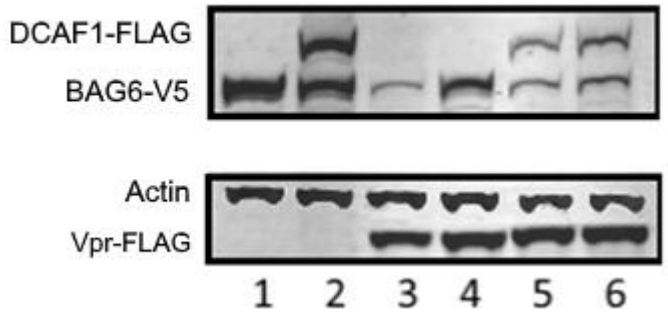

Figure 29. Inhibition of the proteasome reverses the ability of Vpr to degrade BAG6. $4x10^5$ 293T cells were plated in 6-well plates the day before transfection with 1ug pLX304-BAG6, 0.5ug Vpr-GFP, or 0.5ug VprQ65R-GFP as indicated below. 32 hours post-transfection. cells, as indicated, were treated with 20uM MG-132. 48 hours post-transfection, cell lysates were geenerated and immunoblotting was performed using anti V-5, anti-actin, and anti-GFP antibodies.

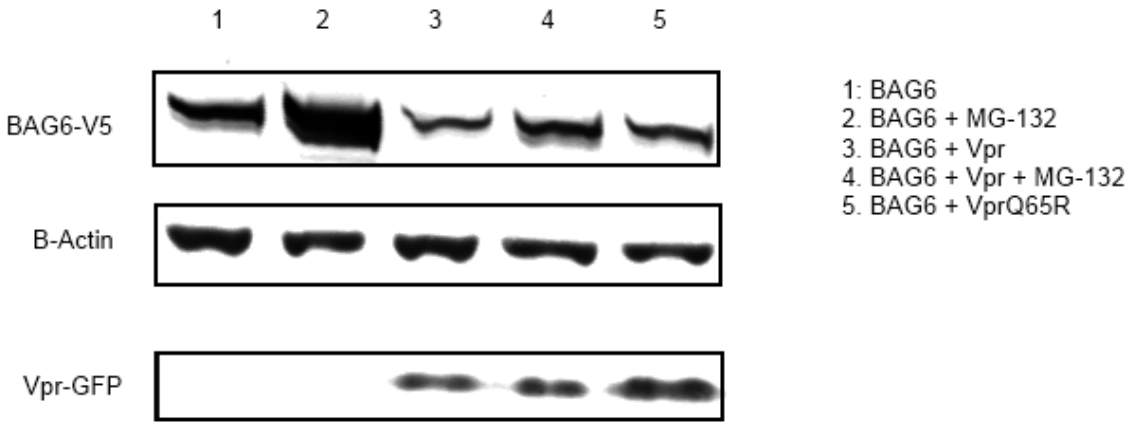

Figure 30. BAG6 co-immunoprecipitates with DCAF1. 293T 2x10^6 293T cells were plated in 10cm plates the day before transfection with BAG6-V5 (4ug in lanes 1 and 3) and DCAF1-FLAG (6ug in lanes 2 and 3), as depicted. 48 hours later, cell lysates were generated and used for Co-IP with rabbit anti-V5 antibody. IP and raw lysate samples were detected by immunoblotting with mouse anti-V5 or mouse anti-FLAG antibodies to detect BAG6 and DCAF1 expression, respectively.

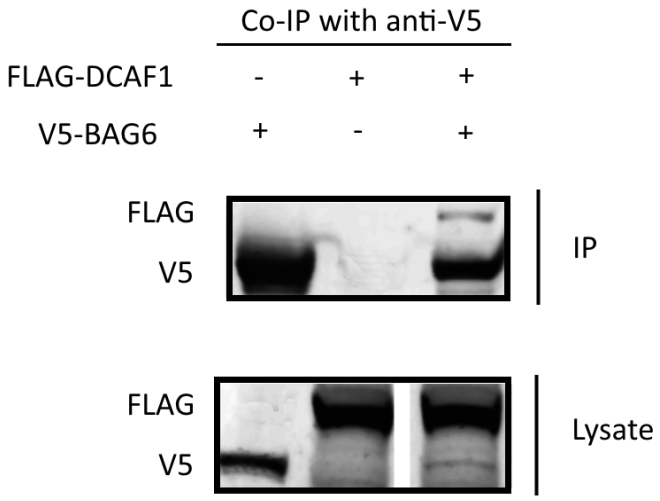

Figure 31. **Expression of BAG6 mutant proteins**. **(a)** $4x10^5$ 293T cells were plated in 6-well plates the day before transfection with 1ug each of BAG6-V5, ΔUBL-V5, ΔBAG-V5, ΔC-V5, or ΔN-V5. Forty-eight hours later, immunoblotting with mouse anti-V5, anti-GFP, and anti-actin antibodies was performed. **(b)** Effects of Increasing Amounts of Vpr on BAG6 mutant protein expression. 293T cells were transfected with 0.5ug BAG6-V5, 0.5ug ΔBAG-V5, 4ug ΔBAG, or 1ug ΔC-V5 (respective lanes 1), with 0.1ug Vpr-GFP (respective lanes 2), or with 0.3ug Vpr-GFP (respective lanes 3). Forty-eight hours later, immunoblotting was performed with the aforementioned antibodies. **(c)** ΔUBL is resistant to Vpr-mediated degradation. 293T cells were transfected with 0.5 ug of BAG6-V5 or ΔUBL-V5 together with either 0.1ug or 0.2ug of Vpr-GFP. Plotted are the expression levels of BAG6-V5 and ΔUBL-V5 as a function of increasing amounts of Vpr-GFP.

a.

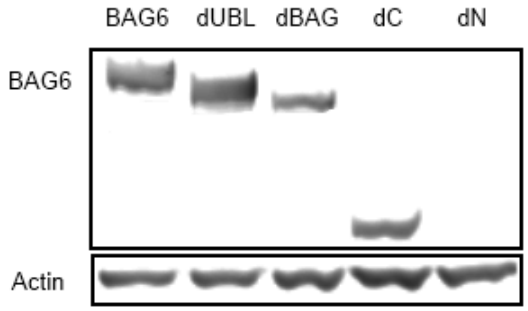

Figure 31, continued.

b.

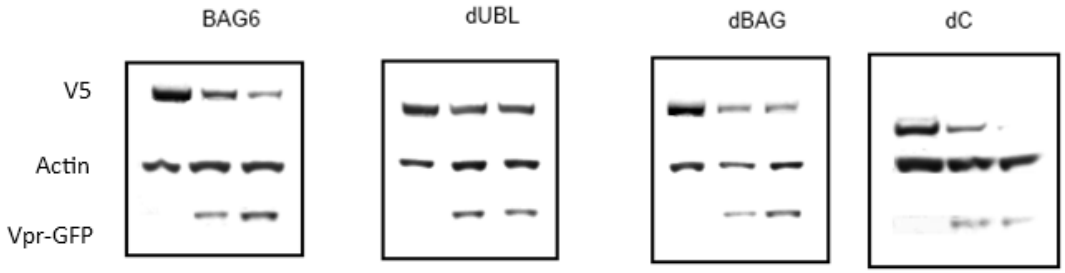

c.

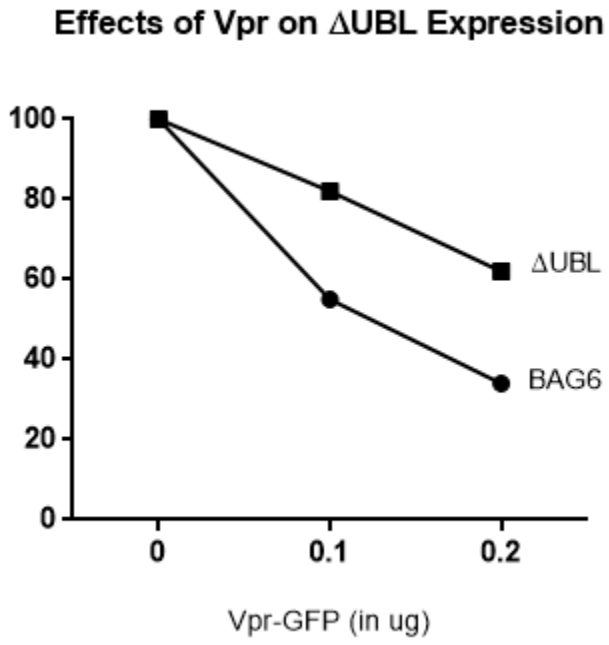

Figure 32. Diminished binding capacity of ΔUBL to DCAF1. A) 293T 2x10^6 293T cells were plated in 10cm plates the day before transfection with 4ug Vpr-GFP and 6ug BAG6-V5 (lane 1) or 4ug Vpr-GFP and 6ug ΔUBL-V5 (lane 2), as depicted. 48 hours later, cell lysates were generated and used for Co-IP with rabbit anti-V5 antibody. IP and raw lysate samples were detected by immunoblotting with mouse anti-V5 or mouse anti-FLAG antibodies to detect BAG6 and DCAF1 expression, respectively. B) In lane 1, 293T were transfected with 6ug DCAF1-FLAG and 6ug BAG6-V5; and 6ug DCAF1-FLAG and 6ug ΔUBL-V5 in lane 2. for Co-IP with rabbit anti-V5 antibody. IP and raw lysate samples were detected as above.

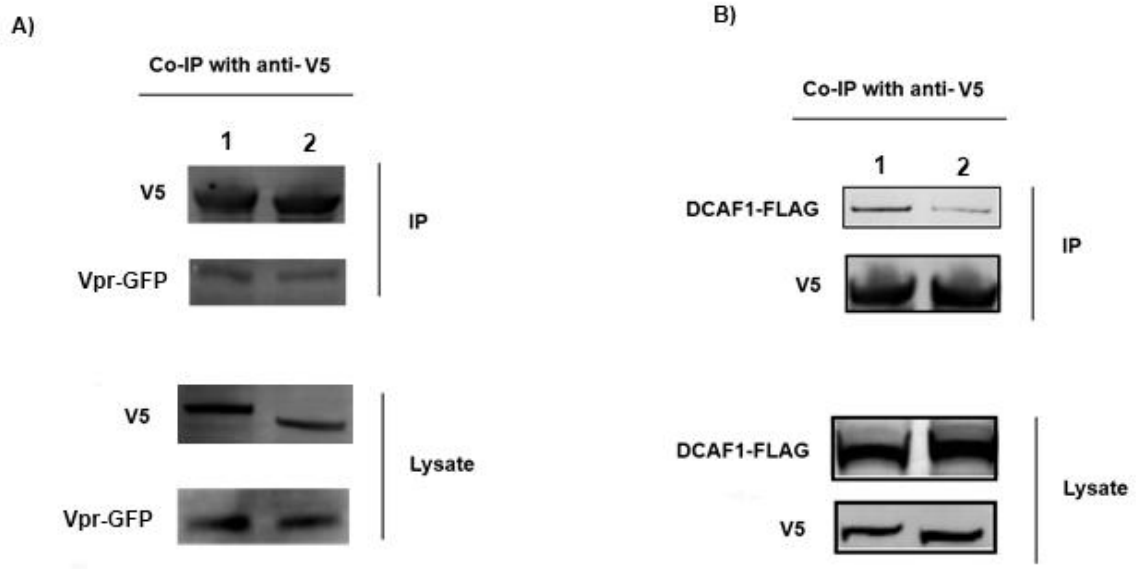

Figure 33. Effects of viral challenge on endogenous BAG6 during the early infection. $1x10^6$ Jurkat-pLKO control cells were seeded in 24-well plates in 1mL RPMI and pretreated with 75ug/mL cycloheximide (CHX) or DMSO vehicle for 30 minutes prior to challenge with HIV-GFP. Cells were then collected, pelleted, and frozen at -80°C at 0h, 2h, and 4h post-infection for the purpose of concurrent cell lysate generation the next day. Immunoblotting was then performed using anti-BAG6 and anti-actin antibodies to determine the effects of HIV-GFP on endogenous BAG6 expression. **(a)** Changes in BAG6 expression are plotted below as a percent of uninfected cells, which were set to 100%. (b) A representative western blot example of the decrease in endogenous BAG6 expression, revealed by CHX, in the presence of HIV-GFP.

a.

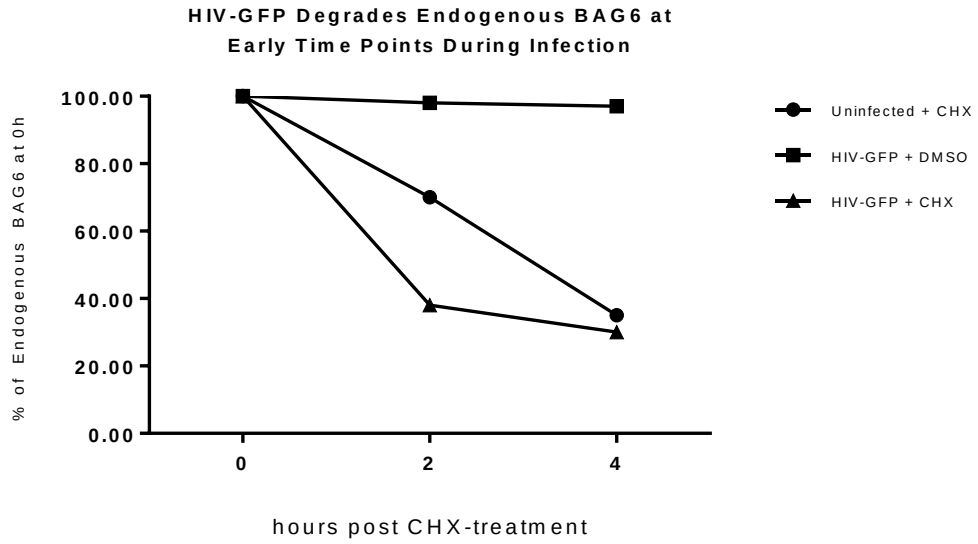

Figure 33, continued.

b.

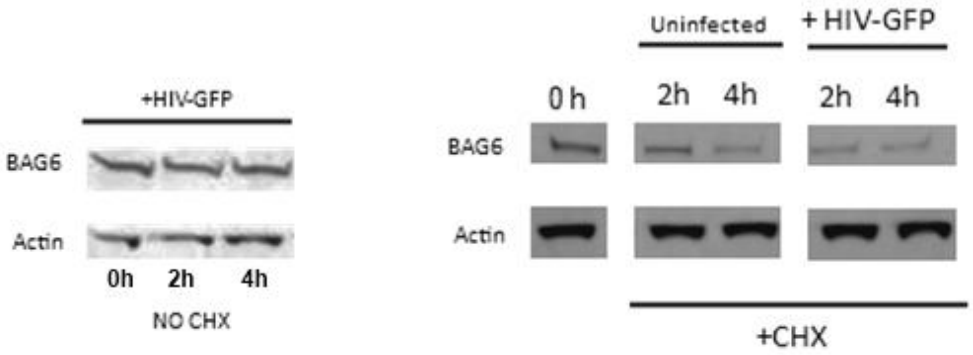

Figure 34. Proposed model for BAG6:Vpr interaction. Within the cytoplasm of the infected cell, Vpr tightly associates with the pre-integration complex as it undergoes reverse transcription concurrent with its translocation towards the nucleus for import. a) PIC-associated Vpr then binds to and ubiquitinates immediately proximal BAG6 for the purpose of enhancing the efficiency of the replication cycle in a hitherto unknown manner. b) In knockdown cells, BAG6 is no longer available to Vpr as a binding partner and its ubiquitination can no longer occur. Consequently, reduced efficiency of the replication cycle is observed.

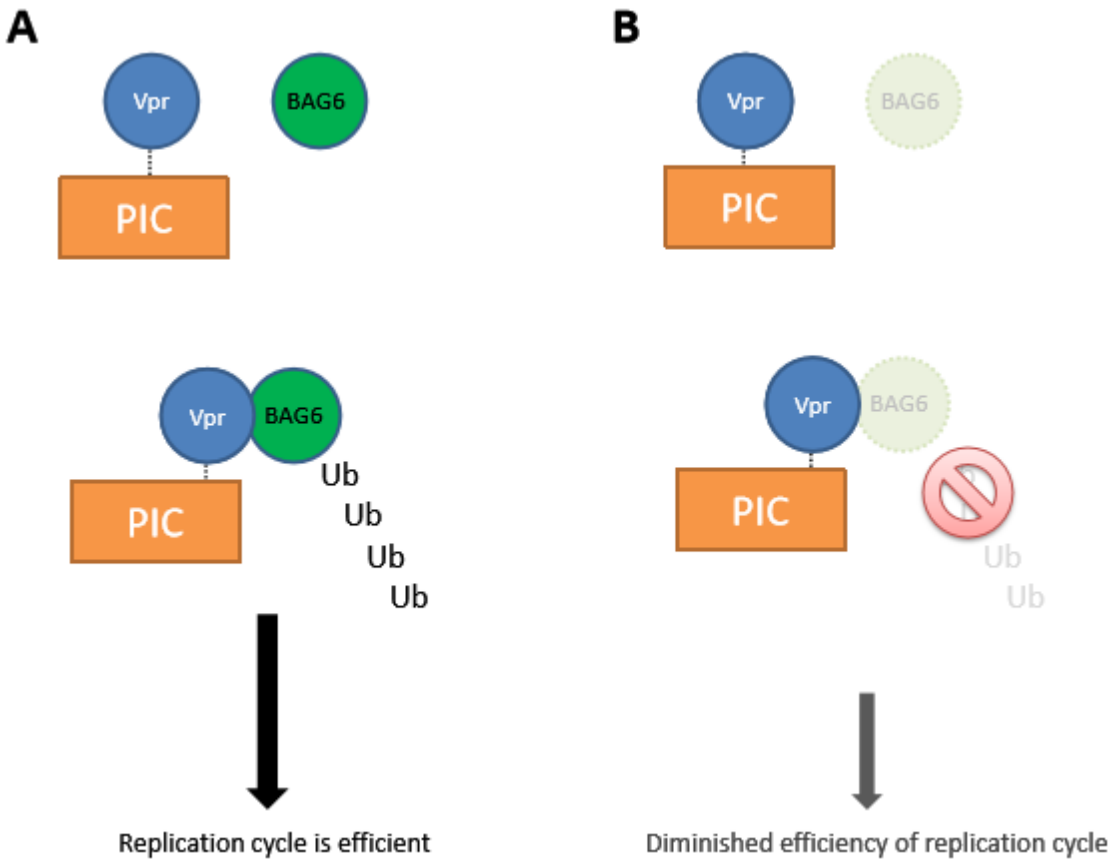

CHAPTER 4

DISCUSSION

The HIV/AIDS pandemic represents the greatest global health challenge in modern history. While HAART can effectively prolong life by controlling the HIV-1 infection and prevention of subsequent onset of AIDS, current treatment strategies have limitations. From an operational and logistical standpoint, providing over 30 million people globally with treatment for the duration of their lives poses a great, and quite possibly an unsustainable challenge (UNAIDS, 2016). Moreover, lifelong treatment adherence can be difficult for both economical and clinical reasons. Although rare, antiretroviral-drug resistance still poses a problem, particularly for those individuals who are unable to fully adhere to treatment. Drug toxicities, complex drug–drug interactions, and consequent immune dysfunction have substantial health consequences.

To that end, alternative strategies to inhibit HIV-1 replication, which supplement or even supplant current therapies are considered to be a very attractive goal worth pursuing. In theory, these endeavors may provide a so-called functional cure, whereby individuals can control their ongoing HIV-1 infection and prevent associated pathologies. Thus understanding how a virus only capable of encoding for a handful of viral proteins evolved in a manner that enables not only circumvention of the immune system, but also usurpation of normal cellular pathways is both fascinating from a biological standpoint and of the highest clinical relevance.

One such alternative approach to treatment is host-directed antiviral therapy that circumvents the emergence of viral resistance by targeting critical host component or

cellular pathways that HIV-1, as an obligate intracellular pathogen, intimately relies on. Thus by better characterizing host factors the virus usurps to its benefit, an unprecedented combination therapy encompassing numerous technological and biological advancements may be deployed. As HIV-1 infection is an exceedingly complex process whereby the virus utilizes many host cell processes to aid in its successful replication, all HIV-1 viral proteins are known to interact with at least one host protein (Lever and Jeang, 2011). Many potential interactions however have not yet been elucidated or are still poorly understood. Thus, there is a need to further investigate the relationship between viral proteins and host proteins, as the latter have already shown promise of being utilized as novel therapeutic targets (Dorr et al., 2005; Kellam et al., 2006). A concrete example of this paradigm shift whereby host protein activity is targeted by a drug as opposed to the pathogen is the fusion inhibitor maravircoc, a newer member of HAART, which binds to the HIV-1 co-receptor CCR5 and prevents virally mediated membrane fusion with the host cell (Dorr et al., 2005).

In spite of FDA-approved use of Marinol for treatment of HIV-associated anorexia, HIV-positive individuals have a higher prevalence of illicit cannabis use than that of the general population (Braitstein et al. 2001; Chitsaz et al. 2013; Furler et al. 2004; Harris et al. 2014). Although drug use generally correlates with non-adherence to HAART, which contributes to virological rebound, cannabis use in fact has not been linked to a decrease in HAART adherence (Ghosh et al. 2014; Kino and Chrousos, 2003; Slawson et al., 2015). In fact, several studies have shown cannabinoids to restrict HIV-1 replication and slow disease progression *in vitro* and *in vivo* (Peterson et al., 2004; Rock et al., 2007, Molina et al., 2010; Costantino et al., 2012; reviewed in Molina et al., 2015.

Such findings can be largely attributed to the pleiotropic on cells expression profiles these compounds have (Kaminski et al., 1998), adversely affecting the normal viral lifecycle. We thus sought to identify novel host factors that are both responsive to cannabinoid treatment and associated with HIV-1 replication, with the long-term goal that better characterization of the cellular factors implicated in the viral lifecycle may lead to the development of novel host-target antiretroviral therapies.

At the time when this project first began, the approach of leveraging still-new next-generation sequencing technology greatly facilitated host genome-wide investigations into HIV-1-dependency factors (Fellay et al., 2007; Brass et al. 2008, König et al., 2008; Zhou et al., 2008; Bushman et al., 2009). Hundreds of cellular proteins were revealed as prospective host factors utilized by HIV-1 in some capacity. Of course, many of these proposed factors were indeed false positives generated as an artifact of experimental variability among the various studies (Prussia, et al., 2011), confirming the importance of subsequent experimental validation using standard molecular approaches. Thus to characterize the broad effects of cannabinoids on viral infection, we utilized a targeted transcriptomic analysis approach, by means of RNA-Seq, to identify molecular regulatory mechanisms through which suppressive effects on HIV-1 infection may be occurring. From our results we confirmed the protective effects of cannabinoids on HIV-1 infection among T-cell lines (Table 1, and Figure 2). Moreover, we successfully identified well-scored hits among host factors that are both modulated by cannabinoids and important for HIV-1 replication (Table 2). Most importantly however, we were able to functionally validate our transcriptomic workflow by characterizing the role of the host factor BAG6 during infection, being the first group to do so.

Specifically, our data revealed that cannabinoids reduce BAG6 expression in T-cells (Figure 10). To study the individual importance of BAG6 within the infection context, we successfully generated stable BAG6-knockdown cells (Figure 14) and proceeded with their viral challenge. We were thus able to recapitulate the cannabinoid-mediated phenotype of restricted HIV-1 replication (Figures 16, 23, and 25). It is also very interesting to note that we observed a similar decrease in infection upon challenge of BAG6-knockdown cells compared to control cells with either replication-competent NL4-3 or replication-deficient HIV-GFP virus. We thus concluded that BAG6 knockdown in fact has effect on the early stages of the viral cycle, prior to the onset of the consequences of *env* deletion in the replication-deficient virus. And so through the targeted modulation of the expression of a single host protein, we were able reconstitute the effects of the broadly acting cannabinoids, revealing a potential mode of their action during viral challenge. More significantly however, we for the first time revealed the importance of BAG6 expression to the viral lifecycle.

Additionally, we were the first group to experimentally validate the findings of a mass-spectrometry study (Jäger et al., 2013) that had previously recognized BAG6 as a prospective binding partner to the HIV-1 viral accessory protein Vif (Figures 17 and 18). In fact, viral accessory proteins, as a field of study, truly gained prominence over the past 15 years with the discovery of the interaction between A3G and Vif. Since then, numerous other host restriction factors, many of which are very efficiently counteracted by viral proteins, had been identified (Abdel-Mohsen et al., 2013). We were however unable to appreciate, or study in further detail, the significance of the Vif:BAG6 interaction during viral challenge (Figures 23 and 25). With Vif being characterized

primarily within the context of its ability to degrade, by leveraging the host proteasome, the host restriction factor APOBEC3-G (Sheehy et al., 2002; reviewed in Feng et al., 2014), a factor not expressed in our cell model (Figure 20), it is not surprising that we could not detect differences in viral replication between challenge of BAG6-knockdown cells with wild-type or Vif-deficient virus. Of course, it is important to note that not every host factor serves as a restriction factor. Viral accessory viral proteins are oftentimes packaged within incoming virions and are key facilitators of the usurpation of host factors to the benefit of the virus, especially during the early stages of infection prior to integration and subsequent translation of viral proteins (Malim et al., 2008). And so we cannot exclude the possibility that the significance of the BAG6:Vif interaction becomes more apparent in virally challenged A3G-expressing, BAG6-knockdown cells. Thus it would be very interesting to study the interplay between these two proteins in other, more salient cell models to determine if an intricate complex of BAG6, A3G, and Vif exists. Intriguingly, a recent finding revealed an interplay between Vif and Vpr, another HIV-1 viral accessory protein, in their ability to degrade A3G (Zhou et al., 2015), in addition to reports of certain overlap in their functionalities (Wang et al., 2008; Wang et al., 2011). For that reason, we had decided to focus our efforts on determining the effect of Vpr on the infective capacity of the virus in BAG6 knockdown cells.

Fascinatingly, we determined that Vpr-deficient virus was less infectious than wild-type virus in knockdown cells, revealing the BAG6:Vpr interaction to be the key cellular protein - viral protein interaction in our infection model (Figure 30). Using overexpression experiments we next determined that BAG6 was bound to and degraded by Vpr (Figures 26 and 27). This effect of Vpr represented a novel, previously unreported

function of this viral accessory protein. In fact, Vpr had been shown to bind to only a handful of other host proteins, emphasizing the relatively limited knowledge base of its interactive capacity. Importantly, Vpr is known to mediate the proteasomal degradation of its binding partners through the recruitment of a cellular E3 ubiquitin ligase complex by utilizing the adapter protein DCAF1 (Schrofelbauer et al., 2005; Wen et al., 2012; reviewed by Guenzel et al., 2014). We not only determined that BAG6 degradation by Vpr is enhanced in the presence of DCAF1, but that DCAF1 alone binds to BAG6 and is sufficient to induce BAG6 degradation (Figures 28 and 30). Thus, the paradigm of Vpr usurping DCAF1 for the targeted degradation of a host protein can be applied to BAG6 as well (Wen et al., 2012; Maudet et al., 2013).

Taken together, our two major conclusions from this study are as follows: BAG6 knockdown reduces HIV-1 infection; and Vpr targets BAG6 for proteasomal degradation. At first glance, these two statements seem incongruous. After all, it would appear the end result is the same - a decrease in BAG6 at the protein level - regardless if it occurs via cannabinoids or shRNA, or if the virus actively promotes its destruction. Thus if the virus utilizes Vpr for BAG6 removal to its own benefit, why would a global reduction in BAG6 result in reduced infection? Does HIV-1 not prefer a cellular environment where BAG6 expression is minimal? To negotiate these conflicting results, we will provide our thoughts on two proposed hypotheses that explain the role of BAG6 in HIV-1 infection.

Our first hypothesis is that Vpr engages the host proteasome to ubiquitinate BAG6 not for the purposes of degradation of the latter, but for modification of its function, which will subsequently aid in the successful completion of the viral lifecycle. In fact, ubiqutination is not only meant for the degradation of proteins, but is also

important in regulating a broad host of cellular processes such as signal transduction, cell division, and protein trafficking (Mukhopadhyay and Riezman, 2007). Importantly, from our results we were never able to overtly detect any changes in global endogenous BAG6 expression upon viral challenge at any point during infection, be it early time points following viral challenge (Figure 33 and 34) or the full 6 days post infection. Thus by utilizing the *de novo* protein synthesis inhibitor cycloheximide we could specifically observe BAG6 protein expression at very early time point in the infection and effectively gauge what the effect of Vpr presence, if any, was on BAG6 turnover. In the absence of infection and, therefore of Vpr expression, the half-life of BAG6 was ~3 hours. A third of the original BAG6 amount degraded every two hours post-cycloheximide treatment, culminating with two-thirds gone by four hours. Presence of Vpr however accelerated the degradation of BAG6 such that two-thirds of the original amount of protein was already gone by two hours post-treatment, a two-fold increase over the rate of natural turnover of the protein. Thus under normal conditions, the rate of BAG6 turnover exceeds that of the modest ability of Vpr to selectively degrade it, hence there was always an effective "surplus" of BAG6 such that we could never examine the level of protein expression during infection without using cycloheximide. With Vpr being encapsidated within virions and being present in the cytosol during the early phases of the viral lifecycle, it is therefore possible that the interaction of BAG6 with Vpr is a localized one. After all, Vpr is known to associate with the capsid, as well as the RT and PIC complexes (Suzuki and Craigie, 2007). As Vpr is released into the cytoplasm during viral capsid uncoating, what the virus in fact may aim for is a localized microenvironment, proximal to capsid, that is rich in the ubiquitinated form of BAG6, which then helps to facilitate the normal

progression of the viral lifecycle, such as improving the efficiency of the reverse transcription process, or increasing the nuclear import rate of the pre-integration complex (Guenzel, et al., 2014). And so the degradation of BAG6, which we observe in our cell system, could simply be a side effect of ubiquitination, and not what the virus explicitly strives to achieve. With cannabinoid treatment or shRNA transduction the global levels of BAG6 are drastically decreased, with the cytoplasm becoming deficient for BAG6. Consequently, BAG6 is no longer available as a target for Vpr-mediated ubiquitination, resulting in reduced infection. Taken together, these findings suggest the existence of a physiological link between early events of the viral life cycle and the modification of BAG6 by virion-associated Vpr. Although it would be very interesting to study the exact interplay between virion-associated Vpr and endogenous BAG6 at very early times post viral entry, even with advanced visualization techniques such as fluorescence resonance energy transfer (FRET) microscopy, the relatively few hundred Vpr molecules incorporated within the virion may impose technical challenges (Lavallee et al., 1994; Bachand et al., 1999). Alternatively, identifying the residues on BAG6 to which Vpr mediates ubiquitin attachment could be a viable approach. In doing so, we could generate cell lines that express BAG6 incapable of being ubiquitinated by Vpr. By virally challenging these cells, we could then test the hypothesis that the process of BAG6 ubiquitination is beneficial to the virus, as here we would be expecting a decrease in infection, similarly as in BAG6 knockdown cells. Analogously, identifying residues within Vpr, which mediate binding to BAG6 and its subsequent ubiquitination, could also be accomplished. Thus by generating a virus expressing such a Vpr mutant, we would have yet another way of confirming our supposition.

Our second hypothesis is that the knockdown of BAG6 effectively removes its presence as a chaperoning protein from the cytoplasm, possibly permitting the cytoplasmic accumulation of an unidentified factor that is somehow detrimental to the virus. In fact, BAG6 is involved in the quality control of mislocalized or misfolded proteins (Minami et al., 2010; Hessa et al, 2011). It is hypothesized that this occurs by means of its "holdase" activity whereby certain aggregation-prone proteins are safely bound to and shuttled to appropriate cellular subcompartments for further processing (Lee and Ye, 2013; Rodrigo-Brenni et al., 2014). Knockdown of BAG6 may therefore permit accumulation of this putative factor within the cytoplasm and proximal to the incoming virion, with adverse consequences to viral infection. It is therefore possible that Vpr actually engages both BAG6, perhaps as a scaffolding protein, and DCAF1, as an adapter protein to the proteasome, for the purposes of enhancing the efficacy of targeted degradation of this unknown factor. Thus in the absence of BAG6, Vpr may still retain some capacity to directly engage DCAF1 for the clearance of this factor, perhaps through residual BAG6 expression in spite of effective protein ablation (Figure 14). In the absence of Vpr however, the virus cannot clear this factor efficiently, and therefore may be adversely affected by its accumulation. To test this hypothesis, we can characterize the interactome of BAG6 to determine which of the proteins BAG6 binds to is the putative factor. Pulldown experiments with BAG6 can be performed and complexes subsequently resolved on a native polyacrylamide gel to retain association between complex members. Binding partners can then be identified by mass spectrometry. By doing so, we may generate a list of numerous potential hits. By determining which of these hits most likely represents the kind of factor consistent with our data, i.e. one whose increased

concentration in the cytoplasm has deleterious effects on viral replication, we can perform systematic functional assays, such as targeted knockdown with shRNA, to decrease cytosolic concentration of these factors individually. By challenging these cells with wildtype or Vpr-deficient virus, we would be able to determine if the downregulation of any of these putatively adverse factors can restore Vpr-deficient replication to levels comparable to wildtype replication.

The ultimate purpose of this study was to establish a novel workflow utilizing biologically active compounds that exert pleiotropic modulatory effects, such as cannabinoids, that leverages modern transcripotomic techniques to identify novel host factors which are implicated in HIV-1 infection. By identifying cellular factors which are usurped by the virus to its advantage, as we have done so with BAG6, the hope is to develop novel treatments that target the immutable host instead of the ever-changing virus. Specifically, the introduction of a BAG6 dominant negative mutant protein which is either unable to bind to Vpr or is protected from Vpr-mediated degradation could also be a viable treatment option, especially in tandem with current HAART therapy. Alternatively, a pharmacological inhibitor of the BAG6:Vpr interaction could be introduced by gene therapy which would abrogate the consequences of this binding. In doing so, key steps of the viral replication cycle may be significantly hindered in a manner the highly mutagenic nature of the viral genome cannot overcome, as in the major concern with targeting the virus with current state-of-the-art approaches (Wang et al., 2016). Thus, current HAART regimens may be significantly altered in the future to encompass personalized treatment that caters on an individual-HIV-positive basis, and not with the broad strokes with which we attempt to aid HIV-affected individuals today.

BIBLIOGRAPHY

Abrams DI, Hilton JF, Leiser RJ et-al. Short-term effects of cannabinoids in patients with HIV-1 infection: a randomized, placebo-controlled clinical trial. Ann. Intern. Med. 2003;139 (4): 258-66.

Abdel-mohsen M, Raposo RA, Deng X, et al. Expression profile of host restriction factors in HIV-1 elite controllers. Retrovirology. 2013;10:106.

Abrams DI, Jay CA, Shade SB et-al. Cannabis in painful HIV-associated sensory neuropathy: a randomized placebo-controlled trial. Neurology. 2007;68 (7): 515-21.

Adachi A, Gendelman HE, Koenig S et-al. Production of acquired immunodeficiency syndrome-associated retrovirus in human and nonhuman cells transfected with an infectious molecular clone. J. Virol. 1986;59 (2): 284-91.

Adachi A, Gendelman HE, Koenig S, Folks T, Willey R, Rabson A, Martin MA. Production of acquired immunodeficiency syndrome-associated retrovirus in human and nonhuman cells transfected with an infectious molecular clone. J Virol 59:284-291, 1986.

Adamson CS, Freed EO. Novel approaches to inhibiting HIV-1 replication. Antiviral Res. 2010;85(1):119-41.

Aiken C. Viral and cellular factors that regulate HIV-1 uncoating. Curr Opin HIV AIDS. 2006;1(3):194-9.

Angers, S., Li, T., Yi, X., MacCoss, M.J., Moon, R.T., Zheng, N. Molecular architecture and assembly of the DDB1-CUL4A ubiquitin ligase machinery. Nature Letters, 443; pp. 590-593 (2006).

Arhel N, Genovesio A, Kim KA, et al. Quantitative four-dimensional tracking of cytoplasmic and nuclear HIV-1 complexes. Nat Methods. 2006;3(10):817-24.

Arhel N, Kirchhoff F. Host proteins involved in HIV infection: new therapeutic targets. Biochim Biophys Acta. 2010;1802(3):313-21.

Arhel N. Revisiting HIV-1 uncoating. Retrovirology. 2010;7:96.

Ashburner M, Ball CA, Blake JA et-al. Gene ontology: tool for the unification of biology. The Gene Ontology Consortium. Nat. Genet. 2000;25 (1): 25-9.

Bacchetti P, Moss AR. Incubation period of AIDS in San Francisco. Nature. 1989;338(6212):251-3.

Balliet JW, Kolson DL, Eiger G, et al. Distinct effects in primary macrophages and lymphocytes of the human immunodeficiency virus type 1 accessory genes vpr, vpu, and nef: mutational analysis of a primary HIV-1 isolate. Virology. 1994;200(2):623-31.

Balter, M. How Does HIV Overcome the Body's T Cell Bodyguards?Science , New Series, Vol. 278, No. 5342 (Nov. 21, 1997), pp. 1399-1400.

Baltimore, David. Expression of animal virus genomes. Bacteriol Rev. 1971;35(3):23541
Banerji J, Sands J, Strominger JL, Spies T. A gene pair from the human major histocompatibility complex encodes large proline-rich proteins with multiple repeated motifs and a single ubiquitin-like domain. Proc Natl Acad Sci USA. 1990;87(6):2374-8.

Bangsberg DR, Hecht FM, Charlebois ED, et al. Adherence to protease inhibitors, HIV-1 viral load, and development of drug resistance in an indigent population. AIDS. 2000;14(4):357-66.

Berger EA. Introduction: HIV co-receptors solve old questions and raise many new ones. Semin Immunol. 1998;10(3):165-8.

Binici J, Koch J. BAG-6, a jack of all trades in health and disease. Cell Mol Life Sci. 2014;71(10):1829-37.

Boden D, Hurley A, Zhang L, et al. HIV-1 drug resistance in newly infected individuals. JAMA. 1999;282(12):1135-41.

Braitstein P, Kendall T, Chan K, et al. Mary-Jane and her patients: sociodemographic and clinical characteristics of HIV-positive individuals using medical marijuana and antiretroviral agents. AIDS. 2001;15(4):532-3.

Brass AL, Dykxhoorn DM, Benita Y et-al. Identification of host proteins required for HIV infection through a functional genomic screen. Science. 2008;319 (5865): 921-6.
Bredt BM, Higuera-alhino D, Shade SB et-al. Short-term effects of cannabinoids on immune phenotype and function in HIV-1-infected patients. J Clin Pharmacol. 2002;42 (11 Suppl): 82S-89S.

Burdo TH, Lackner A, Williams KC. Monocyte/macrophages and their role in HIV neuropathogenesis. Immunol Rev. 2013;254(1):102-13.

Busch MP, Satten GA. Time course of viremia and antibody seroconversion following human immunodeficiency virus exposure. Am J Med. 1997;102(5B):117-24.

Bushman FD, Craigie R. Activities of human immunodeficiency virus (HIV) integration protein in vitro: specific cleavage and integration of HIV DNA. Proc Natl Acad Sci USA. 1991;88(4):1339-43.

Bushman FD, Malani N, Fernandes J et-al. Host cell factors in HIV replication: meta-analysis of genome-wide studies. PLoS Pathog. 2009;5 (5): e1000437.

Buzon MJ, Martin-gayo E, Pereyra F, et al. Long-term antiretroviral treatment initiated at primary HIV-1 infection affects the size, composition, and decay kinetics of the reservoir of HIV-1-infected CD4 T cells. J Virol. 2014;88(17):10056-65.

Cabral GA, Griffin-thomas L. Emerging role of the cannabinoid receptor CB2 in immune regulation: therapeutic prospects for neuroinflammation. Expert Rev Mol Med. 2009;11 : e3.

Casey klockow L, Sharifi HJ, Wen X, et al. The HIV-1 protein Vpr targets the endoribonuclease Dicer for proteasomal degradation to boost macrophage infection. Virology. 2013;444(1-2):191-202.

Catz SL, Kelly JA, Bogart LM, et al. Patterns, correlates, and barriers to medication adherence among persons prescribed new treatments for HIV disease. Health Psychol. 2000;19:124-133.

Chaisson RE, Osmond D, Moss AR, Feldman HW, Bernacki P. HIV, bleach, and needle sharing. Lancet. 1987;1(8547):1430.

Chan DC, Fass D, Berger JM, Kim PS. Core structure of gp41 from the HIV envelope glycoprotein. Cell. 1997;89(2):263-73.
Chang L-J, Urlacher V, Iwakuma T, Cui Y, Zucali J. Efficacy and safety analyses of a recombinant human immunodeficiency virus type 1 derived vector system. Gene Ther 6:715?728, 1999.

Charneau P, Alizon M, Clavel F. A second origin of DNA plus-strand synthesis is required for optimal human immunodeficiency virus replication. J Virol. 1992;66(5):2814-20.

Charneau P, Mirambeau G, Roux P, Paulous S, Buc H, Clavel F. HIV-1 reverse transcription. A termination step at the center of the genome. J Mol Biol. 1994;241(5):651-62.

Charo IF, Ransohoff RM. The many roles of chemokines and chemokine receptors in inflammation. N. Engl. J. Med. 2006;354 (6): 610-21.

Chitsaz E, Meyer JP, Krishnan A, et al. Contribution of substance use disorders on HIV treatment outcomes and antiretroviral medication adherence among HIV-infected persons entering jail. AIDS Behav. 2013;17 Suppl 2:S118-27.

Chu C, Selwyn PA. Complications of HIV infection: a systems-based approach. Am Fam Physician. 2011;83 (4): 395-406.

Chun TW, Justement JS, Murray D, et al. Rebound of plasma viremia following cessation of antiretroviral therapy despite profoundly low levels of HIV reservoir: implications for eradication. AIDS. 2010;24(18):2803-8.

Chun TW, Stuyver L, Mizell SB, et al. Presence of an inducible HIV-1 latent reservoir during highly active antiretroviral therapy. Proc Natl Acad Sci USA. 1997;94(24):13193-7.

Ciechanover A, Elias S, Heller H, Hershko A. "Covalent affinity" purification of ubiquitin-activating enzyme. J Biol Chem. 1982;257(5):2537-42.

Clever J, Sassetti C, Parslow TG. RNA secondary structure and binding sites for gag gene products in the 5' packaging signal of human immunodeficiency virus type 1. J Virol. 1995;69(4):2101-9.

Coiras M, López-huertas MR, Pérez-olmeda M, Alcamí J. Understanding HIV-1 latency provides clues for the eradication of long-term reservoirs. Nat Rev Microbiol. 2009;7(11):798-812.

Compton AA, Hirsch VM, Emerman M. The host restriction factor APOBEC3G and retroviral Vif protein coevolve due to ongoing genetic conflict. Cell Host Microbe. 2012;11(1):91-8.

Costantino CM, Gupta A, Yewdall AW et-al. Cannabinoid receptor 2-mediated attenuation of CXCR4-tropic HIV infection in primary CD4+ T cells. PLoS ONE. 2012;7 (3): e33961.

Dalgleish AG, Beverley PC, Clapham PR, Crawford DH, Greaves MF, Weiss RA. The CD4 (T4) antigen is an essential component of the receptor for the AIDS retrovirus. Nature. 1984;312(5996):763-7.

Deeks SG, Lewin SR, Havlir DV. The end of AIDS: HIV infection as a chronic disease. Lancet. 2013;382(9903):1525-33.

DeHart, J.L., Zimmerman, E.S., Ardon, O., Monteiro-Filho, C.M.R., Arganaraz, E.R., Planelles, V. HIV-1 Vpr activates the G2 checkpoint through manipulation of the ubiquitin proteasome system. Virology Journal (2007).

Del portillo A, Tripodi J, Najfeld V, Wodarz D, Levy DN, Chen BK. Multiploid inheritance of HIV-1 during cell-to-cell infection. J Virol. 2011;85(14):7169-76.
Demuth DG, Molleman A. Cannabinoid signalling. Life Sci. 2006;78 (6): 549-63.
Deng H, Liu R, Ellmeier W, et al. Identification of a major co-receptor for primary isolates of HIV-1. Nature. 1996;381(6584):661-6.

Doong H, Vrailas A, Kohn EC. What's in the 'BAG'?--A functional domain analysis of the BAG-family proteins. Cancer Lett. 2002;188(1-2):25-32.

Dorr P, Westby M, Dobbs S et-al. Maraviroc (UK-427,857), a potent, orally bioavailable, and selective small-molecule inhibitor of chemokine receptor CCR5 with broad-spectrum anti-human immunodeficiency virus type 1 activity. Antimicrob. Agents Chemother. 2005;49 (11): 4721-32.

Dorr P, Westby M, Dobbs S, et al. Maraviroc (UK-427,857), a potent, orally bioavailable, and selective small-molecule inhibitor of chemokine receptor CCR5 with broad-spectrum anti-human immunodeficiency virus type 1 activity. Antimicrob Agents Chemother. 2005;49(11):4721-32.

Dragic T, Litwin V, Allaway GP et-al. HIV-1 entry into CD4+ cells is mediated by the chemokine receptor CC-CKR-5. Nature. 1996;381 (6584): 667-73.

Dybul M. Approaches to interrupting HAART for the treatment of HIV infection. IAPAC sessions 2001, July 18-19, 2001 - Chicago. IAPAC Mon. 2001;7(8):232-4.

Elsohly, M.A. (2002). Chemical constituents of cannabis. In:Cannabis and Cannabinoids. Pharmacology, Toxicology and Therapeutic Potential. eds. Grotenherm en, F. & Russo, E. pp. 27–36. NewYork: Haworth Press Inc.

Engelman A, Mizuuchi K, Craigie R. HIV-1 DNA integration: mechanism of viral DNA cleavage and DNA strand transfer. Cell. 1991;67(6):1211-21.

Fellay J, Shianna KV, Ge D et-al. A whole-genome association study of major determinants for host control of HIV-1. Science. 2007;317 (5840): 944-7.

Feng Y, Broder CC, Kennedy PE, Berger EA. HIV-1 entry cofactor: functional cDNA cloning of a seven-transmembrane, G protein-coupled receptor. Science. 1996;272(5263):872-7.

Finzi D, Hermankova M, Pierson T, et al. Identification of a reservoir for HIV-1 in patients on highly active antiretroviral therapy. Science. 1997;278(5341):1295-300.

Fischl MA, Richman DD, Grieco MH et-al. The efficacy of azidothymidine (AZT) in the treatment of patients with AIDS and AIDS-related complex. A double-blind, placebo-controlled trial. N. Engl. J. Med. 1987;317 (4): 185-91.

Flexner C. HIV drug development: the next 25 years. Nat Rev Drug Discov. 2007;6(12):959-66.

Forsman A, Weiss RA. Why is HIV a pathogen?. Trends Microbiol. 2008;16(12):555-60.
Frankel AD, Young JA. 1998. HIV-1: fifteen proteins and an RNA. Annu Rev Biochem 67: 1–25

Furler MD, Einarson TR, Millson M, Walmsley S, Bendayan R. Medicinal and recreational marijuana use by patients infected with HIV. AIDS Patient Care STDS. 2004;18(4):215-28.

Galiègue S, Mary S, Marchand J et-al. Expression of central and peripheral cannabinoid receptors in human immune tissues and leukocyte subpopulations. Eur. J. Biochem. 1995;232 (1): 54-61.

Gallaher WR. Detection of a fusion peptide sequence in the transmembrane protein of human immunodeficiency virus. Cell. 1987;50(3):327-8.

Gallay P, Swingler S, Song J, Bushman F, Trono D. HIV nuclear import is governed by the phosphotyrosine-mediated binding of matrix to the core domain of integrase. Cell. 1995;83(4):569-76.

Gea-banacloche JC, Migueles SA, Martino L, et al. Maintenance of large numbers of virus-specific CD8+ T cells in HIV-infected progressors and long-term nonprogressors. J Immunol. 2000;165(2):1082-92.

Gelderblom HR, Gentile M, Scheidler A, Özel M, Pauli G. Zur Struktur und Funktion bei HIV. AIFO 1993, 5: 231.

Gheysen D, Jacobs E, De foresta F, et al. Assembly and release of HIV-1 precursor Pr55gag virus-like particles from recombinant baculovirus-infected insect cells. Cell. 1989;59(1):103-12.

Ghosh S, Preet A, Groopman JE et-al. Cannabinoid receptor CB2 modulates the CXCL12/CXCR4-mediated chemotaxis of T lymphocytes. Mol. Immunol. 2006;43 (14): 2169-79.

Gibbs JS, Regier DA, Desrosiers RC. Construction and in vitro properties of HIV-1 mutants with deletions in "nonessential" genes. AIDS Res Hum Retroviruses 10:343-350, 1994.

Glass M, Dragunow M, Faull RL. Cannabinoid receptors in the human brain: a detailed anatomical and quantitative autoradiographic study in the fetal, neonatal and adult human brain. Neuroscience. 1997;77 (2): 299-318.

Goff SP. Host factors exploited by retroviruses. Nat Rev Microbiol. 2007;5(4):253-63.
Goh WC, Rogel ME, Kinsey CM, et al. HIV-1 Vpr increases viral expression by manipulation of the cell cycle: a mechanism for selection of Vpr in vivo. Nat Med. 1998;4(1):65-71.

Goodenow M, Huet T, Saurin W, Kwok S, Sninsky J, Wain-hobson S. HIV-1 isolates are rapidly evolving quasispecies: evidence for viral mixtures and preferred nucleotide substitutions. J Acquir Immune Defic Syndr. 1989;2(4):344-52.

Gorter R., Seefried M., Volberding P. (1992). Dronabinol effects on weight in patients with HIV infection. AIDS;6(1):127.

Gramberg T, Sunseri N, Landau NR. Accessories to the crime: recent advances in HIV accessory protein biology. Curr HIV/AIDS Rep. 2009;6(1):36-42.

Gray F, Adle-biassette H, Chretien F et-al. Neuropathology and neurodegeneration in human immunodeficiency virus infection. Pathogenesis of HIV-induced lesions of the brain, correlations with HIV-associated disorders and modifications according to treatments. Clin. Neuropathol. 20 (4): 146-55.

Grulich AE, Van leeuwen MT, Falster MO et-al. Incidence of cancers in people with HIV/AIDS compared with immunosuppressed transplant recipients: a meta-analysis. Lancet. 2007;370 (9581): 59-67.

Guenzel CA, Hérate C, Benichou S. HIV-1 Vpr-a still "enigmatic multitasker". Front Microbiol. 2014;5:127.

Guss DA. The acquired immune deficiency syndrome: an overview for the emergency physician, Part 1. J Emerg Med. 12 (3): 375-84.

Haas AL, Bright PM, Jackson VE. Functional diversity among putative E2 isozymes in the mechanism of ubiquitin-histone ligation. J Biol Chem. 1988;263(26):13268-75.
Haffar OK, Popov S, Dubrovsky L, et al. Two nuclear localization signals in the HIV-1 matrix protein regulate nuclear import of the HIV-1 pre-integration complex. J Mol Biol. 2000;299(2):359-68.

Hakre S, Chavez L, Shirakawa K, Verdin E. Epigenetic regulation of HIV latency. Curr Opin HIV AIDS. 2011;6(1):19-24.

Hall HI, Holtgrave DR, Maulsby C. HIV transmission rates from persons living with HIV who are aware and unaware of their infection. AIDS. 2012;26(7):893-6.

Hallenberger S, Bosch V, Angliker H, Shaw E, Klenk HD, Garten W. Inhibition of furin-mediated cleavage activation of HIV-1 glycoprotein gp160. Nature. 1992;360(6402):358-61.

Harris RS, Hultquist JF, Evans DT. The restriction factors of human immunodeficiency virus. J Biol Chem. 2012;287(49):40875-83.

He J, Choe S, Walker R, Di marzio P, Morgan DO, Landau NR. Human immunodeficiency virus type 1 viral protein R (Vpr) arrests cells in the G2 phase of the cell cycle by inhibiting p34cdc2 activity. J Virol. 1995;69(11):6705-11.

Hecht FM, Busch MP, Rawal B, et al. Use of laboratory tests and clinical symptoms for identification of primary HIV infection. AIDS. 2002;16(8):1119-29.

Hecht FM. Measuring HIV treatment adherence in clinical practice. AIDS Clin Care. 1998;10(8):57-9.

Heinzinger NK, Bukrinsky MI, Haggerty SA, et al. The Vpr protein of human immunodeficiency virus type 1 influences nuclear localization of viral nucleic acids in nondividing host cells. Proc Natl Acad Sci USA. 1994;91(15):7311-5.

Hershko A. The ubiquitin pathway of protein degradation and proteolysis of ubiquitin-protein conjugates. Biochem Soc Trans. 1991;19(3):726-9.

Hessa T, Sharma A, Mariappan M, Eshleman HD, Gutierrez E, Hegde RS. Protein targeting and degradation are coupled for elimination of mislocalized proteins. Nature. 2011;475(7356):394-7.

Hopkins AL, Groom CR. Target analysis: a priori assessment of druggability. Ernst Schering Res Found Workshop. 2003;(42):11-7.

Howlett AC, Barth F, Bonner TI et-al. International Union of Pharmacology. XXVII. Classification of cannabinoid receptors. Pharmacol. Rev. 2002;54 (2): 161-202.

Howlett AC, Johnson MR, Melvin LS et-al. Nonclassical cannabinoid analgetics inhibit adenylate cyclase: development of a cannabinoid receptor model. Mol. Pharmacol. 1988;33 (3): 297-302.

Hoxie JA, June CH. Novel cell and gene therapies for HIV. Cold Spring Harb Perspect Med. 2012;2(10)

Hrecka K, Gierszewska M, Srivastava S, et al. Lentiviral Vpr usurps Cul4-DDB1[VprBP] E3 ubiquitin ligase to modulate cell cycle. Proc Natl Acad Sci USA. 2007;104(28):11778-83.

Hrecka K, Hao C, Gierszewska M, et al. Vpx relieves inhibition of HIV-1 infection of macrophages mediated by the SAMHD1 protein. Nature. 2011;474(7353):658-61.

Huang Y, Paxton WA, Wolinsky SM, et al. The role of a mutant CCR5 allele in HIV-1 transmission and disease progression. Nat Med. 1996;2(11):1240-3.

Hübner A, Kruhoffer M, Grosse F, Krauss G. Fidelity of human immunodeficiency virus type I reverse transcriptase in copying natural RNA. J Mol Biol. 1992;223(3):595-600.

Hugen PW, Burger DM, Aarnoutse RE, et al. Therapeutic drug monitoring of HIV-protease inhibitors to assess noncompliance. Ther Drug Monit. 2002;24(5):579-87.

Jäger S, Cimermancic P, Gulbahce N, et al. Global landscape of HIV-human protein complexes. Nature. 2012;481(7381):365-70.

Jegede O, Babu J, Di santo R, Mccoll DJ, Weber J, Quiñones-mateu M. HIV type 1 integrase inhibitors: from basic research to clinical implications. AIDS Rev. 2008;10(3):172-89.

Jolly C, Sattentau QJ. Retroviral spread by induction of virological synapses. Traffic. 2004;5(9):643-50.

Jowett JB, Planelles V, Poon B, Shah NP, Chen ML, Chen IS. The human immunodeficiency virus type 1 vpr gene arrests infected T cells in the G2 + M phase of the cell cycle. J Virol. 1995;69(10):6304-13
.
Kaminski NE. Regulation of the cAMP cascade, gene expression and immune function by cannabinoid receptors. J. Neuroimmunol. 1998;83 (1-2): 124-32.
Kawahara H, Minami R, Yokota N. BAG6/BAT3: emerging roles in quality control for nascent polypeptides. J Biochem. 2013;153(2):147-60.

Kellam P, Weiss RA. Infectogenomics: insights from the host genome into infectious diseases. Cell. 2006;124 (4): 695-7.

Kellam P. Attacking pathogens through their hosts. Genome Biol. 2006;7(1):201.
King RW, Deshaies RJ, Peters JM, Kirschner MW. How proteolysis drives the cell cycle. Science. 1996;274(5293):1652-9.

Kino T, Chrousos GP. AIDS-related insulin resistance and lipodystrophy syndrome. Curr Drug Targets Immune Endocr Metabol Disord. 2003;3(2):111-7.

Klein TW, Newton C, Larsen K et-al. Cannabinoid receptors and T helper cells. J. Neuroimmunol. 2004;147 (1-2): 91-4.

Klein TW, Newton C, Larsen K et-al. The cannabinoid system and immune modulation. J. Leukoc. Biol. 2003;74 (4): 486-96.

Klein TW, Newton CA, Nakachi N et-al. Delta 9-tetrahydrocannabinol treatment suppresses immunity and early IFN-gamma, IL-12, and IL-12 receptor beta 2 responses to Legionella pneumophila infection. J. Immunol. 2000;164 (12): 6461-6.

König R, Zhou Y, Elleder D et-al. Global analysis of host-pathogen interactions that regulate early-stage HIV-1 replication. Cell. 2008;135 (1): 49-60.

Laguette N, Benkirane M. How SAMHD1 changes our view of viral restriction. Trends Immunol. 2012;33(1):26-33.

Laguette N, Brégnard C, Hue P, et al. Premature activation of the SLX4 complex by Vpr promotes G2/M arrest and escape from innate immune sensing. Cell. 2014;156(1-2):134-45.

Lahouassa H, Daddacha W, Hofmann H, et al. SAMHD1 restricts the replication of human immunodeficiency virus type 1 by depleting the intracellular pool of deoxynucleoside triphosphates. Nat Immunol. 2012;13(3):223-8.

Le rouzic E, Belaïdouni N, Estrabaud E, et al. HIV1 Vpr arrests the cell cycle by recruiting DCAF1/VprBP, a receptor of the Cul4-DDB1 ubiquitin ligase. Cell Cycle. 2007;6(2):182-8.

Le rouzic E, Morel M, Ayinde D, et al. Assembly with the Cul4A-DDB1DCAF1 ubiquitin ligase protects HIV-1 Vpr from proteasomal degradation. J Biol Chem. 2008;283(31):21686-92.

Lecapitaine NJ, Zhang P, Winsauer P et-al. Chronic Δ-9-tetrahydrocannabinol administration increases lymphocyte CXCR4 expression in rhesus macaques. J Neuroimmune Pharmacol. 2011;6 (4): 540-5.

Lee JG, Ye Y. Bag6/Bat3/Scythe: a novel chaperone activity with diverse regulatory functions in protein biogenesis and degradation. Bioessays. 2013;35(4):377-85.
Lever AM, Jeang KT. Insights into cellular factors that regulate HIV-1 replication in human cells. Biochemistry. 2011;50 (6): 920-31.

Lever AM, Jeang KT. Insights into cellular factors that regulate HIV-1 replication in human cells. Biochemistry. 2011;50(6):920-31.

Li J, Xu F, Hu S, et al. Characterization of the interactions between SIVrcm Vpx and red-capped mangabey SAMHD1. Biochem J. 2015;468(2):303-13.

Liu K, Lu H, Hou L, et al. Design, synthesis, and biological evaluation of N-carboxyphenylpyrrole derivatives as potent HIV fusion inhibitors targeting gp41. J Med Chem. 2008;51(24):7843-54.

Low-beer S, Yip B, O'shaughnessy MV, Hogg RS, Montaner JS. Adherence to triple therapy and viral load response. J Acquir Immune Defic Syndr. 2000;23(4):360-1.

Lum JJ, Cohen OJ, Nie Z, et al. Vpr R77Q is associated with long-term nonprogressive HIV infection and impaired induction of apoptosis. J Clin Invest. 2003;111(10):1547-54.

M. Day: Patient Adherence To HAART Regimens: Challenges For Physician Assistants And Health Care Providers. The Internet Journal of Academic Physician Assistants. 2003 Volume 3 Number 1. DOI: 10.5580/2063

Malim MH, Bieniasz PD. HIV Restriction Factors and Mechanisms of Evasion. Cold Spring Harb Perspect Med. 2012;2(5):a006940.
Malim MH, Emerman M. HIV-1 accessory proteins--ensuring viral survival in a hostile environment. Cell Host Microbe. 2008;3(6):388-98.

Malim MH. APOBEC proteins and intrinsic resistance to HIV-1 infection. Philos Trans R Soc Lond, B, Biol Sci. 2009;364(1517):675-87.

Manel N, Hogstad B, Wang Y, Levy DE, Unutmaz D, Littman DR. A cryptic sensor for HIV-1 activates antiviral innate immunity in dendritic cells. Nature. 2010;467(7312):214-7.

Mangeat B, Turelli P, Caron G, Friedli M, Perrin L, Trono D. Broad antiretroviral defence by human APOBEC3G through lethal editing of nascent reverse transcripts. Nature. 2003;424(6944):99-103.

Margottin F, Bour SP, Durand H, et al. A novel human WD protein, h-beta TrCp, that interacts with HIV-1 Vpu connects CD4 to the ER degradation pathway through an F-box motif. Mol Cell. 1998;1(4):565-74.

Maudet C, Sourisce A, Dragin L, et al. HIV-1 Vpr induces the degradation of ZIP and sZIP, adaptors of the NuRD chromatin remodeling complex, by hijacking DCAF1/VprBP. PLoS ONE. 2013;8(10):e77320.

Mcdonald D, Vodicka MA, Lucero G, et al. Visualization of the intracellular behavior of HIV in living cells. J Cell Biol. 2002;159(3):441-52.

Mcnabb J, Ross JW, Abriola K, Turley C, Nightingale CH, Nicolau DP. Adherence to highly active antiretroviral therapy predicts virologic outcome at an inner-city human immunodeficiency virus clinic. Clin Infect Dis. 2001;33(5):700-5.

Mcnamara LA, Collins KL. Hematopoietic stem/precursor cells as HIV reservoirs. Curr Opin HIV AIDS. 2011;6(1):43-8.

Melikyan GB, Markosyan RM, Hemmati H, Delmedico MK, Lambert DM, Cohen FS. Evidence that the transition of HIV-1 gp41 into a six-helix bundle, not the bundle configuration, induces membrane fusion. J Cell Biol. 2000;151(2):413-23.

Minagar A, Commins D, Alexander JS et-al. NeuroAIDS: characteristics and diagnosis of the neurological complications of AIDS. Mol Diagn Ther. 2008;12 (1): 25-43.
Minami R, Hayakawa A, Kagawa H, Yanagi Y, Yokosawa H, Kawahara H. BAG-6 is essential for selective elimination of defective proteasomal substrates. J Cell Biol. 2010;190(4):637-50.

Mocroft A, Ledergerber B, Katlama C, et al. Decline in the AIDS and death rates in the EuroSIDA study: an observational study. Lancet. 2003;362(9377):22-9.
Molina PE, Winsauer P, Zhang P et-al. Cannabinoid administration attenuates the progression of simian immunodeficiency virus. AIDS Res. Hum. Retroviruses. 2011;27 (6): 585-92.

Mukhopadhyay D, Riezman H. Proteasome-independent functions of ubiquitin in endocytosis and signaling. Science. 2007;315(5809):201-5.

Murphy, K., Travers, P., Walport, M., & Janeway, C. (2008). *Janeway's immunobiology*. New York: Garland Science.

Nazli A, Kafka JK, Ferreira VH, et al. HIV-1 gp120 induces TLR2- and TLR4-mediated innate immune activation in human female genital epithelium. J Immunol. 2013;191(8):4246-58.

Neil SJ, Zang T, Bieniasz PD. Tetherin inhibits retrovirus release and is antagonized by HIV-1 Vpu. Nature. 2008;451(7177):425-30.

Ochsenbauer-jambor C, Jones J, Heil M, Zammit KP, Kutsch O. T-cell line for HIV drug screening using EGFP as a quantitative marker of HIV-1 replication. BioTechniques. 2006;40(1):91-100.

Ono A, Orenstein JM, Freed EO. Role of the Gag matrix domain in targeting human immunodeficiency virus type 1 assembly. J Virol. 2000;74(6):2855-66.

Orenstein JM, Gaetz HP, Yachnis AT, Frankel SS, Mertens RB, Didier ES. Disseminated microsporidiosis in AIDS: are any organs spared?. AIDS. 1997;11(3):385-6.

Ott DE. Cellular proteins detected in HIV-1. Rev Med Virol. 2008;18(3):159-75.

Ott M, Geyer M, Zhou Q. The control of HIV transcription: keeping RNA polymerase II on track. Cell Host Microbe. 2011;10(5):426-35.

Ozkaynak E, Finley D, Varshavsky A. The yeast ubiquitin gene: head-to-tail repeats encoding a polyubiquitin precursor protein. Nature. 1984;312(5995):663-6.

Palella FJ, Delaney KM, Moorman AC et-al. Declining morbidity and mortality among patients with advanced human immunodeficiency virus infection. HIV Outpatient Study Investigators. N. Engl. J. Med. 1998;338 (13): 853-60.

Pantaleo G, Fauci AS. Introduction: recent advances in the pathogenesis of human immunodeficiency virus infection. Springer Semin Immunopathol. 1997;18(3):253-6.

Pasternak AO, Lukashov VV, Berkhout B. Cell-associated HIV RNA: a dynamic biomarker of viral persistence. Retrovirology. 2013;10:41.

Paterson DL, Swindells S, Mohr J et-al. Adherence to protease inhibitor therapy and outcomes in patients with HIV infection. Ann. Intern. Med. 2000;133 (1): 21-30.

Paxton W, Connor RI, Landau NR. Incorporation of Vpr into human immunodeficiency virus type 1 virions: requirement for the p6 region of gag and mutational analysis. J Virol. 1993;67(12):7229-37.

Pery E, Rajendran KS, Brazier AJ, Gabuzda D. Regulation of APOBEC3 proteins by a novel YXXL motif in human immunodeficiency virus type 1 Vif and simian immunodeficiency virus SIVagm Vif. J Virol. 2009;83(5):2374-81.

Peterson PK, Gekker G, Hu S et-al. Cannabinoids and morphine differentially affect HIV-1 expression in CD4(+) lymphocyte and microglial cell cultures. J. Neuroimmunol. 2004;147 (1-2): 123-6.

Pickart CM, Rose IA. Ubiquitin carboxyl-terminal hydrolase acts on ubiquitin carboxyl-terminal amides. J Biol Chem. 1985;260(13):7903-10.

Pickart CM, Vella AT. Ubiquitin carrier protein-catalyzed ubiquitin transfer to histones. Mechanism and specificity. J Biol Chem. 1988;263(29):15076-82.

Planelles V, Bachelerie F, Jowett JB, et al. Fate of the human immunodeficiency virus type 1 provirus in infected cells: a role for vpr. J Virol. 1995;69(9):5883-9.

Planelles V, Jowett JB, Li QX, Xie Y, Hahn B, Chen IS. Vpr-induced cell cycle arrest is conserved among primate lentiviruses. J Virol. 1996;70(4):2516-24.
Pollard VW, Malim MH. The HIV-1 Rev protein. Annu Rev Microbiol. 1998;52:491-532.

Prussia A, Thepchatri P, Snyder JP, Plemper RK. Systematic approaches towards the development of host-directed antiviral therapeutics. Int J Mol Sci. 2011;12(6):4027-52.

Raborn ES, Marciano-cabral F, Buckley NE et-al. The cannabinoid delta-9-tetrahydrocannabinol mediates inhibition of macrophage chemotaxis to RANTES/CCL5: linkage to the CB2 receptor. J Neuroimmune Pharmacol. 2008;3 (2): 117-29.

Rasaiyaah J, Tan CP, Fletcher AJ, et al. HIV-1 evades innate immune recognition through specific cofactor recruitment. Nature. 2013;503(7476):402-5.

Ravid T, Hochstrasser M. Diversity of degradation signals in the ubiquitin-proteasome system. Nat Rev Mol Cell Biol. 2008;9(9):679-90.

Re F, Braaten D, Franke EK, Luban J. Human immunodeficiency virus type 1 Vpr arrests the cell cycle in G2 by inhibiting the activation of p34cdc2-cyclin B. J Virol. 1995;69(11):6859-64.

Revised Classification System for HIV Infection and Expanded Surveillance Case Definition for AIDS Among Adolescents and Adults, 1993. JAMA. 1993;269(6):729-730.

Robinson HL. New hope for an AIDS vaccine. Nat Rev Immunol. 2002;2(4):239-50.
Rock RB, Gekker G, Hu S et-al. WIN55,212-2-mediated inhibition of HIV-1 expression in microglial cells: involvement of cannabinoid receptors. J Neuroimmune Pharmacol. 2007;2 (2): 178-83.

Rodrigo-brenni MC, Gutierrez E, Hegde RS. Cytosolic quality control of mislocalized proteins requires RNF126 recruitment to Bag6. Mol Cell. 2014;55(2):227-37.

Rogel ME, Wu LI, Emerman M. The human immunodeficiency virus type 1 vpr gene prevents cell proliferation during chronic infection. J Virol. 1995;69(2):882-8.

Romani B, Cohen EA. Lentivirus Vpr and Vpx accessory proteins usurp the cullin4-DDB1 (DCAF1) E3 ubiquitin ligase. Curr Opin Virol. 2012;2(6):755-63.
Russell RA, Pathak VK. Identification of two distinct human immunodeficiency virus type 1 Vif determinants critical for interactions with human APOBEC3G and APOBEC3F. J Virol. 2007;81(15):8201-10.

Sattentau Q. Avoiding the void: cell-to-cell spread of human viruses. Nat Rev Microbiol. 2008;6(11):815-26.

Sattentau QJ, Moore JP. Conformational changes induced in the human immunodeficiency virus envelope glycoprotein by soluble CD4 binding. J Exp Med. 1991;174(2):407-15.

Schaeffer, E., Geleziunas, R., and Greene, Warner C. Human Immunodeficiency Virus Type I Nef Functions at the Level of Virus Entry by Enhancing Cytoplasmic Delivery of Virions. J of Virol. 75(6): 2993-3000, 2001.

Schröfelbauer B, Yu Q, Zeitlin SG, Landau NR. Human immunodeficiency virus type 1 Vpr induces the degradation of the UNG and SMUG uracil-DNA glycosylases. J Virol. 2005;79(17):10978-87.

Sheehy AM, Gaddis NC, Malim MH. The antiretroviral enzyme APOBEC3G is degraded by the proteasome in response to HIV-1 Vif. Nat Med. 2003;9(11):1404-7.

Sierra-aragón S, Walter H. Targets for inhibition of HIV replication: entry, enzyme action, release and maturation. Intervirology. 2012;55 (2): 84-97.

Siliciano JD, Kajdas J, Finzi D, et al. Long-term follow-up studies confirm the stability of the latent reservoir for HIV-1 in resting CD4+ T cells. Nat Med. 2003;9(6):727-8.

Slawson G, Milloy MJ, Balneaves L, et al. High-intensity cannabis use and adherence to antiretroviral therapy among people who use illicit drugs in a Canadian setting. AIDS Behav. 2015;19(1):120-7.

Smith MH, Ploegh HL, Weissman JS. Road to ruin: targeting proteins for degradation in the endoplasmic reticulum. Science. 2011;334(6059):1086-90.

Smith RL, De boer R, Brul S, Budovskaya Y, Van spek H. Premature and accelerated aging: HIV or HAART?. Front Genet. 2012;3:328.
Smythe W, Khandelwal A, Merle C, et al. A semimechanistic pharmacokinetic-enzyme turnover model for rifampin autoinduction in adult tuberculosis patients. Antimicrob Agents Chemother. 2012;56(4):2091-8.

Sorin M, Kalpana GV. Dynamics of virus-host interplay in HIV-1 replication. Curr HIV Res. 2006;4(2):117-30.

Stivahtis GL, Soares MA, Vodicka MA, Hahn BH, Emerman M. Conservation and host specificity of Vpr-mediated cell cycle arrest suggest a fundamental role in primate lentivirus evolution and biology. J Virol. 1997;71(6):4331-8.

Stoltzfus CM, Madsen JM. Role of viral splicing elements and cellular RNA binding proteins in regulation of HIV-1 alternative RNA splicing. Curr HIV Res. 2006;4(1):43-55.

Stopak K, de Noronha C, Yonemoto W, Greene WC. HIV-1 Vif blocks the antiviral activity of APOBEC3G by impairing both its translation and intracellular stability. Mol Cell12:591-601, 2003.

Sheehy AM, Gaddis NC, Choi JD, Malim MH. Isolation of a human gene that inhibits HIV-1 infection and is suppressed by the viral Vif protein. Nature 8:646-650, 2002.

Stremlau M, Owens CM, Perron MJ, Kiessling M, Autissier P, Sodroski J. The cytoplasmic body component TRIM5alpha restricts HIV-1 infection in Old World monkeys. Nature. 2004;427(6977):848-53.

Suspène R, Rusniok C, Vartanian J-P, Wain-Hobson S. 2006. Twin gradients in APOBEC3 edited HIV-1 DNA reflect the dynamics of lentiviral replication. Nucleic Acids Res 34: 4677–4684.

Suzuki Y, Craigie R. The road to chromatin - nuclear entry of retroviruses. Nat Rev Microbiol. 2007;5(3):187-96.

Trono D, Van lint C, Rouzioux C, et al. HIV persistence and the prospect of long-term drug-free remissions for HIV-infected individuals. Science. 2010;329(5988):174-80.

Ugolini S, Moulard M, Mondor I, et al. HIV-1 gp120 induces an association between CD4 and the chemokine receptor CXCR4. J Immunol. 1997;159(6):3000-8.
United Nations Joint Programme on HIV/AIDS (UNAIDS) (2011). Global HIV/AIDS Response, Epidemic update and health sector progress towards universal access.
Van damme N, Guatelli J.

HIV-1 Vpu inhibits accumulation of the envelope glycoprotein within clathrin-coated, Gag-containing endosomes. Cell Microbiol. 2008;10(5):1040-57.

Veronese FD, Rahman R, Kalyanaraman VS, et al. Monoclonal antibodies to HTLV-III451 gp41: delineation of an immunoreactive conserved epitope in the transmembrane region of divergent isolates of HIV-1. AIDS Res Hum Retroviruses. 1989;5(5):479-86.

Von schwedler UK, Stray KM, Garrus JE, Sundquist WI. Functional surfaces of the human immunodeficiency virus type 1 capsid protein. J Virol. 2003;77(9):5439-50.

Wainberg MA, Friedland G. Public health implications of antiretroviral therapy and HIV drug resistance. JAMA. 1998;279(24):1977-83.

Wainberg Z, Oliveira M, Lerner S, Tao Y, Brenner BG. Modulation of stress protein (hsp27 and hsp70) expression in CD4+ lymphocytic cells following acute infection with human immunodeficiency virus type-1. Virology. 1997;233(2):364-73.

Wang F, Song W, Brancati G, Segatori L. Inhibition of endoplasmic reticulum-associated degradation rescues native folding in loss of function protein misfolding diseases. J Biol Chem. 2011;286(50):43454-64.

Wang J, Reuschel EL, Shackelford JM, et al. HIV-1 Vif promotes the G_1- to S-phase cell-cycle transition. Blood. 2011;117(4):1260-9.

Wang J, Shackelford JM, Selliah N, et al. The HIV-1 Vif protein mediates degradation of Vpr and reduces Vpr-induced cell cycle arrest. DNA Cell Biol. 2008;27(5):267-77.

Wang Z, Gerstein M, Snyder M. RNA-Seq: a revolutionary tool for transcriptomics. Nat. Rev. Genet. 2009;10 (1): 57-63.

Wang G, Zhao N, Berkhout B, Das AT. CRISPR-Cas9 Can Inhibit HIV-1 Replication but NHEJ Repair Facilitates Virus Escape. Mol Ther. 2016;24(3):522-6.

Watters SA, Mlcochova P, Gupta RK. Macrophages: the neglected barrier to eradication. Curr Opin Infect Dis. 2013;26(6):561-6.

Wen X, Casey klockow L, Nekorchuk M, Sharifi HJ, De noronha CM. The HIV1 protein Vpr acts to enhance constitutive DCAF1-dependent UNG2 turnover. PLoS ONE. 2012;7(1):e30939.

Wen X, Duus KM, Friedrich TD, De noronha CM. The HIV1 protein Vpr acts to promote G2 cell cycle arrest by engaging a DDB1 and Cullin4A-containing ubiquitin ligase complex using VprBP/DCAF1 as an adaptor. J Biol Chem. 2007;282(37):27046-57.

Westlake TM, Howlett AC, Bonner TI et-al. Cannabinoid receptor binding and messenger RNA expression in human brain: an in vitro receptor autoradiography and in situ hybridization histochemistry study of normal aged and Alzheimer's brains. Neuroscience. 1994;63 (3): 637-52.

Wong JK, Günthard HF, Havlir DV, et al. Reduction of HIV-1 in blood and lymph nodes following potent antiretroviral therapy and the virologic correlates of treatment failure. Proc Natl Acad Sci USA. 1997;94(23):12574-9.

Wong-staal F. The AIDS virus. What we know and what we can do about it. West J Med. 1991;155(5):481-7.

Yao XJ, Subbramanian RA, Rougeau N, Boisvert F, Bergeron D, Cohen EA. Mutagenic analysis of human immunodeficiency virus type 1 Vpr: role of a predicted N-terminal alpha-helical structure in Vpr nuclear localization and virion incorporation. J Virol. 1995;69(11):7032-44.

Yong-Hui Zheng, Dan Irwin, Takeshi Kurosu, Kenzo Tokunaga, Tetsutaro Sata and B. Matija Peterlin. Human APOBEC3F Is Another Host Factor That Blocks Human Immunodeficiency Virus Type 1 Replication. J. Virology78:6073-6076, 2004.

Yu Q, Chen D, König R, Mariani R, Unutmaz D, Landau NR. APOBEC3B and APOBEC3C are potent inhibitors of simian immunodeficiency virus replication. J Biol Chem. 2004;279(51):53379-86.

Yu X, Yu Y, Liu B, et al. Induction of APOBEC3G ubiquitination and degradation by an HIV-1 Vif-Cul5-SCF complex. Science. 2003;302(5647):1056-60.

Zhang H, Zhou Y, Alcock C, Kiefer T, Monie D, Siliciano J, Li Q, Pham P, Cofrancesco J, Persaud D and Sliciano RF. Novel Single-Cell-Level Phenotypic Assay for Residual Drug Susceptibility and Reduced Replication Capacity of Drug-Resistant Human Immunodeficiency Virus Type 1. J of Virology 78:1718-1729, 2004.

Zhang L, Ramratnam B, Tenner-racz K, et al. Quantifying residual HIV-1 replication in patients receiving combination antiretroviral therapy. N Engl J Med. 1999;340(21):1605-13.

Zhao X, Su H, Yin G et-al. High transfection efficiency of porcine peripheral blood T cells via nucleofection. Vet. Immunol. Immunopathol. 2011;144 (3-4): 179-86.

Zhao Y, Zheng Z, Cohen CJ et-al. High-efficiency transfection of primary human and mouse T lymphocytes using RNA electroporation. Mol. Ther. 2006;13 (1): 151-9.

Zhou D, Wang Y, Tokunaga K, Huang F, Sun B, Yang R. The HIV-1 accessory protein Vpr induces the degradation of the anti-HIV-1 agent APOBEC3G through a VprBP-mediated proteasomal pathway. Virus Res. 2015;195:25-34.

Zhou H, Xu M, Huang Q et-al. Genome-scale RNAi screen for host factors required for HIV replication. Cell Host Microbe. 2008;4 (5): 495-504.